Author:
Mottram, N. J

Title:
Boundary effects in nematic liquid crystal layers.

Boundary Effects in Nematic Liquid Crystal Layers

N. J. Mottram

A thesis submitted to the University of Bristol in accordance with the requirements for the degree of Doctor of Philosophy in the Faculty of Engineering

February 1996.

Abstract

The influence of the glass plates on liquid crystal display characteristics has, for a long time, been understood to be of critical importance. The present work therefore considers the effects of certain changes in the boundaries on the performance of liquid crystal displays and on certain liquid crystal structures. In the first half of the thesis the phenomenon important to the use of liquid crystal layers as displays is considered. This *Freedericksz effect* is investigated for a liquid crystal layer that consisting of a sample of liquid crystal material sandwiched between two non-planar glass plates. Certain display characteristics are then found for these novel boundaries and the possibility for a new type of bistable device is suggested.

In the second half of the thesis the effects of boundaries on defects within the liquid crystal sample are investigated. Defects are known to have a great influence on the appearence and behavior of a liquid crystal and changes to the nature of the boundaries of the liquid crystal layer are found to greatly affect the structure of the defects. Two types of defects are considered, the disclination line and the twist wall. Analytical and numerical solutions are found and the critical behaviour of these defects to changes in parameters such as boundary orientation and temperature is considered.

Acknowledgements

I would like to thank my supervisor, Prof. S. J. Hogan for his guidance, support and encouragement during this project. I am also very grateful to Stuart, Rhona, Trevor, Steve, Richard, Ed, Eric and everyone in 93/95 Woodland Road both past and present. Their help, advice and occasional trips to the Plane Tree have made my time in Bristol a lot more rewarding.
I would also like to thank my family for all their encouragement and my friends from Sandbach, Oxford and Bristol. Without the help of all the people at 40 Aberdeen Road the last three years would not have been so eventful.
This work was funded by the Engineering and Physical Sciences Research Council and my mum. I am extremely grateful to both of them.

Declaration

The work presented in this thesis was carried out by the author at the University of Bristol between September 1992 and February 1996 and is original unless otherwise acknowledged in the text or by reference.
This work has not been previously submitted at this or any other university.

Contents

Chapter 1

Introduction

1.1 Liquid crystals

The three common states of matter, solid, liquid and gas, are different because the molecules in each state have a different degree of order. In the (crystalline) solid state there exists a rigid arrangement of molecules which stay in that position and orientation with a small amount of variation from molecular vibration. To maintain this arrangement there are large forces holding the molecules in place and therefore a solid is difficult to deform. In the liquid phase the molecules have no fixed position or orientation and are free to move in a random fashion and the liquid state has less order than the solid state. The random motions of the molecules mean that the intermolecular attractive forces that kept a solid together are now only strong enough to keep the liquid molecules fairly close together. A liquid can therefore be easily deformed. In the gas state the random motion of the molecules has increased to overcome the intermolecular forces and the molecules eventually spread out to fill any container that holds them. The order in a liquid that derived from the closeness of the molecules has therefore been lost in a gas which consequently has less order than the liquid. The probability of molecules in a certain region being in a rigid arrangement and of the same orientation can be used to define a positional and orientational order which is greatest in the solid state and least in the gaseous state.

The differences between the three states can be attributed to the temperature of the substance. Temperature is a measure of the randomness of the molecules

and therefore the higher the temperature the less order exists and increasing temperature will cause the transition from a solid to a liquid and then to a gas.

The *thermotropic* liquid crystalline phase occurs in some substances in a temperature region between the solid and liquid states. In this state the substance possesses some properties of both liquids and solids. A liquid crystal is a fluid like a liquid but is anisotropic in its optical and electro-magnetic characteristics like a solid. The positional order in a solid may be lost when the liquid crystal is formed but the orientational order is not. It is this orientational order that accounts for the anisotropies of the substance. The molecules are not constrained to be at a fixed point in space but they do align in roughly the same direction (Figure 1.1)

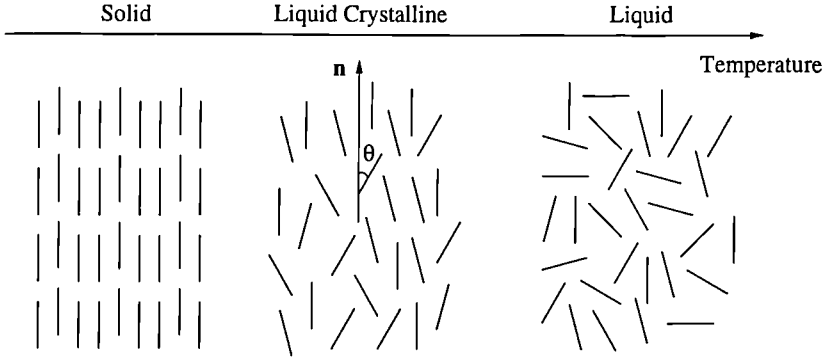

Figure 1.1: Illustration of the solid, liquid crystal and liquid phases. The lines represent molecules.

Using this average direction the anisotropic nature of the liquid crystal state may be modelled by defining a *director* $\mathbf{n}(\mathbf{r})$ which is the unit vector in the direction of the average molecular orientation at the point $\mathbf{r}$ in space. In Figure 1.1 the director can be defined in either direction, up or down, and there is no distinction made between the director and its negative.

Liquid crystalline states can also be found as a result of concentration changes. These *lyotropic* liquid crystals exist in an intermediate concentration region between solute/solvent ratios of 1 and 0 where the properties of the fluid become anisotropic. The present work will deal with thermotropic liquid crystals only.

1.2 History of liquid crystals

In this section the main developments in the history of liquid crystals will be summarised from the more in depth studies carried out by Collings [22] and Kelker [50].

The discovery of liquid crystals is thought to have occurred nearly 150 years ago although its significance was not fully realised until over a hundred years later. Around the middle of the last century Virchow [86], Mettenheimer [68] and Valentin [85] found that the nerve fibre they were studying formed a fluid substance when left in water which exhibited a strange behaviour when viewed using polarized light. They did not realise this was a different phase but they are attributed with the first observation of liquid crystals. Later, in 1877, Otto Lehmann [58] used a polarizing microscope with a heated stage to investigate the phase transitions of various substances. He found that one substance would change from a clear liquid to a cloudy liquid before crystallising but thought that this was simply an imperfect phase transition from liquid to crystalline. In 1888 Reinitzer [77] conducted similar experiments and was the first to suggest that this cloudy fluid was a new phase of matter. He has consequently been given the credit for the discovery of the liquid crystalline phase. Up till 1890 all the liquid crystalline substances that had been investigated had been naturally occurring and it was then that the first synthetic liquid crystal, *p*-azoxyanisole, was produced by Gatterman and Ritschke [41]. Subsequently more liquid crystals were synthesised and it is now possible to produce liquid crystals with specific predetermined material properties.

In the beginning of this century George Freidel conducted many experiments on liquid crystals and it was he who first explained the orienting effect of electric fields and the presence of defects in liquid crystals. In 1922 he proposed a classification of liquid crystals based upon the different molecular orderings of each substance [38]. It was between 1922 and the World War II that Oseen [73] and Zöcher [89] developed a mathematical basis for the study of liquid crystals.

After the start of the war many scientists believed that the important features of liquid crystals had now been discovered and it wasn't until the 1950's that work by Brown in America [16], Chistiakoff in the Soviet Union [84] and Gray

and Frank in England [44, 35] led to a revival of interest in liquid crystals. Maier and Saupe formulated a microscopic theory of liquid crystals , Frank [35] and later Leslie [59] and Ericksen [31] developed continuum theories for static and dynamic systems and in 1968 scientists from RCA first demonstrated a liquid crystal display. The interest in liquid crystals has grown ever since, partly due to the great variety of phenomena exhibited by liquid crystals and partly because of the enormous commercial interest and importance of liquid crystal displays.

1.3 Nematic liquid crystals

There are many types of liquid crystals such as nematic, chiral nematic, smectic and discotic which all possess different forms of structure, symmetry and order. The liquid crystal represented in Figure 1.1 is a nematic (after the Greek word $\nu\eta\mu\alpha$ for thread) and it is this type of liquid crystal that will subsequently considered. Nematics have a high degree of long-range orientational order but no long-range positional order. Substances which form nematics consist of long thin rigid molecules (Figure 1.2) which, while in the liquid crystalline state, prefer to orient parallel to neighbouring molecules. These substances can therefore possess an anisotropy between the directions parallel and perpendicular to the director. Along these two directions the refractive index of the substance, the shear viscosities and the magnetic suseptibilities are different. The molecules are polar in nature and have a major and minor polar axes which coincide with the direction of the director and perpendicular to it or vice versa.

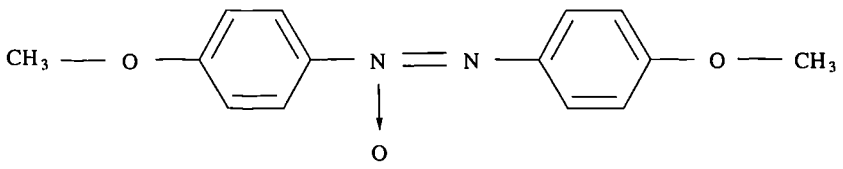

Figure 1.2: A p-azoxyanisole molecule which is liquid crystal in the temperature region $118.2\,\mathrm{deg}\,C < T < 135.3\,\mathrm{deg}\,C$

Two kinds of nematic liquid crystals will be discussed, uniaxial and biaxial.

1.3.1 Uniaxial nematics

Uniaxial nematics may be modelled using rods or sticks (Figure 1.1) to indicate the anisotropic nature of the molecule. The director at a point $\mathbf{r}$ is then the average direction of these rods in some region near $\mathbf{r}$. The amount of order the nematic possesses is defined as the scalar order parameter S. If each molecule forms an angle θ with the director (Figure 1.1) then the scalar order parameter is defined as,

$$S = \frac{1}{2}\langle 3\cos^2\theta - 1\rangle \tag{1.1}$$

where the angular brackets denote a thermal average [24]. When the molecules are all in the direction of the director $\theta = 0$, the substance is crystalline and $S = 1$. When the molecules are oriented randomly then the substance is a liquid and $S = 0$. The scalar order parameter can also be negative and attains its minimum when all the molecules lie in the plane perpendicular to the director $\theta = \pi/2$ and that $S = -1/2$. This situation is physically unrealistic and it will be assumed that the scalar order parameters are positive.

1.3.2 Biaxial nematics

Biaxial nematics may be thought of as long rectangular molecules (Figure 1.3) so that they are two dimensional rather than one dimensional as in the uniaxial case. To describe the orientation two directors $\mathbf{n}_1$ and $\mathbf{n}_2$ are defined corresponding to the average direction of the long and short axes of the molecules. There are then two scalar order parameters defined as,

$$\begin{aligned} S_1 &= \frac{1}{2}\langle 3\cos^2\theta_1 - 1\rangle \\ S_2 &= \frac{1}{2}\langle 3\cos^2\theta_2 - 1\rangle \end{aligned} \tag{1.2}$$

This is a rather simplistic view of biaxial nematics and it should be noted that it is possible to have a uniaxial phase in a substance made of biaxial molecules and a biaxial phase in a substance made of uniaxial molecules [24].

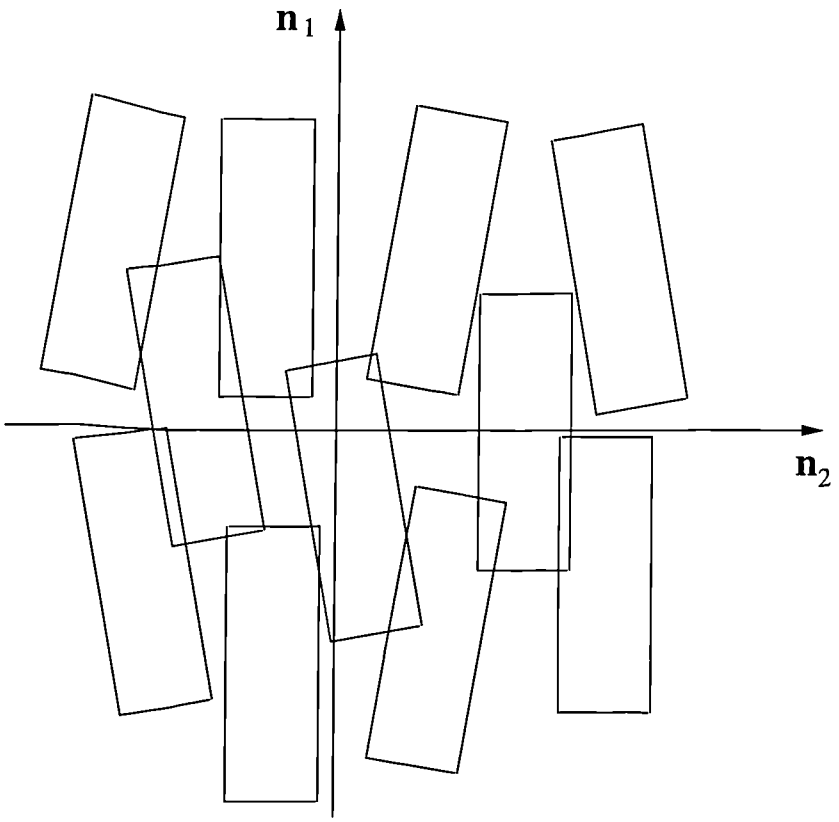

Figure 1.3: Simplistic representation of biaxial nematic liquid crystal with directors $\mathbf{n}_1$ and $\mathbf{n}_2$ defined as the average directions of the major and minor axis of the *rectangular* molecules [24].

1.4 Liquid Crystal Displays

Liquid crystals have a large number of uses but by far their main commercial use is in liquid crystal displays (LCD). A typical LCD consists of a nematic liquid crystal sandwiched between two glass plates which is then placed between two polarizers which are polarized at right angles to each other (Figure 1.4). The plates of glass have dimensions ranging from the order of centimetres for digital watches to metres for large screen VDUs. The distance between the plates is much smaller and is commonly of the order of $10 - 100\mu$m.
The LCD displays information using light and dark regions to produce letters, numbers, pictures etc. The dark regions are formed by aligning the director parallel to the axis of one of the polarizers. Then incident light is extinguished by the effect of the two crossed polarizers. When the director is aligned in

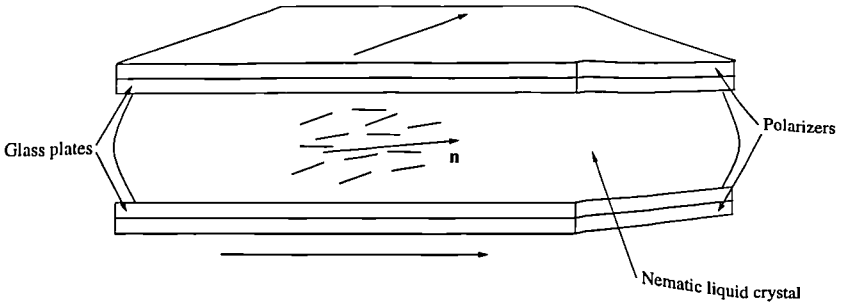

Figure 1.4: Schematic of a nematic liquid crystal display.

a direction not parallel to either axis of polarization the the incident light is changed from plane polarized (from the first polarizer) to elliptically polarized by the nematic anisotropy and therefore some light may pass through the second polarizer and the region is light. Most modern LCDs use twisted nematic layers which consist of a nematic liquid crystal sandwiched between two glass plates that force the director within the layer to rotate in a helix about an axis perpendicular to the glass plates. The presence of this twist in the anisotropic nature of the cell and the internal stress caused by the twist deformation means the LCD has greater transmission properties and faster switching times.
The aligning of the liquid crystal is achieved using the glass plates and magnetic or electric fields. The glass plates are treated by rubbing the plate in one average direction so that either small grooves are left in the glass or possibly long molecules from the abrasive cloth are deposited on the surface. In this way the liquid crystal molecules at the surface align in a direction determined by the direction of the grooves or long molecules. The bulk of the liquid crystal is aligned with this direction by the internal stresses of the substance which induce alignment between neighbouring molecules. Before any external force is introduced the director is therefore in one direction for the whole sample. When a field is applied across the cell orientation of the molecules with the field occurs. This phenomenon is called the Freedericksz effect [36]. It is one of the simplest phenomena that occur in liquid crystal layers when an electromagnetic field is applied. When the major electric or magnetic polar axis of the molecules has been aligned according to the orienting effect of the surfaces and the direction of the electric or magnetic field conflicts with the director the field will compete with the surface to align the liquid crystal. There exists a critical

field strength such that below this value the electromagnetic field cannot overcome the effect of the orienting boundaries but above it the field dominates and the director aligns so that the polar axes of most of the molecules are parallel to the field direction. The exceptions being those molecules near to the boundary. In this way it is possible to obtain two orientations of the bulk director when the field is on or off corresponding to on and off states for the LCD.

1.5 Disclinations

In some nematic samples seen under polarised light, a system of points linked by dark filaments or brushes is observed (Figure 1.5). This phenomenon, called *structures à noyaux* or *schlieren texture*, is formed by discontinuities in orientation called disclination lines. These discontinuities are formed by impurities in the liquid crystal and on the glass surface and by inconsistencies in the alignment at the surface. On a circuit around a disclination line the director rotates by a multiple of π radians. If the cell is viewed through crossed polarizers a system of dark and light regions are observed since the incident light is extinguished in regions where the director is parallel to one of the crossed polarizers. The number of dark regions, or *brushes* is a measure of the strength of the disclination and as can be seen in Figure 1.5 the majority of disclination lines have two or four brushes. These defects can have a great influence on the behaviour of the liquid crystal cell and consequently there structure has been studied in depth.

1.6 Motivation

The motivation for the present work is the need to understand how the boundaries of a liquid crystal display affect the structure and behaviour of a liquid crystal cell. The majority of current analytical work in the subject of liquid crystals assumes the boundary is planar and very simplistic boundary conditions. Recently investigations into the aligning effect of rubbing surfaces have considered non-planar boundaries, shear and oscillatory shear. In the latter, studies have shown that shear has a great influence on the system [46, 65]. In

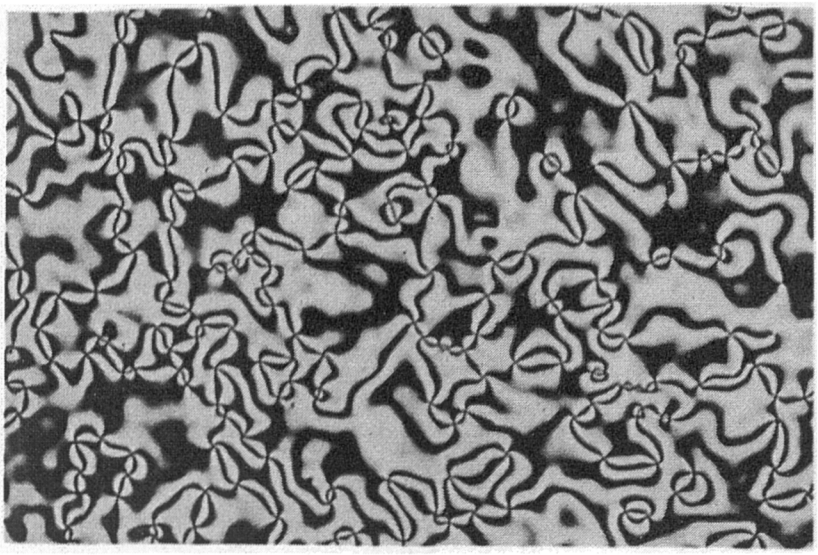

Figure 1.5: Nematic liquid crystal between crossed polarizers. The points where the dark regions converge are disclinations [22].

this thesis the effect of a perturbation to the system in the form of sinusoidal boundaries is considered.
The importance of defects or disclinations in liquid crystal cells motivates us to investigate defects using a relatively new continuum theory [33] paying special attention to the effects of the boundaries and boundary conditions.

1.7 Organisation of the Thesis

In Chapter 2 relevant previous work is discussed and the continuum theory that will be used throughout the thesis is introduced. Chapters 3 to 5 deal with the effects on display characteristics of non-planar boundaries. The bounding glass plates are not assumed to be planar but sinusoidal and in Chapter 3 the configuration of the director within such cells is considered. In Chapter 4 the theory is extended to include a magnetic field applied across the cell and consequently find the critical field strength for the Freedericksz transition for the novel boundaries from the linearised equations. The effect of higher order terms of the equations are then considered and a second transition is found in the solution at a higher field strength. In Chapter 5 the structure of the two

transitions using an amplitude equation type analysis is investigated and the stability characteristics of the various solution paths is found.
In Chapter 6 attention is turned to the effects certain boundaries and boundary conditions have on defects in the liquid crystal layer. In this chapter an introduction to defects is presented and specific attention is given to the two forms of defects considered in the following chapters. In Chapter 7 disclination lines are considered and the director structure of a disclination line attached to the boundary at a single point is found. Then an extended continuum theory is used which allows for biaxiality and changes in the scalar order parameters to consider disclination line cores. In Chapter 8 the same continuum theory is used to investigate twist wall defects in nematic twist layers.
In the final chapter the results of the previous chapters and possible future work are discussed.

Chapter 2

Continuum Theory

In this chapter a brief literature review of previous relevant work and an introduction to the continuum theory used throughout this thesis are given.

2.1 Literature review

A continuum theory of liquid crystals was first proposed in the work of Oseen [73] and Zöcher [89] who introduced the unit vector $\mathbf{n}$ to describe the average orientation of the anisotropic axis of the liquids. This static theory was later re-examined by Frank [35] who presented Oseen's method as a theory of curvature elasticity. The Oseen-Zöcher-Frank formulation describes variations of the director $\mathbf{n}$ corresponding to distortions of the liquid crystals. The free energy of these distortions is then simply a function of the director and any external forces such as a magnetic field. For any particular static system an energy minimization technique can be employed to find the unknown director field. The most widely used continuum theory for the dynamics of liquid crystals, which will be mentioned only briefly, is due to Ericksen [31, 32] and Leslie [59, 60, 61] and in the static limit this theory reduces to the Oseen-Zöcher-Frank theory.

2.1.1 Freedericksz effect

The effects of electric and magnetic fields on liquid crystals was considered by Zöcher [89] and also by Freedericksz and Zolina [36]. The critical behaviour of

the system when a field is applied has subsequently been named the Freedericksz effect. The importance of this effect in the field of liquid crystal displays and in the measurement of material properties of the liquid crystal has meant that a great deal of analytical and experimental studies have been carried out using many different cell configurations and types of liquid crystal (see for example Blinov [12], Frisken and Palffy-Muhoray [39], Kini [52, 53] and Derfel [26, 27]). Due to the commercial need for liquid crystal displays with quick switching times and high contrast much of the research into this area has involved the calculation of the critical field strength and the growth/decay rates of the transition. Our investigation into the Freedericksz effect will concentrate on the effects of non-planar boundaries on the display characteristics of uniaxial nematic liquid crystal cell.

2.1.2 Boundaries

From early on the importance of alignment of liquid crystals was realised and consequently the influence of the glass surfaces in a liquid crystal cell has been widely investigated. Berreman [7] showed that the geometric effects of rubbing the surface are significant in the alignment of the director throughout the whole cell. Investigations into the effects of corrugated surfaces as a model of this rubbing have been carried out by Berreman [8] and more recently by Kawata et al [49], Lee et al [57] and Sugimura and Kawamura [83]. The director may be strongly or weakly anchored and the alignment (or lack of it) of the director at the surfaces of liquid crystal displays plays an extremely important part in the display characteristics [64, 26].

In Chapters 3-5 the director is assumed to be strongly anchored to the surface but that the surface is not planar and in Chapter 6 weak anchoring on a planar surface is considered.

In more recent years interest has grown in how director distortions affect the phase of the liquid crystal. It has been found that boundaries may induce changes in the order (specifically, parameters which govern phase and biaxiality) of the liquid crystal. Investigations by Barberi and Durand [2] and Barbero and Durand [3, 4, 5, 6] have found a significant change in the scalar order parameters near rough surfaces.

2.1.3 Disclinations

The need to describe defects in a continuum model has led to the formulation by Ericksen of a new equilibrium theory [33]. Ericksen introduces the degree of order of the liquid crystal at a point as a dependent variable in the governing equations. In this way he is able to model the core of defects which previously have been largely absent from any rigorous mathematical treatment. This method had been anticipated by earlier authors such as de Gennes [23] and Fan [34]. Landau-de Gennes theory is an equivalent theory (under certain assumptions) and has been used to successfully describe defect cores [40, 80]. Discussion of these theories and the theory used to describe disclinations in this thesis is reserved to a later chapter.

2.1.4 Biaxial liquid crystals

Biaxial liquid crystals were discovered by Yu and Saupe [88] in lyotropic systems (liquid crystals whose phase depends on concentration rather than temperature) and subsequently in thermotropic systems by Malthête et al [20], Chandrasekhar et al [20] and Praeffke et al [75]. Attempts at deriving a macroscopic theory for biaxial liquid crystals has centred on theoretical physics rather than continuum mechanics [15, 42, 48, 66, 79]. Kini [51] used three directors to derive a continuum theory and Leslie et al [63] used the necessary two directors in their extension of the Leslie-Ericksen theory. Biscari with other authors has also used two directors and introduced a degree of biaxiality [9, 10, 11]. It is this latest method that is used to consider uniaxial and biaxial liquid crystals with variable degrees of orientation.

2.2 Continuum theory

In this section a brief outline of the important features of the continuum theory are presented. For a deeper treatment Virga's book on the subject is recommended [87].

A continuum theory must be based on the consideration of quantities that describe the liquid crystal on a macroscopic scale. These quantities will derive from the statistical distribution of the orientation of the molecules within the

liquid crystal. If it is assumed that the orientations of the molecules obey a distribution law whose probability density is f then the first information about the probability distribution comes from its second moments which can be represented by the second order tensor,

$$\mathbf{M} = \int_{S^2} \mathbf{l} \otimes \mathbf{l}\, f(\mathbf{l}) \mathrm{d}a \tag{2.1}$$

where S^2 is the unit sphere, a is the area measure on S^2 and $\mathbf{l}$ denotes an orientation in S^2. It is now possible to define the *order tensor* $\mathbf{Q}$,

$$\mathbf{Q} = \mathbf{M} - \frac{1}{3}\mathbf{I} \tag{2.2}$$

which is therefore a measure of how the second moments of this probability deviate from their isotropic values and can be used to describe the state of the system in a macroscopic theory. It can easily be shown that the trace of $\mathbf{M}$ is 1 and therefore the trace of $\mathbf{Q}$ is zero [87]. Using perpendicular unit basis vectors $\mathbf{n_1}$ and $\mathbf{n_2}$, $\mathbf{Q}$ may therefore be written as,

$$\mathbf{Q} = S_1\, \mathbf{n}_1 \otimes \mathbf{n}_1 + S_2\, \mathbf{n}_2 \otimes \mathbf{n}_2 - \frac{1}{3}(S_1 + S_2)\mathbf{I} \tag{2.3}$$

The eigenvalues of $\mathbf{Q}$ using the basis set $\{\mathbf{n_1},\ \mathbf{n_2},\ \mathbf{k}\}$ are then $\frac{2}{3}S_1 - \frac{1}{3}S_2$, $\frac{2}{3}S_2 - \frac{1}{3}S_1$ and $-\frac{1}{3}S_1 - \frac{1}{3}S_2$. The vectors $\mathbf{n_1}$ and $\mathbf{n_2}$ are termed the *directors* and the scalars S_1 and S_2 are the scalar order parameters.

The free energy density F of the system consists of contributions from the energy associated with distortions of the order parameter from some specified base state, energy from external forces such as magnetic fields, and surface energy. The governing equations may be obtained by minimizing the free energy E of the liquid crystal cell, where in the static case the free energy is the integral of the free energy density over the region occupied by the liquid crystal V.

$$E = \int_V F(\mathbf{Q}) \mathrm{d}v \tag{2.4}$$

where $\mathrm{d}v$ is an element of volume. Three forms of order parameter configurations can be distinguished. The first is the isotropic situation where the molecules are randomly oriented and hence $\mathbf{Q} = \mathbf{0}$ and all the eigenvalues are

the same. The second is *uniaxial* nematics where two of the eigenvalues are the same and the order tensor can be written as,

$$\mathbf{Q} = S\left(\mathbf{n} \otimes \mathbf{n} - \frac{1}{3}\mathbf{I}\right) \tag{2.5}$$

The scalar order parameter S is the degree of orientation of the molecules about the director $\mathbf{n}$. The third situation is the biaxial nematic where all the eigenvalues are distinct and the order parameter may not be simplified from (2.3). The biaxial state becomes uniaxial if $S_1 = S_2$ or when either S_1 or S_2 vanish. The uniaxial or biaxial case becomes isotropic when $S = 0$ or $S_1 = 0 = S_2$ respectively.

2.3 Director configuration

In this system a right-handed set of orthogonal axes $\{\mathbf{i},\ \mathbf{j},\ \mathbf{k}\}$ and corresponding coordinates $(x,\ y,\ z)$ are used. The vertical coordinate is y so that planar bounding plates would be described by the surfaces $y = y_1$ and $y = y_2$. When the surfaces are treated to impose strong or weak boundary conditions, the preferred direction will be in the xy-plane so that when a 2-dimensional model of the liquid crystal cell is considered the x and y axes are horizontal and vertical respectively.

For uniaxial liquid crystals the director $\mathbf{n}$ can be described by spherical polar coordinates r, ϕ and ψ but the condition $\mathbf{n}^2 = 1$ implies that $r = 1$ so that,

$$\mathbf{n} = (\cos(\phi)\cos(\psi),\ \sin(\phi),\ \cos(\phi)\sin(\psi)) \tag{2.6}$$

where ϕ is the angle between the director and the xz-plane and ψ is the azimuthal angle i.e. the angle between the plane containing the director and the y axis and the xy-plane (Figure 2.1). It may also be convenient to occasionally use the angle from the director to the vertical $\varphi = \pi/2 - \phi$.

In later chapters when biaxial nematics are considered the director $\mathbf{n}_1$ will be assumed to lie in the xy-plane and equivalent to the uniaxial director The second director $\mathbf{n}_2$ can be chosen to be a unit vector perpendicular to the uniaxial director (Figure 2.1). The two directors are therefore,

$$\begin{aligned} \mathbf{n}_1 &= (\cos(\phi)\cos(\psi),\ \sin(\phi),\ \cos(\phi)\sin(\psi)) \\ \mathbf{n}_2 &= \mathbf{v} \wedge \mathbf{n}_1 \end{aligned} \tag{2.7}$$

for some vector $\mathbf{v}$.

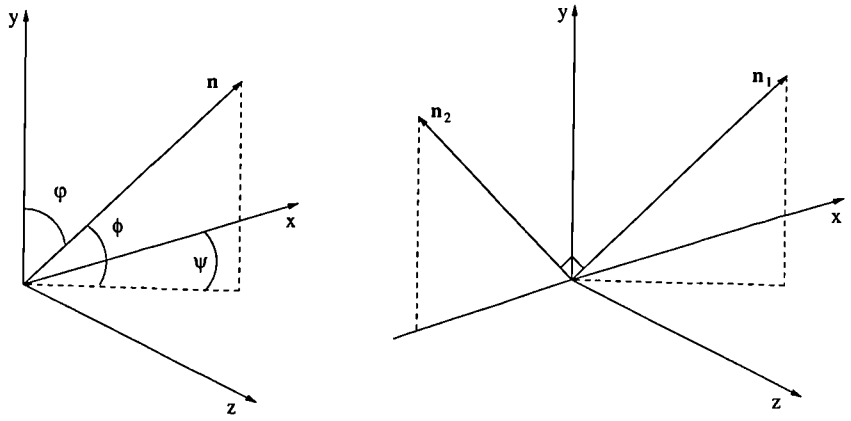

Figure 2.1: Director configuration.

2.4 Boundary conditions

The general boundary condition will be based on the assumption that there is a surface energy term $F_S(\mathbf{Q})$. The free energy is then the sum of the bulk free energy density terms $F_B(\mathbf{Q})$ integrated over the volume occupied by the liquid crystal V and the surface free energy density terms integrated over the boundary ∂V.

$$E = \int_V F_B(\mathbf{Q})\mathrm{d}v + \int_{\partial V} F_S(\mathbf{Q})\mathrm{d}s \tag{2.8}$$

where $\mathrm{d}s$ is an element of surface area. The bulk term may include contributions from elastic distortions and applied fields which will be discussed later. The surface term should reflect the nature of the boundary alignment and order. Therefore if the surface energy is minimum when the order tensor is $\mathbf{Q}_0$ then the surface free energy density may be written as,

$$F_S(\mathbf{Q}) = \mathbf{W}.\mathbf{f}(\mathbf{Q} - \mathbf{Q}_0) \tag{2.9}$$

where the function $\mathbf{f}$ has a minimum at 0 and $\mathbf{W}$ is the *anchoring energy.* One of the simplest forms for the surface energy density will be used [87],

$$\begin{aligned} F_S(\mathbf{Q}) &= F_S(S_1,\ S_2,\ \phi,\ \psi) \\ &= W_1(S_1 - S_{10})^2 + W_2(S_2 - S_{20})^2 + \\ &\qquad W_3 \sin^2(\phi - \phi_0) + W_4 \sin^2(\psi - \psi_0) \end{aligned} \tag{2.10}$$

If one of the variables S_1, S_2, ϕ or ψ deviates away from the *preferred* values S_{10}, S_{20}, ϕ_0 or ψ_0 the free energy will increase. For a specific increase in S_1, say, the energy increase is then determined by the magnitude of the anchoring energy W_1. Since the system will act to resist increases in energy, a large value of W_1 will imply a strong restoring force acting to reduce S_1 to its minimum energy configuration S_{10}. If any of the anchoring energies W_i are infinite then to ensure a finite free energy the corresponding energy density must be zero. For example, for most of this thesis strong anchoring is assumed on ∂V of the scalar order parameters S_1 and S_2 so that $W_1 = W_2 = \infty$ and therefore $S_1 = S_{10}$ and $S_2 = S_{20}$. Strong anchoring of the directors is considered on ∂V in all but Chapter 7 where a uniaxial nematic is considered at boundary that imposes homogeneous weak anchoring. In this case $W_4 = \infty$ but W_3 is finite and the surface energy density has only one term and can be written as $F_S = W \sin^2(\phi)$. The boundary condition is then derived from the minimization of the free energy.

In Chapters 3, 4, 5 and in the first part of Chapter 7 uniaxial liquid crystals with constant scalar order parameters are considered and the governing equations are derived from a minimization of the free energy, leading to Euler-Lagrange equations in the dependent variables, ϕ and ψ. In the last part of Chapter 7 and in Chapter 8 a simplified director structure is chosen but the scalar order parameters are allowed to vary so that the governing equations are the Euler-Lagrange equations with dependent variables ϕ, S_1 and S_2.

Chapter 3

Freedericksz Transition

In the next three chapters the effect of non-planar boundaries will be considered on a liquid crystal layer when a magnetic field is applied. When the field orienting effect is in competition with the aligning effect of the boundaries there is a critical field strength H_c such that below H_c the director is undistorted and alignment is imposed by the boundaries. Above the critical field strength the director aligns with the field everywhere except near the boundaries. At low field strengths and those near the critical field strength value the gradients of distortions of the directors $\mathbf{n}_1$ and $\mathbf{n}_2$ are small and therefore since variations in the scalar order parameters are associated with high distortional energy, it will be assumed that S_1 and S_2 are constant. It is also assumed that the liquid crystal substance is uniaxial. The analysis is thus simplified so that the single director $\mathbf{n}$ is the only dependent variable. The boundaries of the cell are taken to have strong anchoring so that the director is fixed there.

In this chapter the governing equations and the relevant boundary conditions are obtained and then the effects of different boundary conditions and parameter orderings on the simplest system, the linear solution in the absence of a field are considered. In Chapter 4 the linear solution is considered in the presence of a magnetic field and then a perturbation expansion is used to obtain the weakly nonlinear solution. In Chapter 5 the solution is investigated around the transition point by considering the amplitude of the dominant mode. Using this method it is possible to calculate the energy of the system and find the stability of each solution.

3.1 Governing equations

As stated above a uniaxial liquid crystal is considered with constant scalar order parameter (assuming constant temperature). Therefore two of the eigenvalues of $\mathbf{Q}$ are the same ($S_1 = S_2$), and the tensor order parameter can be written as,

$$Q_{ij} = S\left(\mathbf{n}\otimes\mathbf{n} - \frac{1}{3}\mathbf{I}\right)_{ij} = S\left(n_i\, n_j - \frac{1}{3}\,\delta_{ij}\right) \tag{3.1}$$

where S is a constant.

There are two possible ways to proceed, the free energy density F could be considered as a function of Q_{ij} as in Landau-de Gennes theory (see Chapter 7), or alternatively as a function of $\mathbf{n}$. The second description developed by Oseen [73], Zöcher [89] and Frank [35] will be used in the next three chapters. These authors assumed that the typical length over which distortions occur is much greater than the typical molecular length. A continuum theory may then be used so that the structure on the molecular scale can be disregarded and the free energy is determined by the director $\mathbf{n}$ which varies with the space coordinates $\mathbf{r}$ smoothly.

The free energy of the system is then,

$$E = \int_V F(\mathbf{n})\,\mathrm{d}v \tag{3.2}$$

where $dv = dx\,dy\,dz$ is a volume element. The free energy density consists of contributions from surface energy terms $F_S(\mathbf{n})$ and from the bulk free energy which includes distortions of the director field from an undistorted state $F_D(\mathbf{n})$ and external forcing such as magnetic fields $F_H(\mathbf{n})$ and electric fields $F_E(\mathbf{n})$.

$$E = \int_V F_D(\mathbf{n}) + F_H(\mathbf{n}) + F_E(\mathbf{n})\,\mathrm{d}v + \int_{\partial V} F_S(\mathbf{n})\,\mathrm{d}s \tag{3.3}$$

where ds is a surface element. Each of these contributions will now be considered.

3.1.1 Distortional free energy

If the director varies slowly and smoothly so that second and higher order gradients of $\mathbf{n}$ are negligible it is possible to use the assumption that the distortional free energy density F_D is a single-valued function of,

$$n_i \quad n_{i,j} \quad \dot{n}_i \tag{3.4}$$

where, $n_{i,j} = \partial n_i / \partial x_j$ and $\dot{}$ denotes differentiation with respect to time. When the static case is considered it is therefore possible to take,

$$F_D = F_D(n_i, n_{i,j}) \tag{3.5}$$

although it can be shown that this is also the case for the dynamic theory [61]. By considering the relevant symmetries of the nematic liquid crystal (Appendix A) the bulk free energy density may be written as,

$$F_D = \frac{1}{2}K_1 \left(\text{div } \mathbf{n}\right)^2 + \frac{1}{2}K_2 \left(\mathbf{n} \cdot \text{curl } \mathbf{n}\right)^2 + \frac{1}{2}K_3 \left(\mathbf{n} \wedge \text{curl } \mathbf{n}\right)^2 \tag{3.6}$$

Each of these three terms corresponds to a distinct form of distortion (Fig. 3.1). The K_1 term is non-zero when div $\mathbf{n} \neq 0$ and therefore corresponds to a splay deformation of the director. The K_2 term is non-zero when $\mathbf{n} \cdot$ curl $\mathbf{n} \neq 0$ which occurs when the director is twisted. The K_3 term is non-zero when $\mathbf{n} \wedge$ curl $\mathbf{n} \neq 0$ which corresponds to a bending of the director. The coefficients K_1, K_2 and K_3 are the Frank elastic constants corresponding to splay, twist and bend elastic constants.

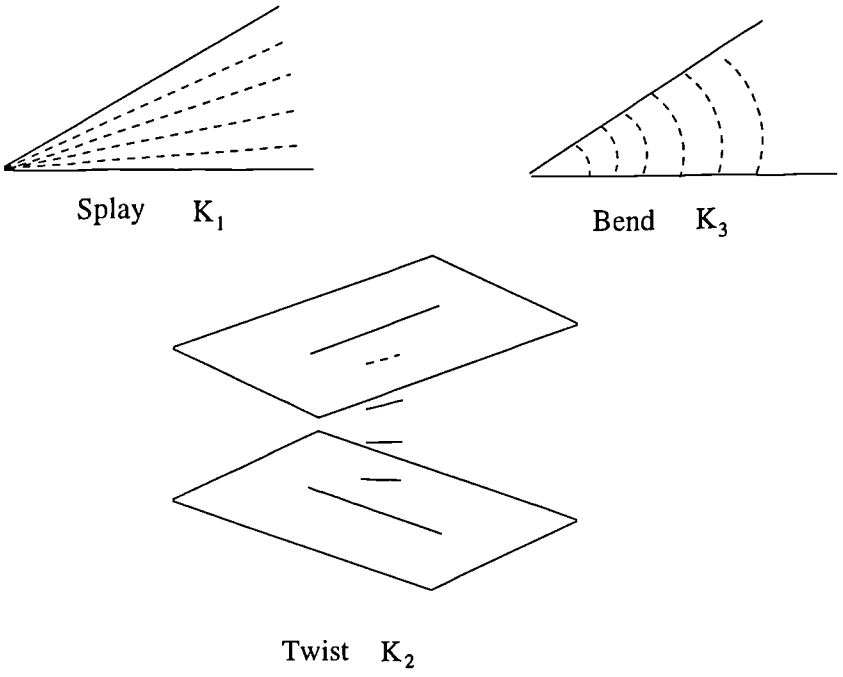

Figure 3.1: The three types of deformation in nematics. Each type may be obtained separately by suitable glass plates.

When one of the coefficients is much smaller than the others, K_2, say, the liquid crystal will find twist deformations more energetically favourable and hence if the liquid crystal is forced to deform it will try to reduce the energy of the system through twisting. For the ease of analysis all three elastic constants are taken to be equal.

$$K_1 = K_2 = K_3 = K \tag{3.7}$$

This *one constant approximation* is not unrealistic since in most nematic liquid crystals the Frank constants are at least of the same order. In MBBA at 22° C the elastic constants are [78],

$$\begin{aligned} K_1 &= 5.30 \pm 0.5 \times 10^{-7} \text{ dyn} \\ K_2 &= 2.20 \pm 0.7 \times 10^{-7} \text{ dyn} \\ K_3 &= 7.45 \pm 1.1 \times 10^{-7} \text{ dyn} \end{aligned} \tag{3.8}$$

It should be mentioned at this point that a liquid crystal cell in which twisting is the only form of deformation is considered (as is later considered in Section 8) then the bend and splay terms in the free energy density (3.6) are zero and the free energy consists of the twist deformation term only. The one constant approximation is then $K = K_2$ since K_1 and K_3 are not present in the free energy. In the same way if only splay and bend deformations are present in the liquid crystal layer then (3.7) is equivalent to the approximation $K_1 = K_3 = K$ since the K_2 term does not enter the free energy. The accuracy of the one constant approximation is therefore determined by the similarity between the elastic constants of the deformations present in the system.
When the one constant approximation is used the free energy density becomes,

$$F_D = \frac{1}{2} K \left((\text{div } \mathbf{n})^2 + (\text{curl } \mathbf{n})^2 \right) \tag{3.9}$$

3.1.2 Field effects

Electric fields

The aligning effect of an electric field $\mathbf{E}$ on a nematic liquid crystal which was described in the introduction can be investigated by deriving the free energy

contribution from the field/director interaction. For a dielectric displacement $\mathbf{D}$ induced by the electric field $\mathbf{E}$ the free energy contribution from the electric effect is,

$$F_E = -\frac{1}{4\pi}\int_0^E \mathbf{D}\cdot \mathrm{d}\mathbf{E} \tag{3.10}$$

and from Maxwell's equations for a sample with no charge carriers the field and displacement vectors must satisfy,

$$\operatorname{div}\mathbf{D} = 0 \tag{3.11}$$

$$\operatorname{curl}\mathbf{E} = 0 \tag{3.12}$$

The dielectric displacement of an anisotropic substance is,

$$\mathbf{D} = \epsilon_\perp \mathbf{E} + \left(\epsilon_\parallel - \epsilon_\perp\right)(\mathbf{E}\cdot\mathbf{n})\ \mathbf{n} \tag{3.13}$$

where $\epsilon_a = \epsilon_\parallel - \epsilon_\perp$, the dielectric anisotropy, is a measure of the difference in the susceptibility to a electric field of a director configuration perpendicular and parallel to the field. The free energy density due to the electric field is therefore,

$$F_E = -\frac{\epsilon_\perp}{8\pi}\mathbf{E}^2 - \frac{\epsilon_a}{8\pi}(\mathbf{n}\cdot\mathbf{E})^2 \tag{3.14}$$

Since each molecule has a permanent electric dipole the first term is dependent on molecular orientation (i.e. the director field $\mathbf{n}$). Not only will the field affect the orientation of the director but the orientation of the director will affect the field. If the dielectric anisotropy or the director field distortion is small the electric field may be assumed to be constant throughout the liquid crystal layer [24]. The first term of the free energy density (3.14) is then constant and may be neglected since it contributes a constant energy to the system which will not affect the minimization.

Magnetic fields

For all practical cases an interaction between the permanent electric dipole of the molecule and an applied magnetic field does not exist. A constant field $\mathbf{H}$

is not affected by the director orientation and the magnetization $\mathbf{M}$ induced by $\mathbf{H}$ is,

$$\mathbf{M} = \chi_{\perp}\,\mathbf{H} + \left(\chi_{\parallel} - \chi_{\perp}\right)(\mathbf{H}\cdot\mathbf{n})\;\mathbf{n} \tag{3.15}$$

and the contribution to free energy density of the magnetic effect, F_H, is,

$$F_H = -\int_0^H \mathbf{M}\cdot\mathrm{d}\mathbf{H} \tag{3.16}$$

Substituting (3.15) in (3.16) leads to,

$$F_H = -\frac{1}{2}\chi_{\perp}\mathbf{H}^2 - \frac{1}{2}\chi_a\,(\mathbf{n}\cdot\mathbf{H})^2 \tag{3.17}$$

Where $\chi_a = \chi_{\parallel} - \chi_{\perp}$. The first term is independent of $\mathbf{n}$ and can be omitted for all situations involving a constant magnetic field H. The constant χ_a is the diamagnetic anisotropy. The constants $\chi_{\parallel}$ and $\chi_{\perp}$ are small ($\chi_{\parallel}$, $\chi_{\perp} \approx 10^{-6}$ for MBBA in cgs electromagnetic units) and the anisotropy χ_a is usually positive and small ($\chi_a \approx 10^{-7}$ for MBBA in cgs electromagnetic units) for nematics.
In subsequent sections a nematic liquid crystal cell with an applied *magnetic* field is only considered noting that for most situations the solutions for the electric field case can be retrieved using the substitution,

$$\frac{\chi_a H^2}{2} \rightarrow \frac{\epsilon_a E^2}{8\pi} \tag{3.18}$$

The field contribution to the free energy density is therefore the second term in (3.17).

3.1.3 Summary

The bulk free energy density of a liquid crystal cell with an applied field $\mathbf{H}$ using the one constant approximation is,

$$F = \frac{1}{2}K\left((\mathrm{div}\;\mathbf{n})^2 + (\mathrm{curl}\;\mathbf{n})^2\right) - \frac{1}{2}\chi_a\,(\mathbf{n}\cdot H)^2 \tag{3.19}$$

With the director configuration (2.6),

$$\mathbf{n} = (\cos(\phi)\cos(\psi),\ \sin(\phi),\ \cos(\phi)\sin(\psi)) \tag{3.20}$$

this becomes,

$$
\begin{aligned}
F \;=\; & \frac{1}{2}K\Big[(\nabla\phi)^2 + \cos^2\phi\,(\nabla\psi)^2 \\
& \quad + 2\left(\sin\phi\cos\phi\,(\phi_{,z}\psi_{,x} - \phi_{,x}\psi_{,z})\right. \\
& \quad\quad + \cos^2\phi\cos\psi\,(\phi_{,y}\psi_{,z} - \phi_{,z}\psi_{,y}) \\
& \quad\quad \left. + \cos^2\phi\sin\psi\,(\phi_{,x}\psi_{,y} - \phi_{,y}\psi_{,x})\right)\Big] \qquad (3.21) \\
& -\frac{1}{2}\chi_a\Big[H_x^2\cos^2\phi\cos^2\psi + H_z^2\cos^2\phi\sin^2\psi \\
& \quad + H_y^2\sin^2\phi + 2\Big(H_zH_x\cos^2\phi\sin\psi\cos\psi \\
& \quad + H_xH_y\sin\phi\cos\phi\cos\psi + H_yH_z\sin\phi\cos\phi\sin\psi)\Big]
\end{aligned}
$$

and the free energy is (3.2),

$$E = \int_V F(\mathbf{n})\,\mathrm{d}v \qquad (3.22)$$

Minimizing with respect to the polar coordinates ϕ and ψ the Euler-Lagrange equations are obtained,

$$\frac{\partial F}{\partial\phi} - \frac{\partial}{\partial x}\left(\frac{\partial F}{\partial\phi_{,x}}\right) - \frac{\partial}{\partial y}\left(\frac{\partial F}{\partial\phi_{,y}}\right) - \frac{\partial}{\partial z}\left(\frac{\partial F}{\partial\phi_{,z}}\right) = 0 \qquad (3.23)$$

$$\frac{\partial F}{\partial\psi} - \frac{\partial}{\partial x}\left(\frac{\partial F}{\partial\psi_{,x}}\right) - \frac{\partial}{\partial y}\left(\frac{\partial F}{\partial\psi_{,y}}\right) - \frac{\partial}{\partial z}\left(\frac{\partial F}{\partial\psi_{,z}}\right) = 0 \qquad (3.24)$$

Together with the relevant boundary conditions from the next section these equations (3.23) and (3.24) with (3.21) describe the system subsequently considered.

3.1.4 Boundary conditions

If the boundaries induce strong anchoring on the liquid crystal the aligning effect of the boundary is strong enough to fix the director on the boundary in one direction $\mathbf{n}_s$. This is equivalent to an infinite anchoring energy W. To minimize the energy integral the director must therefore be $\mathbf{n} = \mathbf{n}_s$ on the boundary. Since the director field on the surface is constant then from Appendix A the surface term F_{24} (A.18) is zero. The surface energy term achieves a minimum only when $\mathbf{n} = \mathbf{n}_s$ on the boundary.

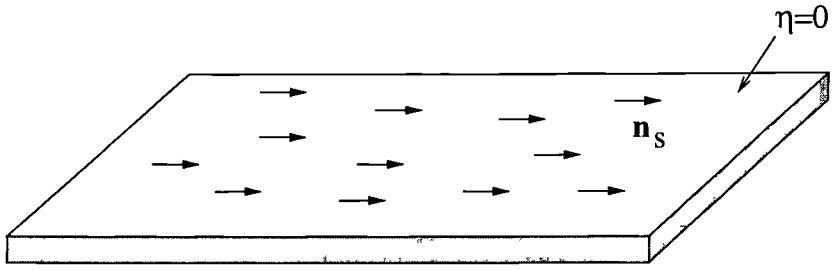

Homogeneous anchoring

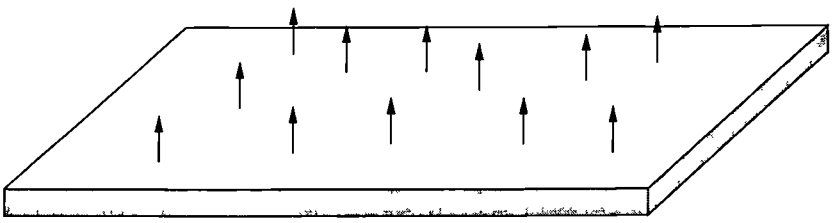

Homeotropic anchoring

Figure 3.2: Homogeneous and homeotropic anchoring on a surface $\eta(x,\ y,\ z) = 0$.

Strong homogeneous and homeotropic anchoring occur when the direction $\mathbf{n}_s$ is respectively parallel or perpendicular to the boundary (Figure 3.2) and the general form of these boundary conditions for a boundary described by the equation $\eta(x,\ y,\ z) = 0$ is,

$$\left.\begin{array}{rcll} \nabla\eta \cdot \mathbf{n_s} & = & 0 & \text{for homogeneous alignment} \\ \nabla\eta \wedge \mathbf{n_s} & = & 0 & \text{for homeotropic alignment} \end{array}\right\} \text{ on } \eta = 0 \qquad (3.25)$$

where $\nabla\eta$ is, by definition, normal to the surface. Three cases are now considered, planar, non-planar and planar with pre-tilt boundaries (Figure 3.3).

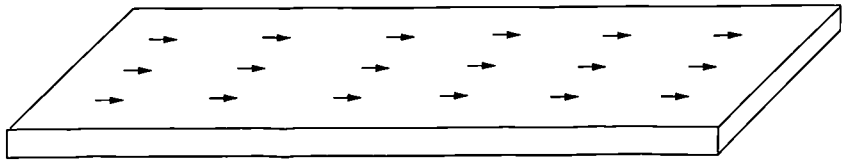

Plane Boundaries

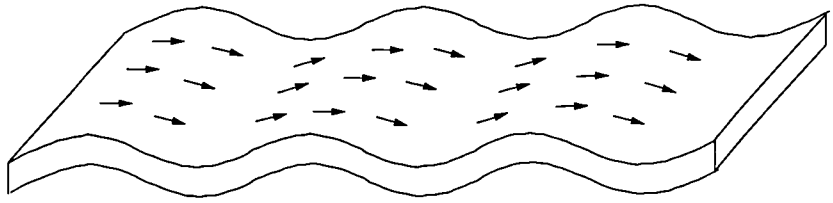

Sinusoidal Boundaries

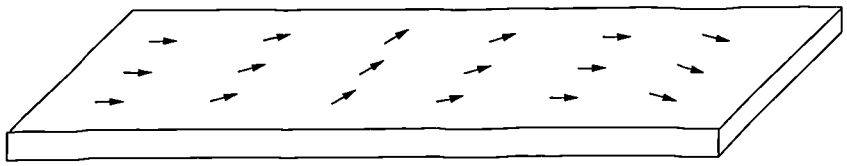

Pre Tilt Boundaries

Figure 3.3: Planar, non-planar and pre-tilt boundaries with homogeneous anchoring of a nematic sample.

Planar boundaries

Without loss of generality it may be assumed that the glass surface has been treated in such a way so that the director aligns with the x axis on the bound-

ary. The preferred direction is therefore $\mathbf{n}_s = (1,\ 0,\ 0)$ and the boundaries are $y = \pm L$ or $\eta = y \mp L$. The boundary conditions are therefore,

$$\left.\begin{array}{lll} \mathbf{n} = (1,\ 0,\ 0) & \text{for homogeneous alignment} \\ \mathbf{n} = (0,\ 1,\ 0) & \text{for homeotropic alignment} \end{array}\right\} \text{ on } y = \pm L \qquad (3.26)$$

For the director configuration, $\mathbf{n} = (\cos(\phi)\cos(\psi),\ \sin(\phi),\ \cos(\phi)\sin(\psi))$

$$\left.\begin{array}{lll} \phi = 0 \quad \psi = 0 & \text{for homogeneous alignment} \\ \phi = \pi/2 \quad \psi = 0 & \text{for homeotropic alignment} \end{array}\right\} \text{ on } y = \pm L \qquad (3.27)$$

In most situations plane boundaries have been successful in modelling liquid crystal cells and consequently they are used, almost without exception, in the investigation of liquid crystal phenomena. It will be shown that non-planar boundaries can cause a significant change in the behaviour of the cell.

Non-planar boundaries

Plane boundaries are used in modelling liquid crystal cells because the simple boundary conditions (3.27) imply the solution should have a shift symmetry $\phi(x) = \phi(x + \lambda)$ for *any* λ. In other words the solution will be independent of x and in most situations the governing equations reduce from partial to ordinary differential equations. The simplification of the system due to this shift symmetry does not occur in non-planar boundaries. Although it is impossible to have independence in x when considering non-planar boundaries a certain amount of symmetry can be retained. Therefore, boundaries that possess the shift symmetry $\phi(x) = \phi(x+\lambda)$ for a fixed λ will be considered. The boundary is therefore periodic with period λ. The obvious choice is sinusoidal boundaries of the form,

$$\begin{aligned} y &= L + A\cos(kx) \\ y &= -L + A\cos(kx + \epsilon) \end{aligned} \qquad (3.28)$$

The surface η is then,

$$\begin{aligned} \eta &= y - L - A\cos(kx) \\ \eta &= y + L - A\cos(kx + \epsilon) \end{aligned} \qquad (3.29)$$

The boundaries have wavenumber k, amplitude A, phase difference ϵ (not to be confused with the electric susceptibilities $\epsilon_{\|}$, $\epsilon_{\perp}$ and ϵ_a which will not appear in the rest of the thesis), mean position $\pm L$ and maximum slope Ak. The boundary conditions are then,

$$\left.\begin{aligned} \psi &= 0 \\ \tan\phi &= -Ak\sin(kx) \end{aligned}\right\} \text{on } y = L + A\cos(kx) \tag{3.30}$$

$$\left.\begin{aligned} \psi &= 0 \\ \tan\phi &= -Ak\sin(kx+\epsilon) \end{aligned}\right\} \text{on } y = -L + A\cos(kx+\epsilon) \tag{3.31}$$

for homogeneous boundary conditions and,

$$\left.\begin{aligned} \psi &= 0 \\ \tan\varphi &= Ak\sin(kx) \end{aligned}\right\} \text{on } y = L + A\cos(kx) \tag{3.32}$$

$$\left.\begin{aligned} \psi &= 0 \\ \tan\varphi &= Ak\sin(kx+\epsilon) \end{aligned}\right\} \text{on } y = -L + A\cos(kx+\epsilon) \tag{3.33}$$

for homeotropic boundary conditions, where $\varphi = \pi/2 - \phi$ is the angle from the director to the y axis. The sinusoidal boundaries in this situation are a perturbation of the plane boundaries and the director on the boundary is perturbed from (1, 0, 0) to $(1+\delta_1,\ \delta_2,\ 0)$ where δ_1 and δ_2 are small. Other authors [8, 83] have used sinusoidal boundaries to model the effect of surface treatment so that the director lies *along* the grooves in the direction (0, 0, 1). This is not the case here. In the present situation the surface is assumed to have been treated so that the director is forced to lie perpendicular to the grooves i.e. in the xy-plane.

Pre-tilt boundaries

Liquid crystal cells can be prepared by treating the surface so that the director is fixed in one direction at a *pre-tilt* angle to the boundary. The surface may in fact be treated so that the pre-tilt angle varies along the surface [57]. It is therefore possible to prepare a surface so that boundary is planar but the boundary condition is sinusoidal,

$$\left.\begin{aligned} \psi &= 0 \\ \tan\phi &= -Ak\sin(kx) \end{aligned}\right\} \text{on } y = L \tag{3.34}$$

$$\left.\begin{aligned} \psi &= 0 \\ \tan\phi &= -Ak\sin(kx+\epsilon) \end{aligned}\right\} \text{on } y=-L \tag{3.35}$$

When strong anchoring is subsequently considered it will be assumed to be homogeneous alignment on non-planar in-phase sinusoidal boundaries (3.30, 3.31 with $\epsilon = 0$). The case of out of phase boundaries is considered for the easier analytical situations (Section 3.2.3) and solutions for homeotropic alignment can be found by a simple transformation of the solution for the homogeneous case (Sections 3.2.2 and 4.1.2).

3.2 Linear zero field configuration

The main features of the different boundaries as well as the dependence of the solution on certain parameter orderings can be obtained from the simplest situation. This is the case when there are no external forces present and the director orientation within the liquid crystal is solely determined by minimisation of the distortion energy due to the sinusoidal boundaries. Strong anchoring at the surfaces is assumed so that the orienting effect of the boundaries, either homogeneous or homeotropic, ensure that the director away from the boundaries lies in the xy-plane. The azimuthal director angle is zero ($\psi = 0$), and the director is therefore,

$$\mathbf{n} = (\cos\phi,\ \sin\phi,\ 0) \tag{3.36}$$

The Euler-Lagrange equations (3.23) and (3.24) with (3.21) reduce to Laplace's equation,

$$\phi_{xx} + \phi_{yy} = 0 \tag{3.37}$$

Four different boundary types can now be considered, to illustrate the main features of the problem.

3.2.1 Homogeneous in-phase non-planar boundaries

When the boundaries are in-phase ($\epsilon = 0$) with homogeneous alignment the transformation that maps sinusoidal to planar boundaries is,

$$
\begin{aligned}
Y &= y - A\cos(kx) \\
X &= x
\end{aligned}
\tag{3.38}
$$

The governing equation (3.37) becomes,

$$
\begin{aligned}
\phi_{XX} + \phi_{YY}\left(1 + (Ak)^2\sin^2(kX)\right) + 2(Ak)\phi_{XY}\sin(kX) & \\
+(Ak)(k)\phi_Y\cos(kX) &= 0
\end{aligned}
\tag{3.39}
$$

Throughout, it will be assumed that the maximum slope of the boundaries, Ak, is small and therefore (3.39) to highest order of Ak is,

$$
\phi_{XX} + \phi_{YY} = 0 \tag{3.40}
$$

The homogeneous boundary conditions are transformed to,

$$
\tan\phi = -Ak\sin(kX) \qquad \text{on} \quad Y = \pm L \tag{3.41}
$$

This problem now has two solutions. The first solution is found using a nondimensionalisation $u = X/L$, $v = Y/L$ so that the changes in the director field occur over distances of the order of the gap width. This solution is,

$$
\phi_1 = -Ak\sin(Lku)\,\frac{\cosh(Lkv)}{\cosh(Lk)} \tag{3.42}
$$

The second solution is found using the nondimensionalisation $u = X/A$, $v = Y/A$ so that the changes in the director field occur over distances of the order of the boundary amplitude,

$$
\phi_2 = \begin{cases} 0 & \text{in the bulk} \\ -(Ak)e^{Ak(\pm v - L/A)}\sin(Aku) & \text{near } v = \pm L/A \end{cases} \tag{3.43}
$$

The main parameters are therefore Ak and Lk which determine the physical configuration of the liquid crystal cell. Two example orderings of these parameters are taken, which demonstrate each of the solutions ϕ_1 and ϕ_2,

$$
Ak \ll 1 \qquad Lk = O(1) \tag{3.44}
$$

$$
Ak \ll 1 \qquad Lk \gg 1/Ak \tag{3.45}
$$

Ordering (3.44) represents a sinusoidal boundary which has a maximum slope that is much less than one, the ratio of gap width $2L$ to the boundary wavelength $2\pi/k$ is of order one (Figure 3.4). Ordering (3.45) represents a boundary which has a maximum slope that is much less than one and the ratio of gap width to the boundary wavelength much greater than one (Figure 3.4).

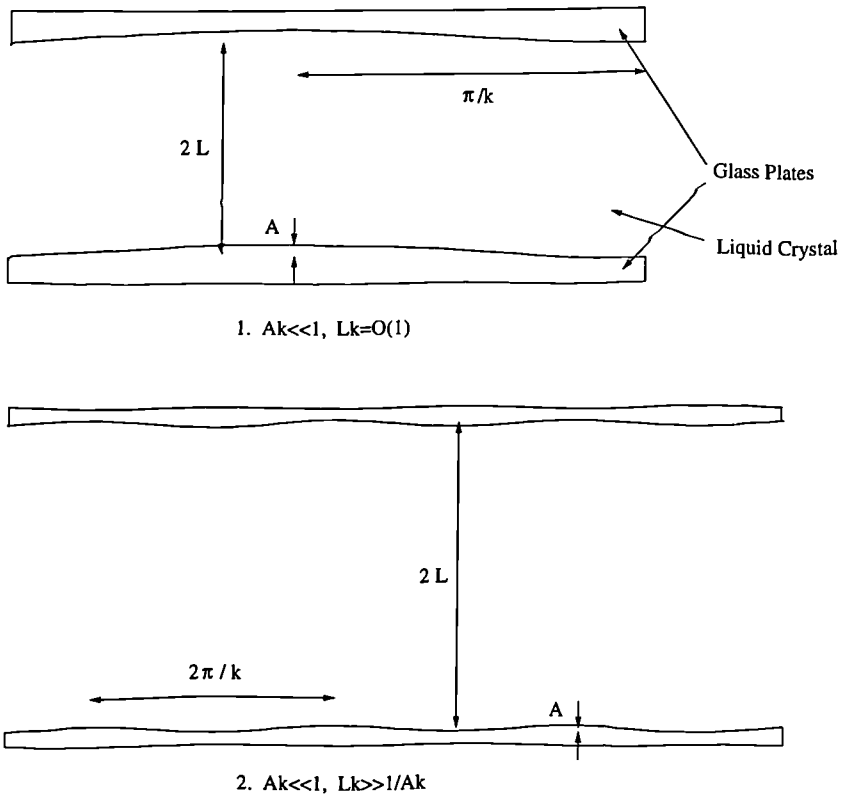

Figure 3.4: Two configurations for the non-planar cell. 1) When $Ak \ll 1$ and $Lk = O(1)$ and 2) When $Ak \ll 1$ and $Lk \gg 1/Ak$.

Many modern liquid crystal displays consist of large bounding plates sandwiching the liquid crystal substance. In large screen LCDs used for television and computer screens these plates can have dimensions of the order of metres whilst the gap width is around $10 - 100\mu$m. There is a risk that under high temperatures these plates will warp and the extremely small aspect ratio of the cell will exaggerate this warping. This situation can be modelled by sinusoidal boundaries described by the first set of parameters (3.44).
A cell that consists of a liquid crystal layer between boundaries that are diffraction gratings can be modelled by ordering (3.45). This cell has been used to

model the orienting effect of the bounding plates on the liquid crystal [83]. In that case the director is assumed to be almost parallel to the grooves of the grating. The present study will investigate the effect of having the director perpendicular to the grooves and consider how this affects the display characteristics.

The director configuration solutions for homogeneous alignment and in-phase boundaries for these two parameter orderings are therefore, (3.42) and (3.43) respectively.

3.2.2 Homeotropic in-phase non-planar boundaries

The above homogeneous boundary solutions can be transformed to give solutions for homeotropic boundary conditions (3.32) and (3.33). The angle $\varphi = \pi/2 - \phi$ satisfies the same governing equations as ϕ and consequently so does $-\varphi$. Then, since the homogeneous boundary conditions can be transformed to the homeotropic boundary conditions using $\phi \rightarrow -\varphi$ it is seen that if ϕ is a solution of the homogeneous problem then $\varphi = -\phi$ is a solution to the homeotropic problem.

3.2.3 Out of phase non-planar boundaries

If the boundaries are not in-phase and have a phase difference $\epsilon \neq 0$ a different transformation of the boundaries must be used. The mappings,

$$\begin{aligned} Y &= y - A\cos\left(kx + \frac{\epsilon}{2}(1 - Y/L)\right) \\ X &= x \end{aligned} \tag{3.46}$$

transform out of phase sinusoidal boundaries in the xy-plane to flat boundaries in the $X - Y$ plane and transform (3.37) to,

$$\begin{aligned} 0 = {} & \phi_{XX} + \left(\frac{1 + A^2k^2\sin^2\Theta}{\Gamma^2}\right)\phi_{YY} + \left(\frac{2Ak\sin\Theta}{\Gamma}\right)\phi_{XY} \\ & \left[\left(Ak^2 + \frac{\epsilon^2 A}{4L^2}\right)\frac{\cos\Theta}{\Gamma^3}\right]\phi_Y \end{aligned} \tag{3.47}$$

where,

$$\Theta = kX + \frac{\epsilon}{2}\left(1 - \frac{Y}{L}\right) \tag{3.48}$$

$$\Gamma = 1 + \frac{A\epsilon}{2L}\sin\Theta \tag{3.49}$$

and the homogeneous boundary conditions are,

$$\tan\phi = \begin{cases} -Ak\sin(kX) & \text{on } Y = L \\ -Ak\sin(kX+\epsilon) & \text{on } Y = -L \end{cases} \tag{3.50}$$

With the first set of parameter orderings, $Ak \ll 1$ and $Lk = O(1)$ and the nondimensionalisation $u = X/L$, $v = Y/L$ the leading order terms of equation (3.47) form Laplace's equation,

$$\phi_{uu} + \phi_{vv} = 0 \tag{3.51}$$

since ϵ is at most order 1. The linearised boundary conditions are,

$$\phi = \begin{cases} -Ak\sin(Lku) & \text{on } v = 1 \\ -Ak\sin(Lku+\epsilon) & \text{on } v = -1 \end{cases} \tag{3.52}$$

To fit the boundary conditions (3.52) solutions of (3.51) are considered to be of the form,

$$\phi = -Ak\, f(v)\, \sin(Lku + g(v)) \tag{3.53}$$

with boundary conditions,

$$f(\pm 1) = 1 \tag{3.54}$$

$$g(1) = 0$$

$$g(-1) = \epsilon \tag{3.55}$$

Substituting (3.53) into (3.51) gives,

$$f'' - (Lk)^2 f - f\,(g')^2 = 0 \tag{3.56}$$

$$2f'\,g' + f\,g'' = 0 \tag{3.57}$$

These equations can be solved with the boundary conditions (3.54). Equation (3.57) can be written as,

$$\left(f^2 g'\right)' = 0 \tag{3.58}$$

and therefore,

$$g' = B/f^2 \tag{3.59}$$

where B is a constant. Substituting g' into (3.56) leads to,

$$f'' f^3 - (Lk)^2 f^4 - B^2 = 0 \tag{3.60}$$

The order of this equation can be reduced by the substitution $p = f'$ to give,

$$p\frac{\mathrm{d}p}{\mathrm{d}f} f^3 - (Lk)^2 f^4 - c_1^2 = 0 \tag{3.61}$$

the solution of is of the form [43],

$$f^2 = a + b\cosh(2Lkv) \tag{3.62}$$

When (3.62) is substituted into (3.59) the solution for g is,

$$g = \begin{cases} \frac{1}{2}\arcsin\left(\frac{b+a\cosh(2Lkv)}{a+b\cosh(2Lkv)}\right) + \frac{1}{2}\left(\epsilon - \frac{\pi}{2}\right) & \text{for } v \geq 0 \\ -\frac{1}{2}\arcsin\left(\frac{b+a\cosh(2Lkv)}{a+b\cosh(2Lkv)}\right) + \frac{1}{2}\left(\epsilon + \frac{\pi}{2}\right) & \text{for } v < 0 \end{cases} \tag{3.63}$$

where a and b are found using the boundary conditions,

$$a = \frac{(\cos(\epsilon)\cosh(2Lk) - 1)}{\cosh^2(2Lk) - 1} \tag{3.64}$$

$$b = \frac{(\cosh(2Lk) - \cos(\epsilon))}{\cosh^2(2Lk) - 1} \tag{3.65}$$

and $B = Lk(b^2 - a^2)^{1/2}$. The solution given by (3.62) and (3.63) relaxes from the boundaries towards the centre of the cell, is statically stable and by substituting $\epsilon = 0$ the in-phase solution (3.42) is recovered.

For the second set of parameter orderings (3.45) and the nondimensionalisation $u = X/A$ and $v = Y/A$ the only change from in-phase to out of phase boundaries is in the lower boundary layer and the solution is,

$$\phi = \begin{cases} 0 & \text{in the bulk} \\ -(Ak)e^{Ak(v-L/A)}\sin(Aku) & \text{near } v = L/A \\ -(Ak)e^{Ak(-v-L/A)}\sin(Aku+\epsilon) & \text{near } v = -L/A \end{cases} \tag{3.66}$$

The bulk of the cell is therefore identical for any phase difference ϵ. The solution for homeotropic boundary conditions is again derived from the homogeneous boundary condition solution.

3.2.4 Pre-tilt boundaries

For this case the boundaries are planar and no transformations are necessary. The governing equation is therefore,

$$\phi_{xx} + \phi_{yy} = 0 \tag{3.67}$$

and the homogeneous boundary conditions are,

$$\begin{aligned} \tan\phi = &\quad -Ak\sin(kx) \quad \text{on } y = L \\ \tan\phi = &\quad -Ak\sin(kx+\epsilon) \quad \text{on } y = -L \end{aligned} \tag{3.68}$$

The similarity of these equations to the linearised non-planar equations leads to an equivalence of the solutions for the two cases. The significant difference between the non-planar and pre-tilt cases arises when higher orders of Ak are considered. The governing equation in the non-planar boundary case is nonlinear whereas the governing equation in the pre-tilt boundary case is linear (and is equation (3.67)).

3.3 Summary

In this chapter the governing equations for the director field in a LCD exhibiting the Freedericksz transition have been formulated and the solution for a simplified case has been found. In Section 3.1 the contributions to the free

energy from director deformations, electric fields, magnetic fields and surface energy terms were considered in turn. The governing equations were then derived from the minimization of the total free energy of the system. When strong anchoring is assumed the boundary conditions for the director field were then found for two new types of surface, the non-planar sinusoidal and the pre-tilt sinusoidal boundaries. In Section 3.2 a solution was found for the linearised system with no external forces (electric or magnetic fields) present. For the non-planar boundaries there are essentially two configurations of interest, corresponding to two orderings of the parameters Ak and Lk and homogeneous in-phase, homeotropic in-phase and homogeneous out of phase boundaries were all considered for each ordering. For pre-tilt boundaries the governing equations are equivalent to the linearised governing equations of the non-planar boundaries and consequently the solution is equivalent.

In the next chapter a magnetic field is introduced to the system and the Freedericksz effect is investigated. The linearised equations are considered for three configurations that exhibit a Freedericksz transition and the critical field is found in each case. A weakly nonlinear analysis is then carried out using the homogeneous in-phase non-planar boundaries with the parameter ordering, $Ak \ll 1$ and $Lk = O(1)$ and a second transition is found at a higher field strength.

Chapter 4

Critical Field Strength

In this chapter the linear and nonlinear effects of applying a magnetic field to a liquid crystal layer are considered. In Section 4.1 the linearised non-planar equations are used to investigate three distinct cell configurations (the pre-tilt case is equivalent to the linearised non-planar case and therefore will not be considered at this point) and find the critical field strength for the Freedericksz effect in each configuration. In Section 4.2 a weakly nonlinear analysis is carried out to investigate higher order terms for a specific configuration.
As described in the Chapter 1, when a field is applied to a liquid crystal cell the Freedericksz effect will not occur unless there is a competition between the aligning effect of the boundaries and the aligning effect of the field. Hence there are three distinct configurations of this problem [18] (Figure 4.1).

1. $\mathbf{H} = (0, H, 0)$ with homogeneous alignment
2. $\mathbf{H} = (H, 0, 0)$ with homeotropic alignment
3. $\mathbf{H} = (0, 0, H)$ with homogeneous alignment

For plane cells these configurations mainly involve splay, bend and twist distortions respectively and can be used to measure experimentally the elastic constants K_1, K_2 and K_3. In non-planar cells splay and bend are introduced by the boundaries and therefore the three configurations involve splay/bend, splay/bend/twist and splay/bend respectively.
Equations (3.23) and (3.24) with (3.21), together with the appropriate boundary conditions, can now be used for each of the above configurations.

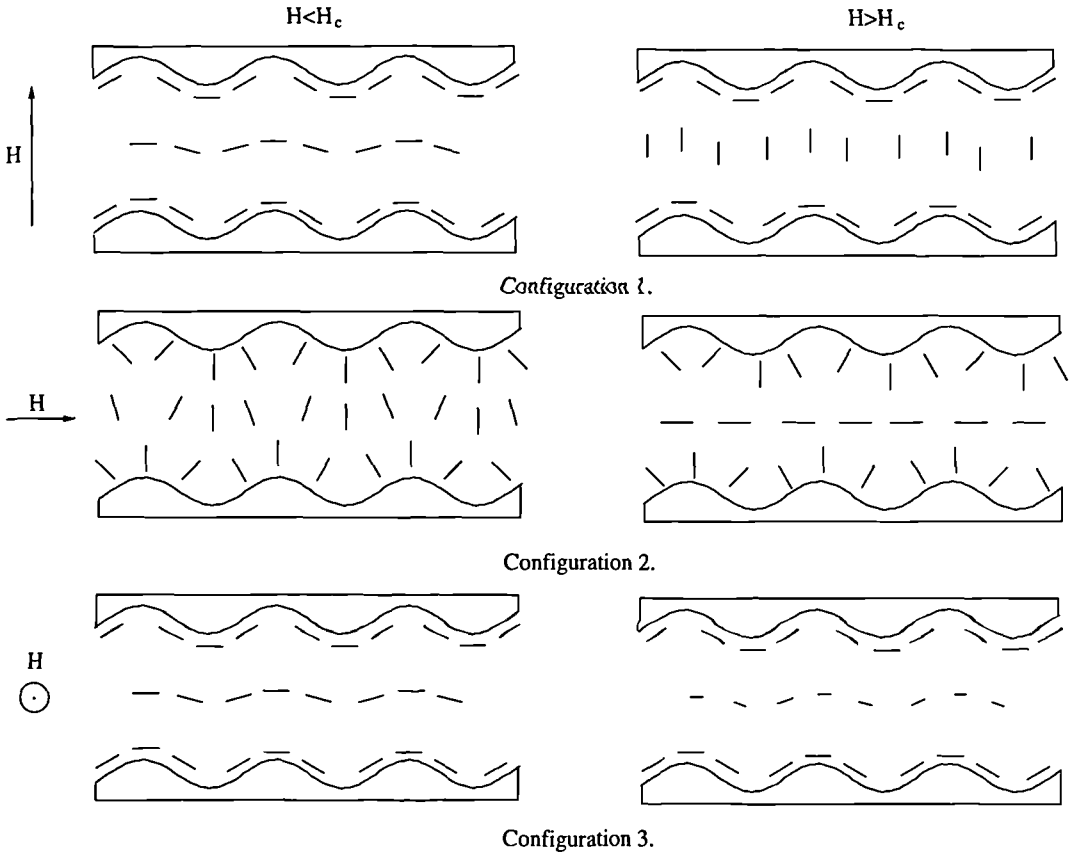

Figure 4.1: Three cell configurations displaying the Freedericksz effect.

4.1 Linear Analysis

4.1.1 Configuration 1

The magnetic field is $\mathbf{H} = (0, H, 0)$. Since the forces on the director have no component in the z direction so that the director lies in the xy-plane and $\mathbf{n} = (\cos\phi(x,y), \sin\phi(x,y), 0)$. Hence (3.23) and (3.24) with (3.21) gives,

$$\phi_{xx} + \phi_{yy} + \frac{\chi_a H^2}{2K}\sin(2\phi) = 0 \tag{4.1}$$

in $-L + A\cos(kx+\mu) < y < L + A\cos(kx)$ with boundary conditions (3.30), (3.31).

This equation is the *elliptic sine-Gordon equation.* The sine-Gordon equation,

$$u_{tt} - \nabla^2 u + \sin u = 0 \tag{4.2}$$

has occurred in many different systems in condensed matter theory. It has been found to be a model for dislocations in crystals [37], flux quanta in Josephson transmission lines [71] and as a model of vortices in superfluid ^{3}He [70]. Both the elliptic sine-Gordon and the sine-Gordon equations have consequently been investigated extensively [13, 14, 25, 47, 67, 81, 82]. The elliptic sine-Gordon equation can be obtained from the sine-Gordon equation either by the transform $t \to iy$ when $\nabla^2 = \partial^2/\partial x^2$ or by considering static solutions when $\nabla^2 = \partial^2/\partial x^2 + \partial^2/\partial y^2$. Since (4.2) exhibits soliton solutions then (4.1) exhibits static soliton solutions. These solitons have been observed in liquid crystal layers with planar boundaries in the form of Helfrich walls (kink solitons) and the director field of a disclination in a field (planar solitons) [55]. For in-phase boundaries and using the transformations (3.38) with the nondimensionalisation $u = X/L$, $v = Y/L$ the governing equation (4.1) is,

$$\begin{aligned}\phi_{uu} + \phi_{vv}\left(1 + (Ak)^2\sin^2(Lku)\right) + 2(Ak)\phi_{uv}\sin(Lku) \\ +(Ak)(Lk)\phi_v\cos(Lku) + \frac{\chi_a H^2 L^2}{2K}\sin(2\phi) \;=\; 0\end{aligned} \tag{4.3}$$

The magnetic field has introduced the parameter $\gamma = \chi_a H^2 L^2/K$ into the governing equation. This parameter is assumed to be of the correct order

to ensure that the field term and the elastic term in (4.3) are comparable. This requires that $\frac{\chi_a H^2 L^2}{2K} \sin(2\phi) = O(\phi_{uu}, \phi_{vv})$ and therefore subsequently the magnetic field parameter γ is assumed to be order one. This region of parameter space includes the classical Freedericksz transition point.
Taking the first set of parameter orderings (3.44) and $\gamma = O(1)$ with only the leading order terms, and equation 4.3 becomes,

$$\phi_{uu} + \phi_{vv} + \frac{\chi_a H^2 L^2}{K}\phi = 0 \tag{4.4}$$

in $-1 < v < 1$ with the boundary conditions (3.41). This leads to the solution,

$$\phi = -Ak \sin(Lku) \frac{\cosh(Lk'v)}{\cosh(Lk')} \tag{4.5}$$

where,

$$Lk' = \sqrt{(Lk)^2 - \frac{\chi_a H^2 L^2}{K}} \tag{4.6}$$

If a magnetic field was applied to the liquid crystal material that had a diamagnetic susceptibility $\chi_a = 0$, the resultant torque on any molecule would be zero and consequently the application of a magnetic field would cause no change to the director configuration. There are therefore two cases of interest, $\chi_a < 0$, or $\chi_a > 0$. The first case implies the major polar axis is the minor molecular axis so that the director aligns perpendicular to the field. The assumption that $Ak \ll 1$ and therefore $\phi \ll 1$ when $H = 0$ has been used. This means there is very little conflict between the field and the polar nature of the molecules. There will not be a Freedericksz effect and the director will simply tend towards $\mathbf{n} = (1, 0, 0)$. The second case, $\chi_a > 0$, implies the major polar axis is the major molecular axis so that the director aligns parallel to the field. In this case a perturbed Freedericksz transition occurs. There is always distortion present in the cell and therefore the initial director configuration is not perpendicular to the field. There is a smooth change from alignment with the boundary to alignment with the field.
As H increases k' becomes zero and then imaginary. The solution (4.5) changes from having a hyperbolic to a sinusoidal v dependence and the solution (4.5) has singularities when,

$$\cosh(Lk') = 0 \tag{4.7}$$

This occurs when,

$$H^2 = H_c^2 = \frac{K}{\chi_a}\left(\frac{(2m-1)^2\pi^2}{4L^2} + k^2\right) \tag{4.8}$$

where m is an integer ($m = 0,\ \pm 1,\ \pm 2\ldots$). The first singularity occurs for $m = 1$ at,

$$H_c^2 = \frac{K}{\chi_a}\left(\frac{\pi^2}{4L^2} + k^2\right) \tag{4.9}$$

Subsequent critical values are outside the parameter space region $\gamma = O(1)$ which is being considered (e.g. $\gamma\,|_{m=2} \approx 9\gamma\,|_{m=1}$). When $k = 0$ the boundaries are flat and the primary critical field becomes,

$$H_c = \frac{\pi}{2L}\sqrt{\frac{K}{\chi_a}} \tag{4.10}$$

which is the classic solution for planar boundaries [18].
Using similar analysis to Section 3.2.1, the second set of parameter orderings, $Ak \ll 1$ and $Lk \gg 1/Ak$, with equation (4.3) leads to the solution,

$$\phi = \begin{cases} 0 & \text{in the bulk} \\ -(Ak)e^{Ak'(\pm v - L/A)}\sin(Aku) & \text{near } v = \pm L/A \end{cases} \tag{4.11}$$

If $\chi_a < 0$ then as H increases k' increases and the boundary layer becomes smaller. In this case there is no Freedericksz transition since the direction of the field does not conflict with the direction of the major polar axis of the molecules. If $\chi_a > 0$ there is a conflict and since the bulk of the liquid crystal is identically oriented as a plane bounded liquid crystal cell it consequently undergoes the Freedericksz transition bifurcation in the same way as a planar cell at the classical field strength (4.10).

4.1.2 Configuration 2

The magnetic field is $\mathbf{H} = (H, 0, 0)$ and the director again lies in the xy-plane so that $\mathbf{n} = (\sin\varphi(x,y),\ \cos\varphi(x,y),\ 0)$. Using the same transformations and nondimensionalisation as Section 4.1.1 and the first set of parameter orderings (3.44) then to leading order (3.23) and (3.24) with (3.21) is,

$$\varphi_{uu} + \varphi_{vv} + \frac{\chi_a H^2 L^2}{K}\varphi = 0 \tag{4.12}$$

in $-1 < v < 1$ with the boundary conditions (3.32).
As for the zero field case the analysis of the homogeneous alignment can be repeated and the solution is $\varphi(u,v) = -\phi(u,v)$ where ϕ is the solution given by (4.5). The critical field is therefore (4.9). Using the second set of parameter orderings (3.45) and a similar analysis to the zero field case it can been seen that the solution is,

$$\varphi = \begin{cases} 0 & \text{in the bulk} \\ (Ak)e^{Ak'(\pm v - L/A)} \sin(Aku) & \text{near } v = \pm L/A \end{cases} \tag{4.13}$$

As with the homogeneously aligned Configuration 1 the bulk of the liquid crystal is oriented like a plane boundary cell and therefore there is a bifurcation at the critical field strength for the Freedericksz transition in a planar cell (4.10).

4.1.3 Configuration 3

The magnetic field is $\mathbf{H} = (0, 0, H)$ and,

$$\mathbf{n} = (\cos\psi(x,y)\cos\phi(x,y),\ \sin\phi,\ \sin\psi\cos\phi) \tag{4.14}$$

Using the same transformations and nondimensionalisation as Section 4.1.2 and the first set of parameter orderings (3.44) then to leading order (3.23) and (3.24) with (3.21) become,

$$\nabla^2\phi - \frac{\nabla^2\cos\psi}{\cos\psi}\phi = 0 \tag{4.15}$$

$$\nabla^2\psi + \frac{\chi_a H^2 L^2}{2K}\sin 2\psi = 0 \tag{4.16}$$

where $\nabla^2 = \frac{\partial^2}{\partial u^2} + \frac{\partial^2}{\partial v^2}$. The boundary conditions are,

$$\begin{aligned} \phi &= -Ak\sin(Lku) \quad \text{on} \quad v = \pm 1 \\ \psi &= 0 \qquad\qquad\ \ \text{on} \quad v = \pm 1 \end{aligned} \tag{4.17}$$

If $\chi_a \leq 0$ then the trivial solution $\psi = 0$ is always statically stable since the force due to the field on the director is in the xy-plane and therefore χ_a is taken to be positive. Linearisation of (4.15) gives,

$$\nabla^2\phi = 0 \tag{4.18}$$

$$\nabla^2\psi + \frac{\chi_a H^2 L^2}{K}\psi = 0 \tag{4.19}$$

with the boundary conditions (4.17). If ψ has a sinusoidal nature in the x direction, as a result of the boundaries, then $\psi(u,v) = \Psi(v)\sin Lku$ and using a similar analysis as before (Section 4.1) (4.18) leads to the critical field strength,

$$H^2 = \frac{K}{\chi_a}\left(\frac{\pi^2}{4L^2} + k^2\right) \tag{4.20}$$

Therefore (4.9) is again the critical field strength. An alternative analysis used in de Gennes and Prost, pg. 90 [24] to consider planar boundaries may be used for non-planar boundaries to obtain the same result. As with the previous configurations (1, 2), the second set of parameter orderings leads to a situation that is similar to the plane boundary liquid crystal cell. The sinusoidal boundaries have negligible effect in the bulk and there is a bifurcation at the classical field strength (4.10).

In this *twisting* configuration it is possible to investigate the dynamics of the Freedericksz transition as the magnetic field is switched from zero to the critical value H_c. The details of this analysis are presented in Appendix B but the main result is that the time taken for the director field to undergo the transition from low amplitude distortion to high amplitude distortion is *greater* than for a liquid crystal layer with plane boundaries.

4.2 Weakly nonlinear analysis

The effects of higher order terms on the linear solution obtained in Section 4.1 will now be considered. Since a solution for homogeneous boundaries can be transformed to a solution for homeotropic boundary conditions (Chapter 3) the only configuration to be considered is a liquid crystal cell with homogeneous boundary conditions (3.30) and (3.31) which, for ease of the analysis, are assumed to be in-phase. The parameter ordering that models a diffraction grating leads to a classical Freedericksz transition and so will not be considered. The parameter ordering, $Ak \ll 1$ and $Lk = O(1)$, which models a warped liquid crystal cell will be used. The order Ak solution of Section 3.1.3 is used as the leading order term in an expansion using Ak as the small parameter. Using the transformations (3.38) and the nondimensionalisation $u = X/L$, $v = Y/L$ the governing equation becomes,

$$\begin{aligned} \phi_{uu} + \phi_{vv}\left(1 + (Ak)^2 \sin^2(Lku)\right) + 2(Ak)\phi_{uv}\sin(Lku) & \\ +(Ak)(Lk)\phi_v \cos(Lku) + \gamma \sin(2\phi) &= 0 \end{aligned} \tag{4.21}$$

where, $\gamma = \frac{\chi_a H^2 L^2}{K}$. The order of γ determines for what range of field strengths the perturbation series solution is valid. Since the Freedericksz transition is to be considered γ is assumed to be of an order that includes the transition field strength. At transition $\gamma = (\pi^2/4) + (Lk)^2$ and so γ is taken as order 1. The form of the expansion series is crucial and a clue to its nature can be found from the boundary conditions (3.41),

$$\tan\phi = -Ak\sin(Lku) \qquad \text{on} \quad v = \pm 1 \tag{4.22}$$

or,

$$\phi = -\arctan(Ak\sin(Lku)) \qquad \text{on} \quad v = \pm 1 \tag{4.23}$$

Using the series expansion for arctan [1] results in,

$$\phi = \left(-Ak + \frac{(Ak)^3}{4} - \frac{(Ak)^5}{8} + \ldots\right)\sin(Lku)$$

$$+\left(-\frac{(Ak)^3}{12}+\frac{(Ak)^5}{16}+\ldots\right)\sin(3Lku) \qquad (4.24)$$
$$+\left(-\frac{(Ak)^5}{80}+\ldots\right)\sin(5Lku)$$
$$+\ldots \qquad \text{on} \quad v=\pm 1$$

This suggests the need for inclusion of terms with wavenumbers different from the boundaries. Since the liquid crystal tends to reduce the distortional energy by relaxing the director angle away from the boundary it can be assumed that the order of the term with wavenumber nLk is equal to the order of that term at the boundary. This means that since the $\sin(2nLku)$ term has order $(Ak)^{2n}$ at the boundary then it will have order $(Ak)^{2n}$ in the bulk. As well as those suggested by the boundary conditions all terms that have a sinusoidal u dependence with wavenumber $(2n+1)Lk$ and terms that have a $\cos(nLku)$ dependence are included. The whole expansion series is therefore,

$$\phi = \sum_{n=1}^{\infty}\left(\left(\sum_{m=n}^{\infty}(Ak)^m\ S_m^n(v)\right)\sin(nLku) + \left(\sum_{m=n}^{\infty}(Ak)^m\ C_m^n(v)\right)\cos(nLku)\right) \qquad (4.25)$$

The set $\{\{\sin(nLku)\},\ \{\cos(nLku)\}\}$ is orthogonal and hence coefficients of $\sin(nLku)$ and $\cos(nLku)$ can be equated after (4.25) is substituted into (4.21). If then the orders of Ak are equated, a series of nonlinear ordinary differential equations is obtained. The equations involving C_m^n have the solution $C_m^n = 0\ \forall m,\ n$. The set of differential equations, up to $O((Ak)^3)$, reduces to,

$$\frac{\mathrm{d}^2}{\mathrm{d}v^2}S_1^1+\left(\gamma-(Lk)^2\right)S_1^1=0 \qquad (4.26)$$

$$\frac{\mathrm{d}^2}{\mathrm{d}v^2}S_2^2+\left(\gamma-4(Lk)^2\right)S_2^2=-\frac{3}{2}(Lk)(Ak)\frac{\mathrm{d}}{\mathrm{d}v}S_1^1 \qquad (4.27)$$

$$\frac{\mathrm{d}^2}{\mathrm{d}v^2}S_3^3+\left(\gamma-9(Lk)^2\right)S_3^3 = \frac{1}{4}(Ak)^2\frac{\mathrm{d}^2}{\mathrm{d}v^2}S_1^1-2(Lk)(Ak)\frac{\mathrm{d}}{\mathrm{d}v}S_2^2-\frac{\gamma}{6}\left(S_1^1\right)^3 \qquad (4.28)$$

$$\frac{\mathrm{d}^2}{\mathrm{d}v^2}S_3^1 + \left(\gamma - (Lk)^2\right) S_3^1 \;=\; -\frac{3}{4}(Ak)^2\frac{\mathrm{d}^2}{\mathrm{d}v^2}S_1^1 + 2(Lk)(Ak)\frac{\mathrm{d}}{\mathrm{d}v}S_2^2 + \frac{\gamma}{6}\left(S_1^1\right)^3 \tag{4.29}$$

which are subject to the boundary conditions (4.24) or,

$$\left.\begin{array}{rcl} S_1^1 &=& -Ak \\ S_2^2 &=& 0 \\ S_3^3 &=& -\frac{(Ak)^3}{12} \\ S_3^1 &=& \frac{(Ak)^3}{4} \end{array}\right\} \text{ on } v = \pm 1 \tag{4.30}$$

The solutions of which are,

$$S_1^1 = -Ak\frac{\cosh\sqrt{((Lk)^2-\gamma)}v}{\cosh\sqrt{((Lk)^2-\gamma)}} \tag{4.31}$$

$$\begin{aligned} S_2^2 \;=\; & \frac{1}{2}\frac{(Ak)^2}{Lk}\sqrt{((Lk)^2-\gamma)}\tanh\sqrt{(((Lk)^2-\gamma))}. \\ & \cdot\left(\frac{\sinh\sqrt{(4(Lk)^2-\gamma)}\,v}{\sinh\sqrt{(4(Lk)^2-\gamma)}} - \frac{\sinh\sqrt{((Lk)^2-\gamma)}\,v}{\sinh\sqrt{((Lk)^2-\gamma)}}\right) \end{aligned} \tag{4.32}$$

$$\begin{aligned} S_3^3 \;=\; & \sigma_1\cosh\sqrt{(9(Lk)^2-\gamma)}v + \sigma_2\cosh\sqrt{((Lk)^2-\gamma)}v \\ & +\sigma_3\cosh\sqrt{(4(Lk)^2-\gamma)}v + \sigma_4\cosh 3\sqrt{((Lk)^2-\gamma)}v \end{aligned} \tag{4.33}$$

$$\begin{aligned} S_3^1 \;=\; & \rho_1\, v\, \sinh\sqrt{(9(Lk)^2-\gamma)}v + \rho_2\cosh\sqrt{((Lk)^2-\gamma)}v \\ & +\rho_3\cosh\sqrt{(4(Lk)^2-\gamma)}v + \rho_4\cosh 3\sqrt{((Lk)^2-\gamma)}v \end{aligned} \tag{4.34}$$

where,

$$\begin{aligned} \sigma_1 \;=\; & -\left(\frac{(Ak)^2}{12} + \sigma_2\cosh\sqrt{((Lk)^2-\gamma)} + \sigma_3\cosh\sqrt{(4(Lk)^2-\gamma)}\right. \\ & \left. + \sigma_4\cosh 3\sqrt{((Lk)^2-\gamma)}\right)\left(\cosh 9\sqrt{((Lk)^2-\gamma)}\right)^{-1} \end{aligned} \tag{4.35}$$

$$\sigma_2 = \frac{(Ak)^3}{96(Lk)^2}\left(\frac{18\left((Lk)^2-\gamma\right)}{\cosh\sqrt{\left((Lk)^2-\gamma\right)}} - \gamma\frac{1}{\cosh^3\left(\sqrt{\left((Lk)^2-\gamma\right)}\right)}\right) \tag{4.36}$$

$$\sigma_3 = \frac{(Ak)^3}{4(Lk)^2}\sqrt{\left((Lk)^2-\gamma\right)}\sqrt{\left(4(Lk)^2-\gamma\right)}\frac{\tanh\sqrt{\left((Lk)^2-\gamma\right)}}{\sinh\sqrt{\left(4(Lk)^2-\gamma\right)}} \tag{4.37}$$

$$\sigma_4 = -\frac{(Ak)^3}{192\cosh^3\left(\sqrt{\left((Lk)^2-\gamma\right)}\right)} \tag{4.38}$$

$$\rho_1 = \left(\frac{\sqrt{\left((Lk)^2-\gamma\right)}}{\cosh\sqrt{\left((Lk)^2-\gamma\right)}} + \frac{3\gamma}{16\sqrt{\left((Lk)^2-\gamma\right)}\cosh^3\left(\sqrt{\left((Lk)^2-\gamma\right)}\right)}\right) \tag{4.39}$$

$$\rho_2 = -\left(\frac{(Ak)^3}{4} - \rho_1\sinh\sqrt{\left((Lk)^2-\gamma\right)} - \rho_3\cosh\sqrt{\left(4(Lk)^2-\gamma\right)} + \rho_1\cosh 3\sqrt{\left((Lk)^2-\gamma\right)}\right)\left(\cosh\sqrt{\left((Lk)^2-\gamma\right)}\right)^{-1} \tag{4.40}$$

$$\rho_3 = \frac{5(Ak)^3}{12(Lk)^2}\sqrt{\left((Lk)^2-\gamma\right)}\sqrt{\left(4(Lk)^2-\gamma\right)}\frac{\tanh\sqrt{\left((Lk)^2-\gamma\right)}}{\sinh\sqrt{\left(4(Lk)^2-\gamma\right)}} \tag{4.41}$$

$$\rho_4 = -\frac{\gamma(Ak)^3}{16\left((Lk)^2-\gamma\right)\cosh^3\left(\sqrt{\left((Lk)^2-\gamma\right)}\right)} \tag{4.42}$$

The first order solution (4.31) is the same as the solution (4.5) and it is clear from the above equations that S_{2n+1}^{2n+1} has singularities at critical field strengths which satisfy the equation,

$$\cosh\sqrt{(2n-1)^2\left((Lk)^2-\gamma\right)} = 0 \tag{4.43}$$

and S_{2n}^{2n} has singularities when,

$$\sinh\sqrt{(2n)^2\left((Lk)^2-\gamma\right)} = 0 \tag{4.44}$$

except when $(2n)^2(Lk)^2 - \gamma = 0$. All these singularities occur at values greater or equal to the critical field strength found in Section 4.1.1 (4.9). These field strengths are,

$$H^2 = \frac{K}{\chi_a}\left[\frac{(2m-1)^2\pi^2}{4L^2} + (2n-1)^2k^2\right] \qquad m,n = 1,2,3\ldots \tag{4.45}$$

and,

$$H^2 = \frac{K}{\chi_a}\left[\frac{(m^2\pi^2}{L^2} + (2n)^2k^2\right] \qquad m,n = 1,2,3\ldots \tag{4.46}$$

If the singularities for S_3^1 are consider it is found that the ρ_4 term (4.42) has a singularity at,

$$\gamma = (Lk)^2 \tag{4.47}$$

There are similar singularities occurring in higher order terms when the equation for S_j^i includes a sinusoidal forcing term that has a different wavenumber to the natural wavenumber prescribed by the left hand side of the equation. In the S_3^1 case the forcing wavenumber is $3\sqrt{((Lk)^2 - \gamma)}$ and the natural wavenumber is $\sqrt{((Lk)^2 - \gamma)}$. This singularity (4.47) occurs before the first singularity in Section 4.1.1 and possibly (depending on the magnitude of Lk) before the classical plane boundary Freedericksz transition field strength.
This would therefore suggest a limit on the perturbation expansion. The lowest order term which contains such a singularity is of order $(Ak)^3$ and to discount this it must be true that $(Ak)^3 \ll Ak$ or,

$$(Ak)^2 \ll 1 \tag{4.48}$$

This gives us some idea as to how large Ak can be before the perturbation expansion is unsatisfactory. Therefore assuming that all terms of order $(Ak)^3$ and smaller are negligible compared to the first two terms the expansion series solution is,

$$\begin{aligned}\phi \;=\; & -Ak\frac{\cosh\sqrt{((Lk)^2-\gamma)}v}{\cosh\sqrt{((Lk)^2-\gamma)}}\sin(Lku) \\ & + \frac{1}{2}\frac{(Ak)^2}{Lk}\sqrt{((Lk)^2-\gamma)}\tanh\sqrt{(((Lk)^2-\gamma))}\ \cdot \\ & \cdot\left(\frac{\sinh\sqrt{(4(Lk)^2-\gamma)}\,v}{\sinh\sqrt{(4(Lk)^2-\gamma)}} - \frac{\sinh\sqrt{((Lk)^2-\gamma)}\,v}{\sinh\sqrt{((Lk)^2-\gamma)}}\right)\sin(2Lku)\end{aligned} \tag{4.49}$$

which is shown in Figure 4.2.

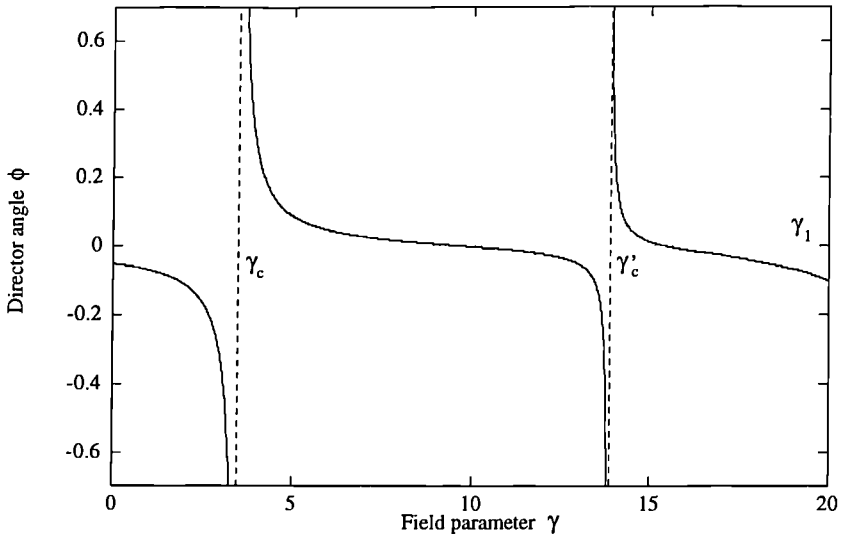

Figure 4.2: Weakly nonlinear solution showing the singularities at γ_c and γ_c' of the director angle (at the point $(\pi/8,\ 0.5)$) versus the field strength parameter γ using the parameters $Ak = 0.1$ and $Lk = 1$.

The assumptions used in deriving this solution were,

1. Configuration parameter orderings, $Ak \ll 1$, $Lk = O(1)$
2. Director angle magnitude, $\phi = O(Ak)$
3. Field parameter ordering, $\gamma = O(1)$

These conditions determine where in parameter space the solution is valid. In Figure 4.2 it can be seen that under the third condition the solution is only valid for $\gamma < \gamma_1$ so that (4.49) contains only two valid singularities at,

$$\gamma_c = \frac{\pi^2}{4} + (Lk)^2 \tag{4.50}$$

and,

$$\gamma_c' = \pi^2 + 4(Lk)^2 \tag{4.51}$$

The solution is not valid for field strengths in a region around the critical field strength where,

$$O\left(\frac{Ak}{\cosh(Lk')}\right) > O(Ak) \tag{4.52}$$

and since $\cosh(Lk') = 0.1$ at the field parameter $\gamma = (Lk)^2 + 2.16$ and $\gamma = (Lk)^2 + 2.78$ then the region around the critical value where the solution is not valid can be approximated to,

$$\gamma \in \left\{(Lk)^2 + 2.16,\ (Lk)^2 + 2.78\right\} = \{\gamma_c - 0.31,\ \gamma_c + 0.31\} \tag{4.53}$$

Similarly for the second singularity the solution is not valid when,

$$\gamma \in \{\gamma_c' - 0.06,\ \gamma_c' + 0.06\} \tag{4.54}$$

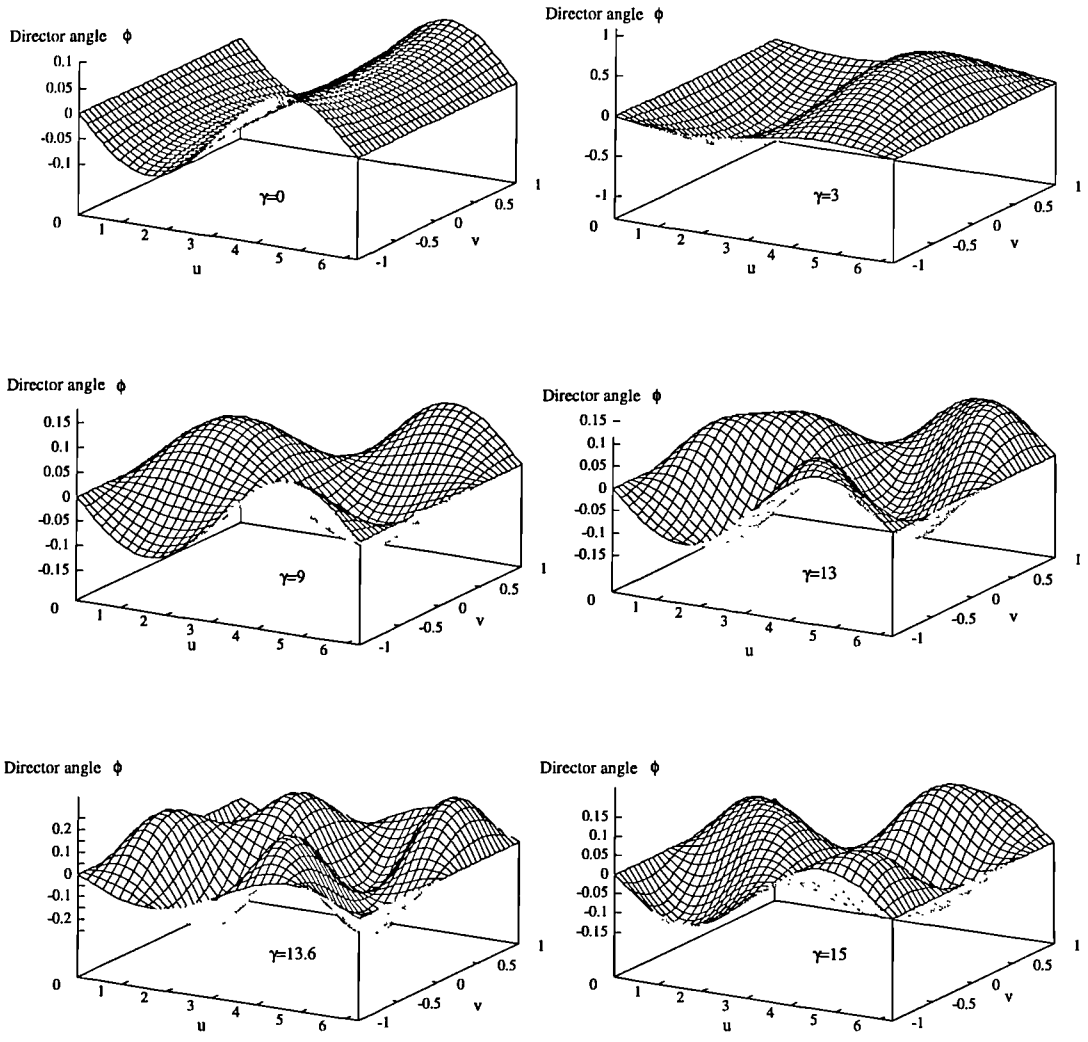

Figure 4.3: Director angle in the cell region $\{0 < x < 2\pi/Lk,\ -1 < v < 1\}$ for different field parameters, γ =0, 3, 9, 13, 13.6, 15.

Figures 4.3 shows the solution at various field strengths. In the classical Freedericksz transition the director angle goes through a pitchfork bifurcation causing the stable configuration to change from $\phi = 0$ to $\phi = \pm\pi/2$. The perturbed solution would be expected to go through a bifurcation (at $\gamma_c = \pi^2/4 + (Lk)^2$) changing the director angle in a similar way so that at higher field strengths the angle is aligned with the field in the vertical direction (at $\phi = \pm\pi/2$). Using the above analysis there is not a smooth transition from a low director angle configuration to $\phi = \pm\pi/2$. Instead the director angle has a *singularity* at critical field strengths. The analysis was only valid for small director angles and therefore the solution (4.49) will not be valid for field strengths close to the critical value where the director angle is large. This solution (4.49) does not therefore imply the physical system has a singularity at the critical field strength but does suggest that there may be a transition from the low angle amplitude configuration to a higher amplitude configuration. Knowing there is a transition and at what point this occurs the system can be analysed around this point in greater detail. In the next chapter these two singularities will be referred to as the *first* and *second* singularities of the expansion series solution. The first singularity from the first term of (4.49) and the second from the second term of (4.49).

4.3 Pre-tilt boundaries

In the previous section the second singularity point was due to a wave-wave interaction between the non-planar boundaries and the linear solution leading to a dominant mode of period π/Lk. This interaction is driven by terms in the governing equation from the transformation of the boundaries. As the boundaries in a pre-tilt cell are planar and do not need a transformation, this interaction does not occur and the director configuration in a pre-tilt cell is in fact the linear approximation to the director configuration in the non-planar cell. The second bifurcation does not occur and as stated previously the second singularity in the linear approximation is outside the relevant parameter region so that there is only one singularity possible in the pre-tilt cell, at the field

strength (4.9).

$$H_c^2 = \frac{K}{\chi_a}\left(\frac{\pi^2}{4L^2} + k^2\right) \tag{4.55}$$

4.4 Summary

In this chapter the Freedericksz transition for liquid crystal layers with non-planar boundaries has been discussed. For the parameter ordering $Ak \ll 1$, $Lk \gg 1/Ak$ a boundary layer solution was found and the Freedericksz transition occured at the classical critical field. In Section 4.1 the parameter ordering $Ak \ll 1$, $Lk \gg 1/Ak$ was used and the linearised equations were solved for three distinct configurations. The resulting solutions have singularities at an infinite number of critical field strengths. Assumptions on the order of the director angle ϕ and the field parameter γ mean that the solution contains only one singularity at a field parameter $\gamma_c = \pi^2/4 + (Lk)^2$ and that the solution is not valid for field strengths in a region around the critical value.

In Section 4.2 effects of higher order terms on the linear solution found in the previous section were considered. An expansion in the small parameter Ak leads to an order $(Ak)^2$ term which contains a singularity at a critical field parameter higher than γ_c and has a wavenumber twice that of the first singularity.

In the next chapter, by considering the amplitude of the dominant mode, the bifurcation structure of each singularity is found and the associated free energies can be calculated.

Chapter 5

Bifurcation and stability analysis

In this chapter the bifurcation structure of the two transitions considered in the previous section will be investigated. There the solution (4.5) modelled the Freedericksz transition as a *singularity* at a critical field strength. Mathematically the director angle ϕ tends to infinity as the field strength tends to the critical value. Physically this would involve the director, and consequently the liquid crystal molecules, spinning and rotating at a faster rate as the field strength approached the critical value. The model uses the precondition that the director angle is small and therefore the solution is only valid when the director angle is of order Ak. This means that the solution of the previous section cannot be used to model the director configuration near to the critical field strength. Using a different approach the system can be analysed as the field strength increases through each of the two singularity/bifurcation points in the parameter regime considered in Section 4.2.

5.1 First Bifurcation

5.1.1 Amplitude Equation

To model the bifurcation more accurately we use an expansion series of the form discussed by [72],

$$\phi = \phi_B + \phi_1 + \phi_2 + \dots \tag{5.1}$$

Here $\phi_i = \phi_i(u,v)$, $\phi_B = S_B\ f(u,v)$ when S_B is the *amplitude* of the perturbation ϕ_B (which will be found later to depend on the field strength), ϕ_i is of order $(Ak)^i$ and $f(u,v)$ has an order larger than $O(Ak)$. The inclusion of the term ϕ_B ensures that the director angle can now take values larger than $O(Ak)$ and it will be possible to model the system through the transition. At low field strength the director orientation is governed by the boundaries, the director angle is of order Ak and hence S_B will be small so that ϕ_1 is the dominant term. When the field is near the critical field strength the director angle increases, the amplitude S_B will increase so that ϕ_B dominates. The transition is therefore from the low field solution ϕ_1 to the high field solution ϕ_B.

It is important to have the correct ordering for the term ϕ_B so that nonlinear terms in the equation, which are relevant during the transition, are included. The nonlinear term of the governing equation is $\sin(2\phi)$. Substituting (5.1) into $\sin(2\phi)$ gives,

$$\begin{aligned}\sin\left(2(\phi_B+\phi_1+\ldots)\right) &= 2(\phi_B+\phi_1+\ldots)-\frac{4}{3}(\phi_B+\phi_1+\ldots)^3+\ldots \\ &= 2(\phi_B+\phi_1+\ldots)-\frac{4}{3}\phi_B^3-4\phi_B^2\phi_1 \\ &\qquad -4\phi_B\phi_1^2-\frac{4}{3}\phi_1^3+\ldots \end{aligned} \tag{5.2}$$

The largest term in this expression is ϕ_B. The next two largest are ϕ_1 and ϕ_B^3. In order to ensure the solution reflects the nonlinearity of the governing equation the orders of these two terms are taken to be equal and therefore $\phi_B = O((Ak)^{1/3})$.

Using the governing equation (4.3) and the boundary conditions 3.41 which are transformed using,

$$\Phi = 2\left(\phi + \arctan(Ak)\ F(v)\ \sin(Lku)\right) \tag{5.3}$$

where F is any smooth function such that $F(\pm 1) = 1$ so that the boundary conditions are now,

$$\Phi = 0 \qquad \text{on } v = \pm 1 \tag{5.4}$$

In modelling the transition, the field parameter is assumed to be close to the critical value γ_c and expansion series of Φ and γ in the small parameter Ak are used to represent the system near γ_c. These expansion series are,

$$\Phi = \Phi_{1/3}(Ak)^{1/3} + \Phi_{2/3}(Ak)^{2/3} + \Phi_1(Ak) + \ldots \tag{5.5}$$

$$\gamma = \gamma_c + \gamma_{1/3}(Ak)^{1/3} + \gamma_{2/3}(Ak)^{2/3} + \ldots \tag{5.6}$$

where $\gamma = (\chi_a H^2 L^2)/K$ is the field strength parameter and γ_c is the critical field strength (of order 1).
Equating all terms which are of the same order a series of governing equations for the expansion terms Φ_i is obtained. The first three equations are,

$$\mathrm{M}\left(\Phi_{1/3}\right) = 0 \tag{5.7}$$

$$\mathrm{M}\left(\Phi_{2/3}\right) = -\gamma_{1/3}\,\Phi_{1/3} \tag{5.8}$$

$$\begin{aligned}\mathrm{M}\left(\Phi_1\right) = {} & -\gamma_{1/3}\,\Phi_{2/3} - \gamma_{2/3}\,\Phi_{1/3} + \frac{\gamma_c}{6}\,{\Phi_{1/3}}^3 \\ & +2\left(\frac{\mathrm{d}^2 F}{\mathrm{d}v^2} - (Lk)^2 F\right)\sin(Lku) + 2\gamma_c F\,\sin(Lku)\end{aligned} \tag{5.9}$$

Where,

$$\mathrm{M} = \frac{\partial^2}{\partial u^2} + \frac{\partial^2}{\partial v^2} + \gamma_c \tag{5.10}$$

The solution from Chapter 4 (4.5) predicts the excited mode $\Phi_{1/3}$ has a u dependence which is sinusoidal of period $2\pi/(Lk)$. The v dependence is determined by the boundary conditions (5.4) giving the solution to (5.7),

$$\Phi_{1/3} = S_{1/3}\,\sin(Lku)\,\cos\left(\frac{\pi}{2}v\right) \tag{5.11}$$

$$\gamma_c = \frac{\pi^2}{4} + (Lk)^2 \tag{5.12}$$

where $S_{1/3}$ is the amplitude of the dominant mode during the bifurcation. The second equation produces a solvability condition $\gamma_{1/3} = 0$ and a solution,

$$\Phi_{2/3} = 0 \tag{5.13}$$

Taking into consideration the solutions of previous chapters (e.g. Chapter 3, equation (3.42)) F is chosen such that,

$$\frac{\mathrm{d}^2F}{\mathrm{d}v^2} - (Lk)^2F = 0 \tag{5.14}$$

then,

$$F = \frac{\cosh(Lkv)}{\cosh(Lk)} \tag{5.15}$$

The third equation therefore becomes,

$$\begin{aligned} \mathrm{M}(\Phi_1) \;=\; & \frac{\gamma_c S_{1/3}^3}{96}\left[9\sin(Lku)\cos\left(\frac{\pi}{2}v\right) + 3\sin(Lku)\cos\left(\frac{3\pi}{2}v\right)\right. \\ & \left. -3\sin(3Lku)\cos\left(\frac{\pi}{2}v\right) - \sin(3Lku)\cos\left(\frac{3\pi}{2}v\right)\right] \\ & -\gamma_{2/3}\, S_{1/3}\sin(Lku)\cos\left(\frac{\pi}{2}v\right) + 2\gamma_c\sin(Lku)\frac{\cosh(Lkv)}{\cosh(Lk)} \end{aligned} \tag{5.16}$$

The last term can be expanded into a Fourier series,

$$F = \frac{\cosh(Lkv)}{\cosh(Lk)} = \left[a_0 + \sum_{i=1}^{\infty} a_i \cos\left(i\frac{\pi}{2}v\right)\right] \tag{5.17}$$

where the Fourier coefficients are,

$$a_i = \frac{2(-1)^i Lk}{(Lk)^2 + \left(\frac{i\pi}{2}\right)^2}\sinh(Lk) \tag{5.18}$$

for $i = 1,\ 2,\ 3\ldots$. Then equation (5.16) can be written as,

$$\begin{aligned} \mathrm{M}(\Phi_1) \;=\; & \left[\frac{3\gamma_c S_{1/3}^3}{32} - \gamma_{2/3}S_{1/3} + 2\gamma_c a_1\right]\sin(Lku)\cos\left(\frac{\pi}{2}v\right) \\ & + \left[\frac{3\gamma_c S_{1/3}^3}{96} - 2\gamma_c a_3\right]\sin(Lku)\cos\left(\frac{3\pi}{2}v\right) \\ & - \left[\frac{\gamma_c S_{1/3}^3}{32}\right]\sin(3Lku)\cos\left(\frac{\pi}{2}v\right) \\ & - \left[\frac{\gamma_c S_{1/3}^3}{96}\right]\sin(3Lku)\cos\left(\frac{3\pi}{2}v\right) \\ & + 2\gamma_c\sin(Lku)\left[a_0 + \sum_{\substack{i=2 \\ i\neq 3}}^{\infty} a_i\cos\left(i\frac{\pi}{2}v\right)\right] \end{aligned} \tag{5.19}$$

The first term of the right hand side of this equation is a resonant forcing term. Since the liquid crystal region is bounded in the v direction the solution *can* contain a secular term in the v coordinate. The solvability condition is not that the coefficient of the resonant term must vanish but that the boundary conditions (5.4) are satisfied. The solution is therefore,

$$\begin{aligned}\Phi_1 &= \lambda_1\, v\, \sin(Lku)\sin\left(\frac{\pi}{2}v\right) \\ &\quad +\lambda_2 \sin(3Lku)\cos\left(\frac{\pi}{2}v\right) \\ &\quad +\lambda_3 \sin(3Lku)\cos\left(\frac{3\pi}{2}v\right) \\ &\quad +\lambda_4 \sin(Lku) \\ &\quad +\sum_{i=2}^{\infty}\delta_i \sin(Lku)\cos\left(i\frac{\pi}{2}v\right)\end{aligned} \tag{5.20}$$

where,

$$\lambda_1 = \frac{1}{\pi}\left(\frac{3\gamma_c S_{1/3}^3}{32} - \gamma_{2/3}S_{1/3} + 2\gamma_c a_1\right) \tag{5.21}$$

$$\lambda_2 = \frac{3S_{1/3}^3}{768(Lk)^2}\left(\frac{\pi^2}{4} + (Lk)^2\right) \tag{5.22}$$

$$\lambda_3 = \frac{S_{1/3}^3}{768} \tag{5.23}$$

$$\lambda_4 = \frac{16}{\pi^2(Lk)}\left(\frac{\pi^2}{4} + (Lk)^2\right)\sinh(Lk) \tag{5.24}$$

$$\delta_i = \frac{8\gamma_c a_i}{\pi^2(1-i^2)} \qquad \text{for } i = 2,4,5,6,7\ldots \tag{5.25}$$

$$\delta_3 = -\frac{\gamma_c}{\pi^2}\left(a_3 + \frac{S_{1/3}^3}{64}\right) \tag{5.26}$$

and the boundary condition $\Phi(\pm 1) = 0$ gives,

$$\lambda_1 + \lambda_4 + \sum_{i=1}^{\infty}(-1)^i\delta_{2i} = 0 \tag{5.27}$$

By integrating $\cos(\pi v/2)\cosh(Lkv)$ in two different ways, firstly using the identity,

$$\cos(A + iB) = \cos A \cosh B - i\sin(A)\sinh(B) \tag{5.28}$$

and secondly using the Fourier expansion (5.17) of $\cosh(Lkv)$ the last term of (5.27) can be reduced with the relation,

$$\frac{\pi}{\gamma_c} = \int_{-1}^{1} \cos\left(\frac{\pi}{2}v\right) \frac{\cosh(Lkv)}{\cosh(Lk)}\, \mathrm{d}v = \frac{\pi}{2\gamma_c} \sum_{i=1}^{\infty} (-1)^i \delta_{2i} + a_1 \tag{5.29}$$

and together with expressions for λ_1 (5.21), λ_4 (5.24) and a_1 (5.18) equation (5.27) gives the solvability condition,

$$S_{1/3}^3 - \frac{32\,\gamma_{2/3}}{3\gamma_c} S_{1/3} + \frac{64\,\pi}{3\gamma_c} = 0 \tag{5.30}$$

This *amplitude equation* governs the development of the dominant mode from low amplitude when the boundary alignment is dominant to high amplitude when the field alignment is dominant. Since $\gamma_{1/3} = 0$, the order $(Ak)^{2/3}$ term of the field parameter expansion (5.6) is a measure of the distance from the critical field parameter γ_c. The dependence of $S_{1/3}$ on $\gamma_{2/3}$ indicates how the solution varies through the transition.
Equation (5.30) has three roots [1],

$$S_{1/3} = z_1 = 2P^{1/2} \cos\left(\frac{\vartheta}{3}\right) \tag{5.31}$$

$$S_{1/3} = z_2 = -\frac{1}{2} z_1 + \sqrt{3} P^{1/2} \sin\left(\frac{\vartheta}{3}\right) \tag{5.32}$$

$$S_{1/3} = z_3 = -\frac{1}{2} z_1 - \sqrt{3} P^{1/2} \sin\left(\frac{\vartheta}{3}\right) \tag{5.33}$$

where,

$$P = \sqrt{\frac{32\gamma_{2/3}}{9\gamma_c}} \tag{5.34}$$

$$\vartheta = \arctan\left(\frac{32\gamma_{2/3}^3}{(9\pi\gamma_c)^2} - 1\right) \tag{5.35}$$

The number of real/imaginary solutions depends on the magnitude of $\gamma_{2/3}$.

$$\gamma_{2/3} < \frac{3}{2}\sqrt[3]{\frac{3\gamma_c\pi^2}{4}} \qquad z_1 \text{ real, } z_2,\ z_3 \text{ complex conjugate roots} \tag{5.36}$$

$$\gamma_{2/3} = \frac{3}{2}\sqrt[3]{\frac{3\gamma_c\pi^2}{4}} \qquad \text{all real roots, } z_2 = z_3 \tag{5.37}$$

$$\gamma_{2/3} > \frac{3}{2}\sqrt[3]{\frac{3\gamma_c\pi^2}{4}} \qquad \text{all real roots, } z_1 > z_2 > z_3 \tag{5.38}$$

$$\vartheta = \arctan\left(\frac{32\gamma_{2/3}^3}{(9\pi\gamma_c)^2} - 1\right) \tag{5.39}$$

It is therefore possible to plot $S_{1/3}$ against $\gamma_{2/3}$ i.e. the amplitude of the dominant mode in the director angle against the measure of the deviation of the field parameter γ from the critical value γ_c to obtain a bifurcation diagram of the transition. As can be seen from Figure 5.1 this is a perturbed pitchfork bifurcation from a low director angle amplitude solution, $\gamma_{2/3} < 0$, and a high amplitude solution $\gamma_{2/3} > 0$. The stability of each of these solutions can be found by considering the energy of the system on each of the branches of the bifurcation diagram.

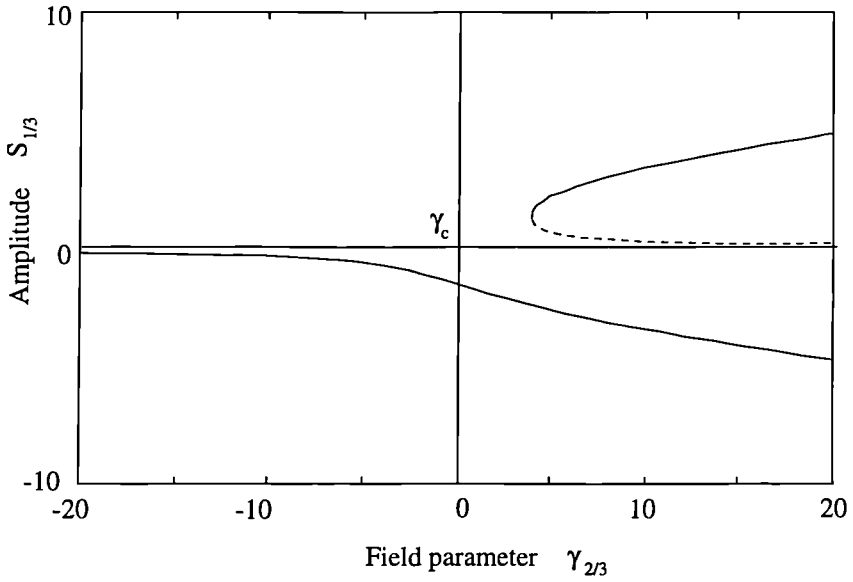

Figure 5.1: Bifurcation diagram for the first transition.

5.1.2 Stability

To investigate the stability of the solution found in the previous section (5.20) with respect to other values of the amplitude $S_{1/3}$ the energies of other possible configurations are compared. The solvability condition determines the

three possible magnitudes of the amplitude $S_{1/3}$. The energy of the system is calculated for any $S_{1/3}$ and can therefore determine the stability of each of the three solutions. The energy of the system is given by [18],

$$E(\Phi) = \int_V (F_D + F_M)\, \mathrm{d}v \tag{5.40}$$

where F_D and F_M are the free energy densities (3.9) and (3.17) and V is the volume enclosed by the bounding plates (of unit length in the z direction). When $\mathbf{n} = (\cos\phi(x,y),\ \sin\phi,\ 0)$ equation (5.40) becomes,

$$E(\Phi) = \int_V \left(K\,(\nabla\phi)^2 - \chi_a H^2 \sin^2\phi\right)\, \mathrm{d}v \tag{5.41}$$

The perturbation solution (5.5), (5.6) will be used with the boundaries transformed using (3.38) and $u = X/L,\ v = Y/L$, the boundary conditions transformed using (5.3). The boundary is periodic with period $2\pi/Lk$ (since the nondimensional variable u is used) and so a configuration solution minimises the energy of the system contained in one period of the boundaries ($0 < u < 2\pi/Lk$) if and only if the solution minimises the energy of the whole system. The energy integral can therefore be carried out using the region $V = \{0 < u < 2\pi/Lk,\ -1 < v < 1,\ 0 < z < 1\}$.
After transforming the boundaries and the boundary conditions (5.41) becomes,

$$\begin{aligned} E \;=\; \frac{K}{Lk}\int_{-1}^{1}\int_{0}^{2\pi/(Lk)} & \frac{1}{4}\left(\Phi_u^2 + J_u^2 - 2\Phi_u J_u\right) \\ & + \frac{(Ak)^2}{4}\sin^2(Lku)\left(\Phi_v^2 + J_v^2 - 2\Phi_v J_v\right) \\ & + \frac{(Ak)}{2}\sin(Lku)(\Phi_v\Phi_u + J_v J_u - \Phi_u J_v - \Phi_v J_u) \\ & + \frac{1}{4}\left(\Phi_v^2 + J_v^2 - 2\Phi_v J_v\right) \\ & - \frac{\chi_a H^2 L^2}{K}\sin^2((\Phi + J)/2)\ \mathrm{d}u\mathrm{d}v \end{aligned} \tag{5.42}$$

where,

$$\Phi \;=\; S_{1/3}\,\sin(Lku)\,\cos\left(\frac{\pi}{2}v\right) + (Ak)\Phi_1 + \ldots \tag{5.43}$$

$$J \;=\; 2(Ak)\sin(Lku)F(v) \tag{5.44}$$

When the expansion series (5.5), (5.6) are substituted into (5.42) the coefficients of $(Ak)^i$ are equated and the leading order term is the $(Ak)^{2/3}$ term,

$$\begin{aligned} E_{2/3} &= \frac{K}{(Lk)}\int_{-1}^{1}\int_{0}^{2\pi/(Lk)} \frac{1}{4}S_{1/3}^2\left((Lk)^2\cos^2(Lku)\cos^2\left(\frac{\pi}{2}v\right)\right. \\ &\quad + \frac{\pi^2}{4}\sin^2(Lku)\sin^2\left(\frac{\pi}{2}v\right) \\ &\quad \left. - \gamma_c\sin^2(Lku)\cos^2\left(\frac{\pi}{2}v\right)\right)\,dudv \end{aligned} \tag{5.45}$$

But $\gamma_c = ((Lk)^2 + \pi^2/4)$ so $E_{2/3} = 0$. The next term is $E_{4/3}$ which reduces to,

$$\begin{aligned} E_{4/3} &= \frac{K}{(Lk)}\int_{-1}^{1}\int_{0}^{2\pi/(Lk)} \frac{(Lk)^2}{2}S_{1/3}\Phi_{1u}\cos(Lku)\cos\left(\frac{\pi}{2}v\right) \\ &\quad - (Lk)^2 S_{1/3}\cos^2(Lku)\cos\left\{\frac{\pi}{2}v\right\}F \\ &\quad - \frac{\pi}{4}S_{1/3}\Phi_{1v}\sin(Lku)\sin\left(\frac{\pi}{2}v\right) \\ &\quad - \frac{\pi}{2}S_{1/3}\sin^2(Lku)\sin\left(\frac{\pi}{2}v\right)F' \\ &\quad - \frac{\gamma_c}{2}S_{1/3}\left[\Phi_1\sin(Lku)\cos\left(\frac{\pi}{2}v\right)\right. \\ &\qquad - 2\sin^2(Lku)\cos\left(\frac{\pi}{2}v\right)F' \\ &\qquad \left. -\frac{S_{1/3}^3}{24}\sin^4(Lku)\cos^4\left(\frac{\pi}{2}v\right)\right] \\ &\quad - \frac{\gamma_{2/3}}{4}S_{1/3}^2\sin^2(Lku)\cos^2\left(\frac{\pi}{2}v\right)\,dudv \end{aligned} \tag{5.46}$$

All the terms involving Φ and its derivatives vanish and the rest of the terms reduce to,

$$\begin{aligned} E_{4/3} = \quad & (Ak)^{4/3}\frac{3\gamma_c K\pi}{256(Lk)}\,S_{1/3}\left[S_{1/3}^3 - \frac{64\gamma_{2/3}}{3\gamma_c}\,S_{1/3} + \frac{256\pi}{3\gamma_c}\right] \\ & + O\left((Ak)^2\right) \end{aligned} \tag{5.47}$$

At a specific field strength γ_c the energy (5.47) has a stationary point when $\partial E/\partial S_{1/3} = 0$. This leads to the amplitude equation (5.30) which confirms that the solution (5.11) with (5.30) occurs at stationary point of the energy.

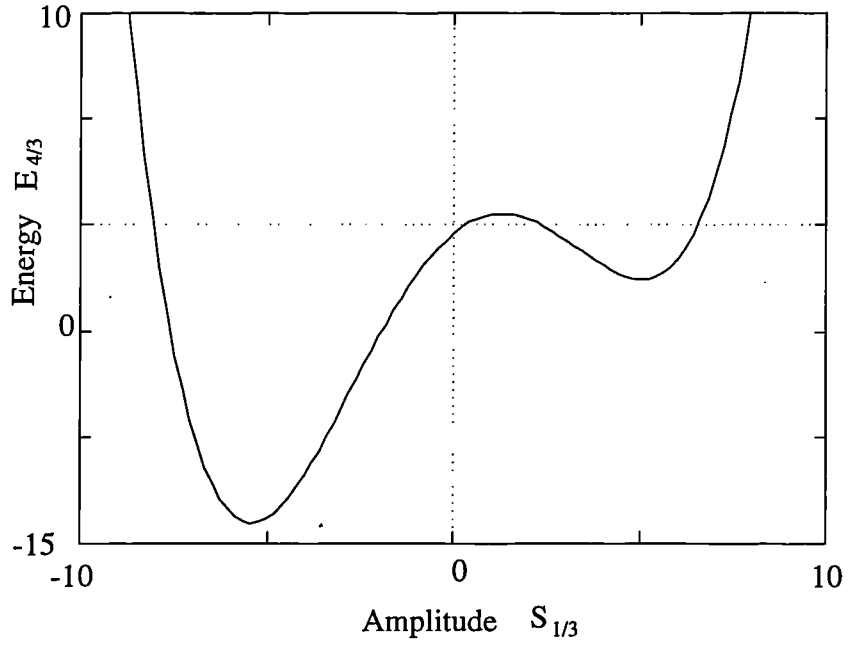

Figure 5.2: Energy versus director amplitude $S_{1/3}$ during the first bifurcation.

The energy functional (5.47) implies that the upper and lower branches are stable and the middle branch is unstable (Figure 5.2).
In the unperturbed system ($k = 0$) the classical Freedericksz transition is a pitchfork bifurcation with stable upper and lower branches. Therefore in a perturbed system a perturbed pitchfork bifurcation as described by (5.30) and (5.47) would be expected.

5.2 Second Bifurcation

5.2.1 Amplitude Equation

In this section the second singularity which occurs at the field strength parameter $(\pi^2 + 4(Lk)^2)$ is considered. If the amplitude of the director angle before the second singularity in the weakly nonlinear solution (4.49) (Figure 4.2) is compared to the three solution branches in the bifurcation analysis the director angle is found to be of order Ak. This suggests that the second transition is a bifurcation of the unstable middle branch solution of the first bifurcation. To investigate this possibility a perturbation of the solution from Section 5.1

on the middle branch is considered in a similar way to the first bifurcation. The form of the solution on the middle branch of the first bifurcation, at the field strength (4.51), and the form of the perturbation used must be carefully considered.

The solution from the first bifurcation following the middle branch of the bifurcation diagram (Figure 5.1) is given by the expansions (5.5) and (5.6) where the first order term solution is (5.11). On the middle branch the amplitude $S_{1/3}$ of this solution is the smallest root of the cubic amplitude equation (5.30). This root can be approximated by assuming $S_{1/3}$ is small so that the $S_{1/3}^3$ term is negligible and hence,

$$S_{1/3} = O\left(\frac{2\pi}{\gamma_{2/3}}\right) \tag{5.48}$$

In the first perturbation analysis of this section the perturbation to the critical field was,

$$\gamma = \frac{\pi^2}{4} + (Lk)^2 + \gamma_{2/3}(Ak)^{2/3} + \gamma_{4/3}(Ak)^{4/3} + \dots \tag{5.49}$$

At the new field strength $\gamma = \pi^2 + 4(Lk)^2$ this implies,

$$\gamma_{2/3}(Ak)^{2/3} = \frac{3}{4}\left(\pi^2 + (Lk)^2\right) \tag{5.50}$$

and consequently $\gamma_{2/3} = O\left((Ak)^{-2/3}\right)$.

Using (5.48) $S_{1/3} = O\left((Ak)^{2/3}\right)$ and therefore the solution on the middle branch at this field strength is the solution (5.5) with the new $S_{1/3}$ ordering above. One consequence of this new ordering is that the first order term of the solution at this point on the middle branch is of order Ak.

The second singularity of the weakly nonlinear solution (4.49) occurs in the second term which has a $\sin(2Lku)$ dependence. The highest order term Φ_i of (5.5) which includes a $\sin(2Lku)$ factor is assumed to cause the instability leading to the second bifurcation. The first term to have a $\sin(2Lku)$ dependence is Φ_2 and the bifurcation is modelled in a similar way to the first bifurcation (5.1) using a perturbation to Φ_2,

$$\Phi = \Phi_B + \Phi_2 + \dots \qquad \text{where } \Phi_B = T_B\, g(u,v) \tag{5.51}$$

so that T_B is the amplitude of the perturbation Φ_B. Following the method used for the first bifurcation (Section 5.1.1) it is found that $B = 2/3$. The full perturbation expansion used is,

$$\Psi = \Phi + \nu = \Psi_{2/3}(Ak)^{2/3} + \Psi_1(Ak) + \Psi_{4/3}(Ak)^{4/3} + \ldots \quad (5.52)$$

$$\gamma = \gamma'_c + \gamma'_{2/3}(Ak)^{2/3} + \gamma'_{4/3}(Ak)^{4/3} + \ldots \quad (5.53)$$

where $\Psi_i = \Phi_i + \nu_i$ and $\Phi = \sum \Phi_i$ is the solution (5.5) on the middle branch of the first bifurcation and $\nu = \sum \nu_i$ is the perturbation to this solution. A transformation of the boundary conditions is used, but instead of the (5.3) the transformation,

$$\Phi = 2\left(\phi + \arctan(Ak)\ F(v)\ \sin(Lku) + (Ak)^2\ G(v)\ \sin(2Lku)\right) \quad (5.54)$$

is used, where F and G are any smooth functions such that $F(\pm 1) = 1$ and $G(\pm 1) = 0$ so that the boundary conditions are as before,

$$\Phi = 0 \qquad \text{on } v = \pm 1 \quad (5.55)$$

After substituting (5.52) and (5.53) into the governing equation ((4.3) with the above transformation) a set of governing equations is obtained for the Ψ_i the first of which is,

$$N\left(\Psi_{2/3}\right) = 0 \quad (5.56)$$

where,

$$\mathrm{N} = \frac{\partial^2}{\partial u^2} + \frac{\partial^2}{\partial v^2} + \gamma'_c \quad (5.57)$$

and since $\Phi_{2/3} = 0$ the solution is,

$$\nu_{2/3} = T_{2/3}\ \sin(2Lku)\sin(\pi v) \quad (5.58)$$

the non-trivial solvability condition is obtained from the order $(Ak)^2$ equation and is,

$$T_{2/3}^3 - \frac{32\ \gamma'_{4/3}}{3\gamma'_c}\ T_{2/3} + \frac{64\ \pi\gamma_c}{3\gamma_c}\left(\frac{1}{4(Lk)^2 + \pi^2} - \frac{1}{(Lk)^2 + \pi^2}\right) = 0 \quad (5.59)$$

which is the amplitude equation for the second bifurcation. In this equation $\gamma'_{4/3}$ is the measure of how the field parameter varies from the critical value γ'_c. It is clear that this equation implies another perturbed pitchfork bifurcation. To find the stability of the different branches of the bifurcation diagram (Figure 5.3) the solution is substituted into the energy functional as before.

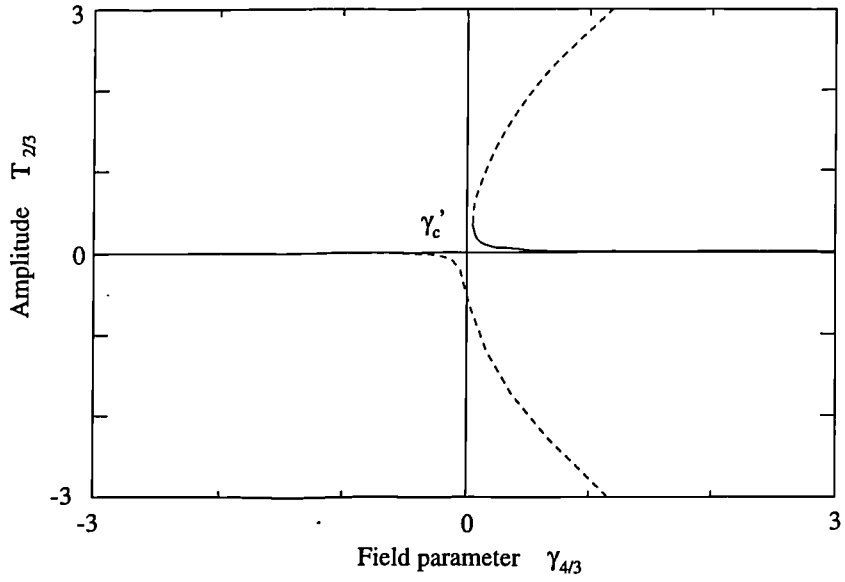

Figure 5.3: Bifurcation diagram for the second transition.

5.2.2 Stability

As in the previous section the free energy of the system which is now a function of $S_{1/3}$ and $T_{2/3}$ is calculated. The resulting energy equation is,

$$E = (Ak)^2 E_2 + (Ak)^{8/3} E_{8/3} + O\left((Ak)^3\right) \tag{5.60}$$

where,

$$E_2 = E_2(S_{1/3}) = aS_{1/3}^2 + bS_{1/3} + c \tag{5.61}$$

$$E_{8/3} = E_{8/3}(T_{2/3}) = T_{2/3}\left(dT_{2/3}^3 + eT_{2/3} + f\right) \tag{5.62}$$

are the first two non-zero terms of the energy with,

$$a = -\frac{K}{\pi Lk}\left(k_1 \tan(k_1)\, \gamma_{2/3}^2\right) \tag{5.63}$$

$$b = -\frac{K}{Lk}\left(2k_1 \tan(k_1)\, \gamma_{2/3}\left(\frac{1}{\gamma_c'} - 2\right)\right) \tag{5.64}$$

$$c = -\frac{K\pi}{Lk}\left(4k_1 \tan(k_1)\, \left(1 - \frac{1}{\gamma_c'}\right) + \frac{\gamma_c'}{\cosh^2(Lk)} + k_4^2 \frac{\tanh(Lk)}{Lk}\right) \tag{5.65}$$

$$d = -\frac{K\pi}{Lk}\left(\frac{21\gamma_c'}{512}\right) \tag{5.66}$$

$$e = -\frac{K\pi}{Lk}\left(\frac{7\gamma'_{4/3}}{16}\right) \tag{5.67}$$

$$f = \frac{K\pi}{Lk}\left(\frac{7\pi\gamma_c}{8}\frac{1}{4(Lk)^2+\pi^2} - \frac{1}{(Lk)^2+\pi^2}\right) \tag{5.68}$$

and,

$$k_1 = \pi^2 + 3(Lk)^2 \tag{5.69}$$

$$k_4 = \pi^2 + 2(Lk)^2 \tag{5.70}$$

$$\gamma_{2/3} = 3\gamma_c = \frac{3}{4}\left(\pi^2 + 4(Lk)^2\right) \tag{5.71}$$

The stationary points occur when $\partial E/\partial S_{1/3} = 0$ and $\partial E/\partial T_{2/3} = 0$. Using (5.60) and (5.61) there are stationary points when $\partial E_2/\partial S_{1/3} = 0$ and $\partial E_{8/3}/\partial T_{2/3} = 0$ or equivalently,

$$0 = S_{1/3} - \frac{b}{a} \tag{5.72}$$

$$0 = T_{2/3}^3 + \frac{3e}{4d}T_{2/3}^2 + \frac{f}{2d}T_{2/3} + \frac{g}{4d} \tag{5.73}$$

The first equation in (5.72) implies the solution is on the middle branch of the first bifurcation. The second (5.73) implies that the solution is (5.58) with (5.59). The form of $E_{8/3}$ tells us that the bifurcation is a perturbed pitchfork bifurcation with the outer two branches unstable and the inner stable (Figure 5.4).

The complete bifurcation diagram and energy diagram are shown in Figures 5.5 and 5.6

5.3 Summary

In this chapter the structure of the two bifurcations found in Chapter 4 was investigated in more detail. By introducing an *amplitude* of the dominant mode for each transition and calculating the governing equation for this amplitude the two singularities were found to be perturbed pitchfork bifurcations. It was found that the first bifurcation is from the stable zero field solution to two stable and one unstable solutions whilst the second is from the unstable branch

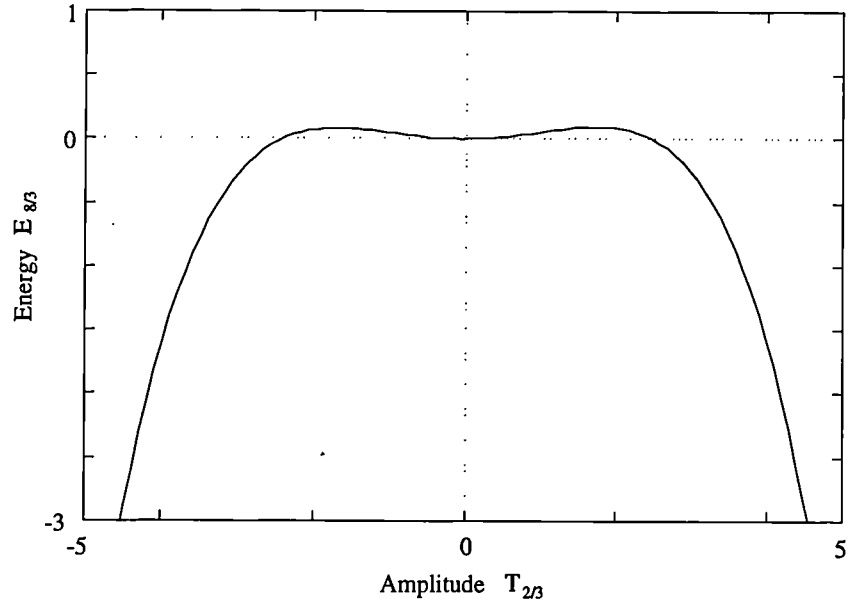

Figure 5.4: Energy versus director amplitude $T_{2/3}$ during the second bifurcation.

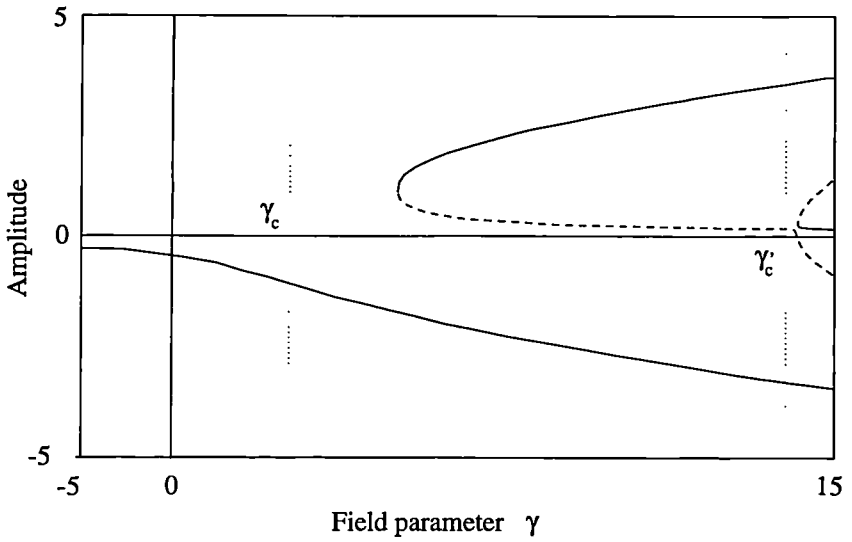

Figure 5.5: Full bifurcation diagram for both transitions.

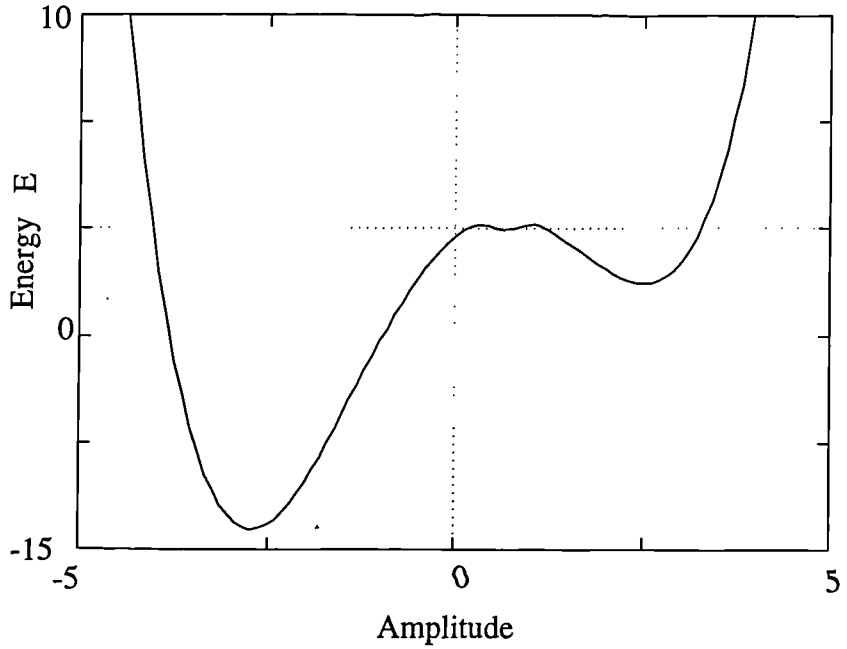

Figure 5.6: Full energy diagram during the second bifurcation.

of the first bifurcation to two unstable and one stable solution. The existence of the *three* stable solutions, two with high director angle amplitude and one with low director angle amplitude leads to the possibility of a new switching device. The system may be able to switch from the high to low director angle amplitude at a fixed electric field strength.

In the rest of this thesis attention is turned to the effects that changes in boundary conditions have on defects. In the next chapter an introduction to defects in nematic liquid crystals is given concentrating on the two types of defects considered in the subsequent chapters. In Chapter 7 the director configuration of disclination lines attached to the boundary of the cell are considered. In the same chapter and in Chapter 8 Ericksen's continuum theory [33] is then used to describe the changes in the scalar order parameters near the cores of defects.

Chapter 6

Defects

In this chapter an introduction to defects in nematic liquid crystals is given. The two forms of defects that will be considered in subsequent chapters are then discussed in more detail.

In a typical nematic liquid crystal the director does not point in the same direction at all points in the sample. There may be adjacent regions within the sample which have different director orientations, between which there will exist a small area where the director must exhibit an abrupt change. If this change is too abrupt the director, which is a macroscopic quantity, cannot be defined and the director field contains a singularity at this point. Whether or not a singularity occurs, these points where the director undergoes an abrupt change are defects.

The presence of these defects determines, to a large extent, the appearance of a particular sample when viewed using a microscope. Since different types of liquid crystal have different symmetries and ordering only specific defect types are allowed within each type of liquid crystal [24]. The study of defects is therefore a major method of classification of liquid crystals. In the next two chapters defects within nematic liquid crystals are considered.

In regions near defects the abrupt change in the orientation of the director corresponds to large internal stresses. This stress would be released if the defects were not present. The occurrence of these stable defects indicates that influences such as electric/magnetic fields and surface orientation are present. This can be seen in Figure 6.1 which shows a nematic sample contained within a capillary tube. The surface of the tube is treated so that the director is

forced to align perpendicular to the surface (homeotropic alignment). In a) the director has no z dependence and the boundary conditions have caused a *line* of singularities in the director field along the z-axis. This configuration may relax to form a pair of *point* singularities positioned on the z (b in Figure 6.1) or to a configuration with no singularities (c in Figure 6.1). In this last configuration the director has a component in the z direction everywhere except at the boundary whereas the configuration in a) never had a component in the z direction. The director in c) is said to have *escaped* into the third dimension and the defect is therefore called an *escaped defect.*

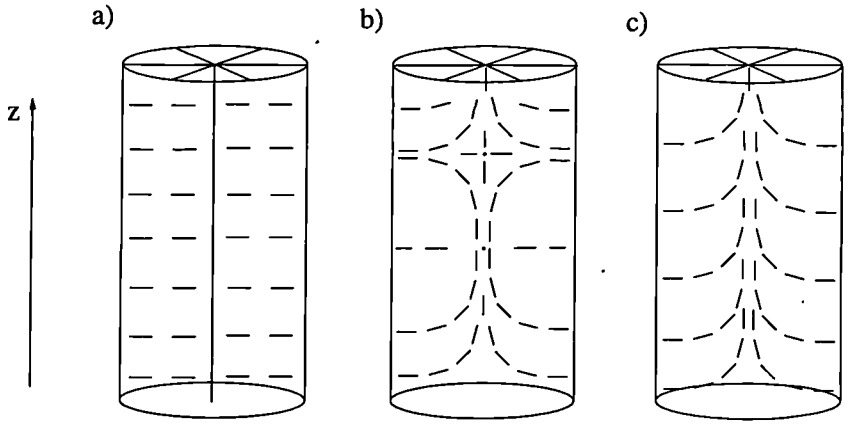

Figure 6.1: Director configurations of a nematic liquid crystal in a capillary tube with homeotropic boundary conditions. a) Line of singularities along the z axis. b) Two point singularities along the z axis. c) No singularity but a defect along the z axis.

It will be seen later (Section 7.1) that in the mathematical description of these defects there is a singularity in the energy density at at any singular point of the director orientation field causing the defect to possess an infinite energy. To eliminate this singularity it is therefore thought that the high stress in the region around these points leads to the presence of a defect *core* [24]. This core has radius r_c, a finite energy E_c (per unit length) and possibly consists of isotropic liquid or biaxial liquid crystal [80]. If this is the case the liquid crystal has melted to reduce the large distortional energy caused by the abrupt change in the director orientation. This core will be investigated in detail in subsequent chapters.

Two types of defect will be considered in the following chapters: the disclination line and the wall defect.

6.1 Disclination line

In the schlieren texture, described by Friedel as structures à noyaux [38], of Figure 1.5 the dark brushes originate from a series of points. These points are defect lines perpendicular to the viewing layer similar to the structures in Figure 6.1 with the z direction perpendicular to the layer. These defects are *disclination lines* and were first studied theoretically by Oseen [73] and Frank [35]. They considered a planar structure so that the director is confined to the xy-plane and is not a function of z as in Figure 6.1 a). The director can therefore be written as $\mathbf{n} = (\cos\phi,\ \sin\phi,\ 0)$. If the one constant approximation is used then the Oseen-Zöcher-Frank free energy density (Appendix A) is,

$$F = \frac{1}{2}K\left(\nabla\phi\right)^2 \tag{6.1}$$

and the Euler-Lagrange equation is then Laplace's equation,

$$\nabla^2\phi = 0 \tag{6.2}$$

If simple director configurations that are independent of $r = (x^2 + y^2)^{1/2}$ and z are sought then the solutions are,

$$\phi = c_1\theta + c_2 \tag{6.3}$$

where c_1 and c_2 are constants and $\theta = \arctan\left(y/x\right)$ is the polar angle in the xy-plane. Since $\phi(0) = \phi(2\pi) + n\pi$ for any integer n then,

$$c_1 = \pm 1/2,\ \pm 1,\ \pm 3/2, \ldots \tag{6.4}$$

The singularity in the director field is along the z axis perpendicular to the layer and the director orientation changes by an angle of $2\pi c_1$ on going around the singular line. The constant c_1 is termed the strength of the disclination lines and the director field for different strength disclinations is shown in Figure 6.2. The defect in the capillary tube shown in Figure 6.1 is therefore a disclination line of strength $+1$.

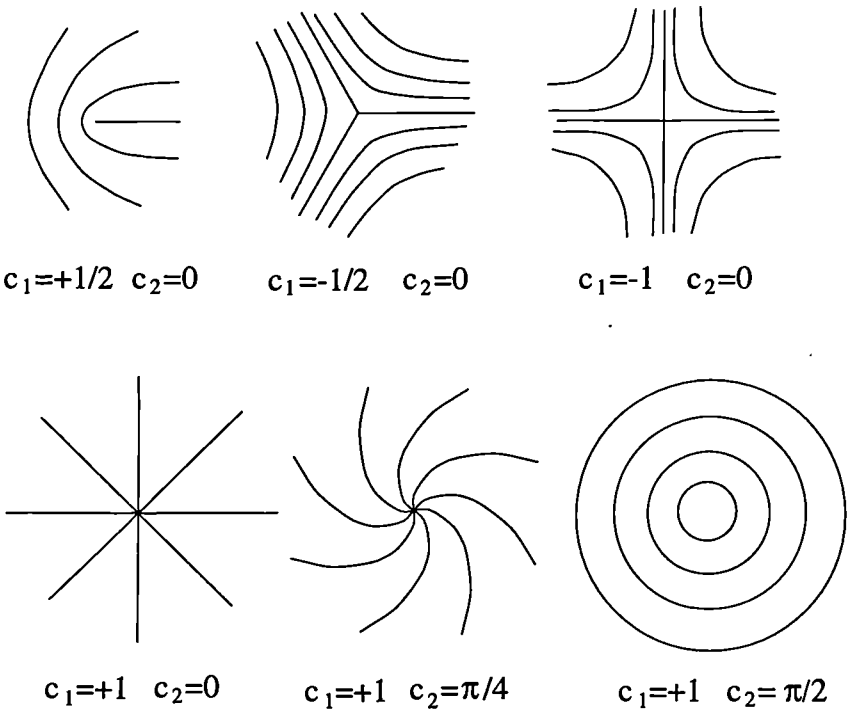

Figure 6.2: Disclination lines (perpendicular to the page) for various values of c_1 and $c_2$in equation (6.3).

When these director configurations are viewed through crossed polarizers the schlieren texture of Figure 1.5 is seen. Incident light will be extinguished when the director is parallel to either of the polarizing directions. This can be seen in Figure 6.3. Using an example of a +1 strength disclination line viewed under crossed polarizers placed at an angle θ_p and $\theta_p + \pi/2$ to the vertical the pattern of light and dark regions is seen to be identical to the schlieren texture near the disclination line. These solutions (6.3) therefore describe extremely well the defect structure in nematic liquid crystal layers viewed through crossed polarizers.

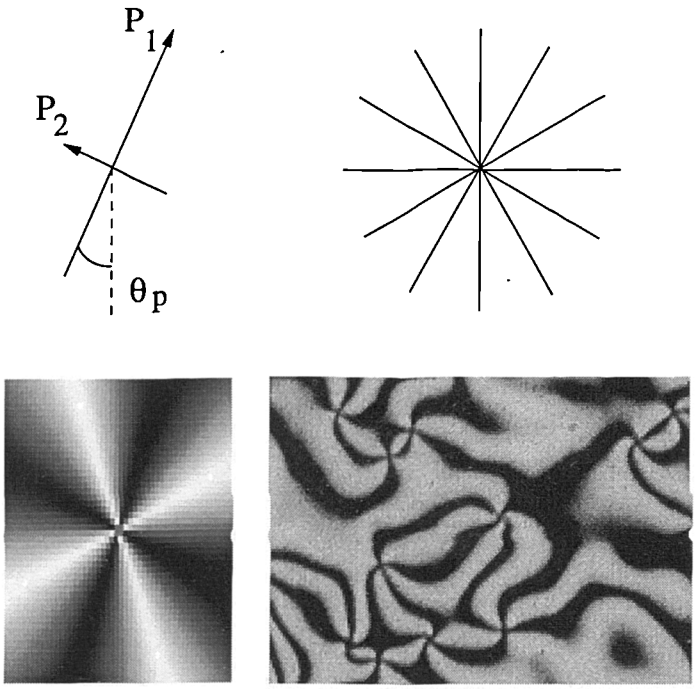

Figure 6.3: Strength +1 disclination line: The crossed polarizers P_1 and P_2 at an angle θ_p to the vertical, the director field (6.3), the director field (6.3) through the crossed polarizers and real disclinations of strength +1 through crossed polarizers (from Figure 1.5).

The above equation of a disclination line (6.3) does not include any variation with the z coordinate and is essentially a description of the director field around the disclination in the *bulk* of the liquid crystal far from the bounding plates.

Close to the boundary the director configuration will be greatly affected by the aligning effect of the treated surface (Section 1.4). This boundary effect is considered in the next chapter.

In the majority of previous work concerned with defects the assumption that the core of the disclination consists of a cylinder of isotropic fluid with a fixed radius r_c and energy E_c is used [24]. Few authors have considered the detailed structure of the core since the Oseen-Zöcher-Frank theory for statics and the Leslie-Ericksen theory for dynamics of liquid crystals does not allow for a phase change from liquid crystalline to isotropic. With the recent development by Ericksen [33] of a continuum theory which allows for phase changes a detailed study of defect cores is possible. In the next chapter the core of a disclination line is considered, not for the highly complicated director structure of a disclination line near the boundary but for the simpler case of a disclination line in the bulk of the liquid crystal sample.

6.2 Wall defects

Wall defects may occur between two adjacent regions of different director orientation when the singularity in the director is not a line or a point as in Figure 6.1 but occurs on a surface. The region of the abrupt change in the director when passing through this surface is called a wall defect. It is easy to see that within the Oseen-Zöcher-Frank theory this surface singularity would relax to distribute the internal stress concentrated at the defect throughout the sample [24]. This is shown in Figure 6.4. In the first diagram there is a surface of singularities in the director on the $z = 0$ plane caused by the abrupt change in the director between two adjacent regions of different orientation. With no external forces present this defect is unstable and the high stress concentrated at the plane $z = 0$ will *smear* out of the plane and the director will vary continuously from one region to the other as in the second diagram of Figure 6.4.

It is possible to stabilise the director configuration seen in Figure 6.4 b) using an electric or magnetic field. Figure 6.5 shows the three possibilities for walls when an electric field is applied in the x direction. The director is aligned parallel to the field everywhere except for a small region where there is an

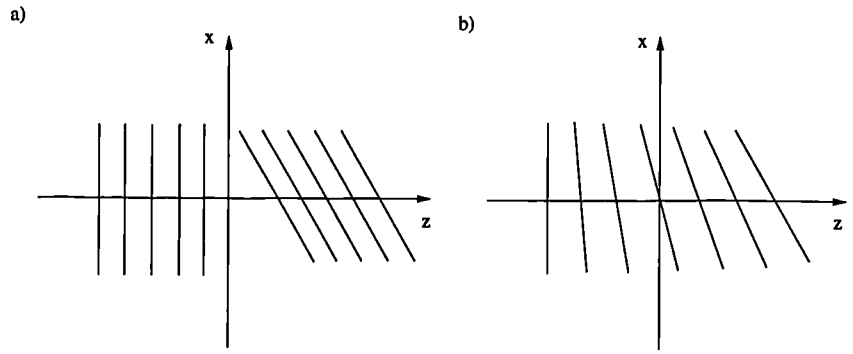

Figure 6.4: Smearing of the director field around a wall defect. Without any external forces the director field with a singularity at $z = 0$ (a) would relax to a continuous distortion configuration (b).

abrupt change from one orientation to another. These walls are similar to Bloch walls in ferromagnetics and were first considered by Helfrich [45].

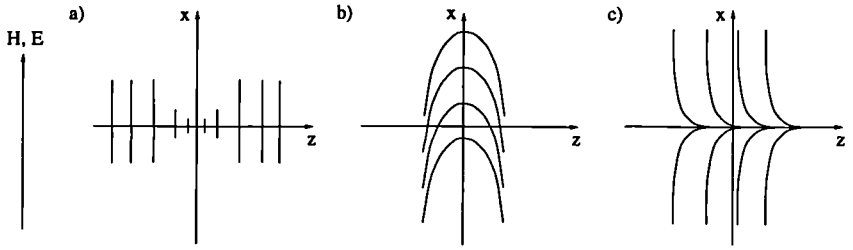

Figure 6.5: Helfrich walls, a) twist wall, b) bend-splay wall parallel to the x axis, c) bend-splay wall parallel to the z axis.

When the theory of Ericksen is used these walls may be stabilised without the use of an electric or magnetic field since the large amount of free energy concentrated at the defect may be reduced by spontaneous *melting* of the liquid crystal to an isotropic state. In the same way that the core of the disclination line in the previous section was isotropic where there was a large distortional energy concentration. In Chapter 8 the possibility of a wall defect occurring in a *twisted nematic layer* is considered. In a twisted nematic layer the aligning effects of the two boundaries are in different directions causing a twist in the layer. The relative stabilities of the two possible configurations, uniform twist throughout the layer or twist wall, are then considered.

6.3 Summary

In this chapter an introduction to defects in nematic liquid crystals has been given with a more detailed discussion on the line disclination and the wall defect. These two forms of defect will subsequently be discussed in Chapters 7 and 8 respectively. The main motivation behind this study is to investigate the influences of various boundary conditions on the defects present in a liquid crystal layer. Using the theory of Oseen-Zöcher-Frank the director configuration of a disclination line near to and attached to a boundary will be discussed in the first part of Chapter 7. The rest of this chapter will be concerned with the detailed structure of the core of a disclination line. Chapter 8 is concerned with the stability of the wall defect in a twisted nematic layer and considers the stabilising effect of melting and biaxiality on the wall defect.

Chapter 7

Disclination Lines

In liquid crystal displays disclination lines can be observed perpendicular to the layer (Figure 1.5). These lines terminate when they *attach* to the bounding plates. Since these boundaries are treated the minimum surface energy configuration occurs when the director is aligned with the preferred direction on the boundary. However the large distortions that exist near the core of the disclination prevent this occurring. The competition between these two aligning effects will be considered in Section 7.1 and 7.2. In Section 7.3 a Ericksen's continuum theory [33] is introduced in order to investigate the core of the disclination line. For analytical and numerical simplification the disclination is taken to lie in the bulk of the liquid crystal sample away from the boundary. The director configuration is greatly simplified and the core structure may then be calculated. A summary of the results obtained in this chapter is then given in Section 7.4.

7.1 Attached disclination lines

The director configuration of a disclination line in the bulk of the liquid crystal sample was found in the previous chapter to be,

$$\phi = c_1\theta + c_2 \tag{7.1}$$

If it is assumed that the disclination is contained within a region of radius $r = R$ and that there exists a disclination core of radius $r = r_c$ with finite energy E_c then the free energy within the sample is,

$$E = \int K\,(\nabla \mathbf{n})^2\,\mathrm{d}v = E_c + \int_0^{2\pi}\int_{r_c}^{R} K\,\frac{\phi_\theta^2}{r^2} r\,\mathrm{d}r\mathrm{d}\theta$$
$$= E_c + 2\pi K {c_1}^2 \ln\left(R/r_c\right) \tag{7.2}$$

If there are *two* disclinations in the sample then the director configuration may be calculated by superposition of solutions of the form (7.1) so that for two disclination lines positioned at $x = -d,\ y = 0$ and $x = d,\ y = 0$ which individually would have the director configurations $\phi = c_{11}\theta + c_{21}$ and $\phi = c_{12}\theta + c_{22}$ respectively then the director angle solution is,

$$\phi = c_{11}\theta_1 + c_{21} + c_{12}\theta_2 + c_{22} \tag{7.3}$$

Where $\theta_1 = \arctan\left(y/(x+d)\right)$ and $\theta_2 = \arctan\left(y/(x-d)\right)$ are the polar angles measured from each of the disclinations (Figure 7.1).

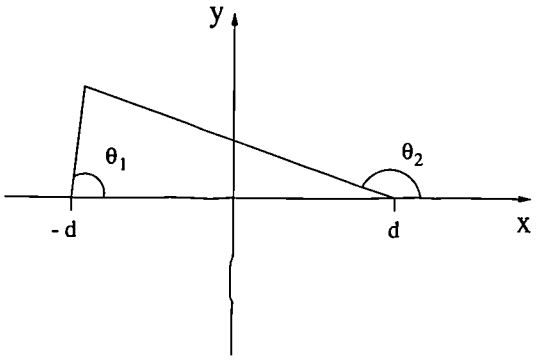

Figure 7.1: Configuration of two disclination lines positioned at $x = -d,\ y = 0$ and $x = d,\ y = 0$.

The corresponding free energy is then,

$$E = 2E_c + \pi K\left(c_{11} + c_{12}\right)^2 \ln\left(R/r_c\right) - 2\pi K c_{11} c_{12} \ln\left(d/r_c\right) \tag{7.4}$$

Equation (7.3) implies that for two disclinations of the same strength ($c_{11} = c_{12}$) the director angle along the line equidistant from both disclinations (where $\theta_1 + \theta_2 = \pi$, $x = 0$ in Figure 7.1) is constant and equal to $\phi = c_{11}\pi + c_{21} + c_{22}$. Equation (7.4) implies that the free energy is independent of R if the two disclinations have opposite strengths ($c_{11} = -c_{12}$) and by differentiation the

force between the two disclination is $2\pi K c_{11} c_{12}/d$. Therefore disclinations with strengths of like signs repel and those of opposite sign attract.
With these results it is possible to calculate the forces of interaction between a disclination and an aligning boundary. If there is a boundary at $x = 0$, say, which exhibits strong homogeneous alignment the director angle must be $\phi = 0$ at $x = 0$. The director configuration around a disclination of strength $+1$ at $x = d$ can therefore be calculated using an image disclination of strength $+1$ placed at $x = -d$ since the director angle along $x = 0$ is then equal to $\phi = \pi$ (equivalent to $\phi = 0$ since $\mathbf{n}^2 = 1$) (Figure 7.2).

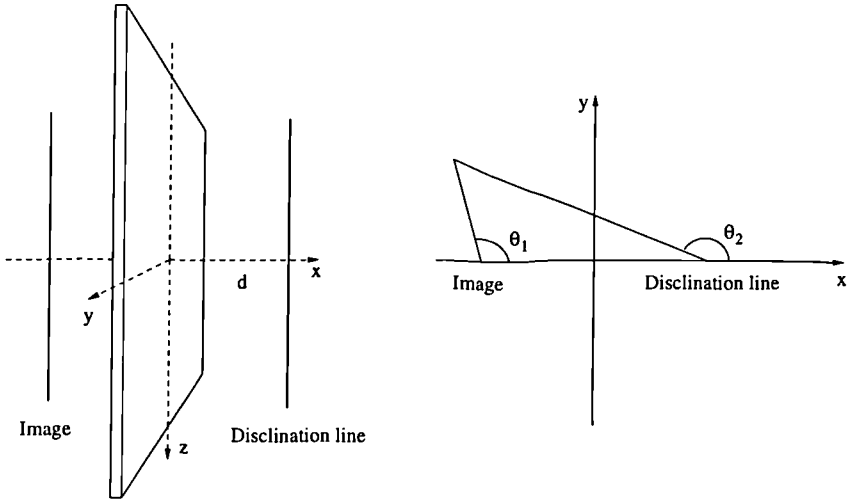

Figure 7.2: Disclination line and its image a distance d from the wall.

The configuration is then,

$$\phi = \theta_1 + \theta_2 \tag{7.5}$$

The force per unit length on the line exerted by the image (or equivalently the boundary) is therefore $f = 2\pi K/d$ away from the boundary. If a disclination line attached to a bounding plate at $x = y = z = 0$ is considered then the anchoring at the surface would cause a repulsive force on the disclination line away from the boundary. With no external influences the disclination line must therefore attach to the boundary at right angles (Figure 7.3).
At large distances from the boundary other effects may influence the orientation of the line such as the other bounding plate, other disclinations, electric

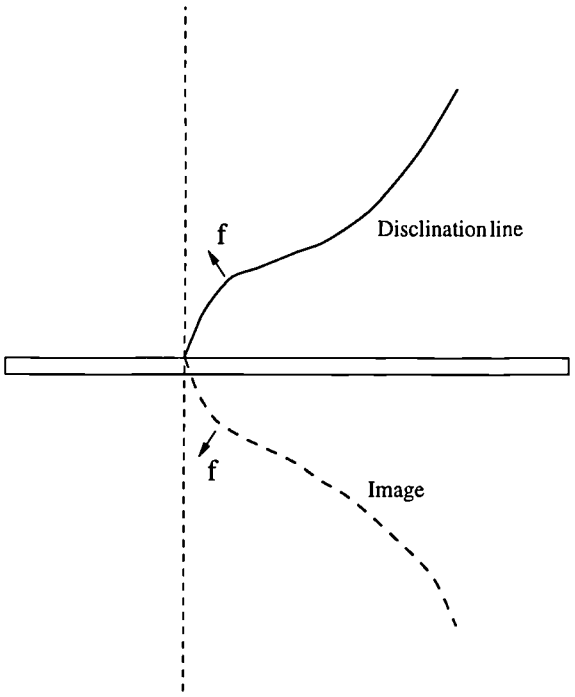

Figure 7.3: The force f on a disclination line *not* attached at right angles to a boundary which, without external influences, would cause it to move perpendicular to the boundary.

or magnetic fields. However, close to the boundary the disclination line will be perpendicular. In the next section the director field is calculated in this region.

7.2 Director configuration of attached lines

Knowing that the disclination attaches at right angles to the boundary, the director configuration, close to the boundary, of an attached line is now investigated. Consider a nematic liquid crystal in the half space $z \geq 0$ with $\mathbf{n} = (\cos\phi(x,y,z), \sin\phi(x,y,z), 0)$ so that the director lies in a plane parallel to the surface $z = 0$. Then assume that there is a disclination line along $x = y = 0$ (Figure 7.4) and that the scalar order parameter $S = S_b$ is constant throughout the liquid crystal sample except in the disclination line core $r < r_c$ which has energy E_c. Subsequently the constant core energy will be neglected since it will not affect the minimization of the total free energy.

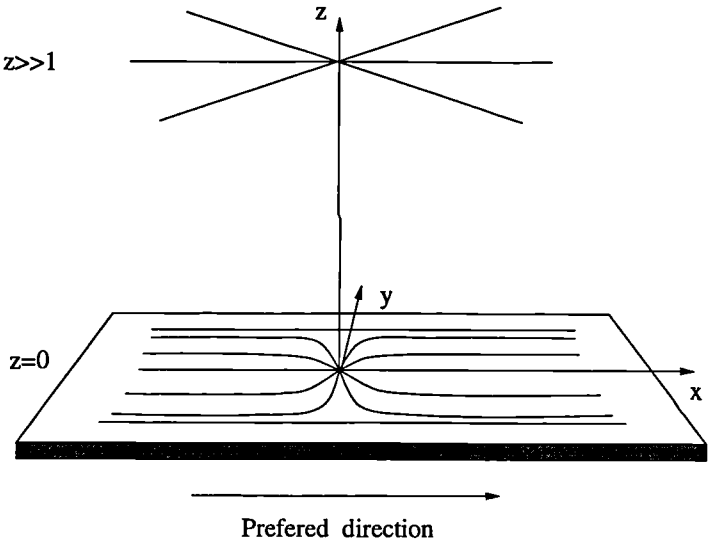

Figure 7.4: Disclination of strength +1 attaching to a treated boundary

The Frank free energy is given by,

$$F = \int_V \frac{1}{2}K_{11}(\operatorname{div}\mathbf{n})^2 + \frac{1}{2}K_{22}(\mathbf{n}\cdot\operatorname{curl}\mathbf{n})^2 + \frac{1}{2}K_{33}(\mathbf{n}\wedge\operatorname{curl}\mathbf{n})^2\,\mathrm{d}v + \int_{S_0} F_0\,\mathrm{d}s \tag{7.6}$$

where $V = \{(x, y, z) : z \geq 0,\ r > r_c\}$, $S_0 = \{(x, y, z) : z = 0,\ r > r_c\}$ and F_0 is the surface energy density for S_0.

Since the boundary is treated there exists a preferred direction at the surface such that the surface energy is minimised when the director at the boundary lies in this direction. To model this preferred direction, which in this case is taken to be parallel to the x axis, the Rapini-Popoular [76] form of the surface energy density,

$$F_0 = W (\sin \phi)^2 \tag{7.7}$$

is taken so that the surface energy density has minima at the director angles $\phi = 0,\ \pi,\ 2\pi, \ldots$ and maxima $\phi = \pi/2,\ 3\pi/2, \ldots$. The boundary is attempting to align the director with the direction $\phi = 0$ (or $\phi = \pi \ldots$). If the anchoring strength, W, is zero then there is no contribution from the surface to the free energy and so the director is free to move in any direction on the boundary. If W is small compared to K then there will be little alignment at the surface and if W is large compared to K then the director will favour alignment in order to reduce the contribution to the energy from the surface term. As $W \to \infty$ the strong anchoring case is reached which insists that $\phi = 0$ on the surface.

Minimization of (7.2) with the one constant approximation leads to the Euler-Lagrange equations,

$$\nabla^2 \phi = 0 \qquad \text{in } z > 0 \tag{7.8}$$

$$\frac{\partial \phi}{\partial z} = \frac{W}{K} \sin 2\phi \qquad \text{on } z = 0 \tag{7.9}$$

Far from the boundary the disclination is not influenced by the alignment effect and therefore the director field is that of a defect in an infinite liquid crystal sample,

$$\phi \to \arctan\left(\frac{x}{y}\right) \qquad \text{as } z \to \infty \tag{7.10}$$

By considering various regions in the liquid crystal layer these equations (7.8, 7.9, 7.10) may be simplified and solved. The first region to be considered is close to the boundary. In order to simplify the equations a form of ϕ_z will be assumed that models the decreasing influence of the boundary alignment

on the director further from the surface $z = 0$. Using the boundary condition (7.9) it will therefore be assumed that ϕ_z near to the boundary has the form,

$$\frac{\partial \phi}{\partial z} = \mu(z) \sin 2\phi \tag{7.11}$$

then by using a Taylor expansion of $\mu(z)$ and the boundary condition (7.9) equation (7.11) may be approximated by,

$$\frac{\partial \phi}{\partial z} = \frac{W}{K} \sin 2\phi \tag{7.12}$$

when $z \ll W/K$. By differentiation,

$$\frac{\partial^2 \phi}{\partial z^2} = \left(\frac{W}{K}\right)^2 \sin 4\phi \tag{7.13}$$

and then (7.8) becomes,

$$\frac{\partial^2 \phi}{\partial x^2} + \frac{\partial^2 \phi}{\partial y^2} + \left(\frac{W}{K}\right)^2 \sin 4\phi = 0 \tag{7.14}$$

This is the elliptic sine-Gordon equation which has been used to model defects in an magnetic field [70]. The governing equation for a defect in an magnetic field can be written as,

$$\frac{\partial^2 \phi}{\partial x^2} + \frac{\partial^2 \phi}{\partial y^2} + \frac{\chi_a H^2}{2K} \sin 4\phi = 0 \tag{7.15}$$

Therefore the effective magnetic field is proportional to W/K. This is encouraging since the magnetic field strength is a measure of the field's ability to orient the director with the field direction. In an equivalent way W/K is the parameter which governs how energetically favourable it is for the director to orientate with the *easy* direction of the boundary compared with the splay distortion of the defect.

A solution of equation (7.14) that has a singularity at $x = y = 0$ is,

$$\phi = \phi_1 = \pm \arctan\left(\frac{\sqrt{1+\zeta^2}}{\zeta} \frac{\sin\left(\frac{W}{K}\zeta\, y\right)}{\sinh\left(\frac{W}{K}\sqrt{1+\zeta^2}\, x\right)}\right) \tag{7.16}$$

where ζ is a constant. This solution (Figure 7.5) is periodic in the y direction and there are an infinite number of singularities at the points $x = 0$, $y = n\pi\left(\frac{K}{W\sqrt{1+\zeta^2}}\right)$. By restricting the solution to be valid only near $y = 0$ and

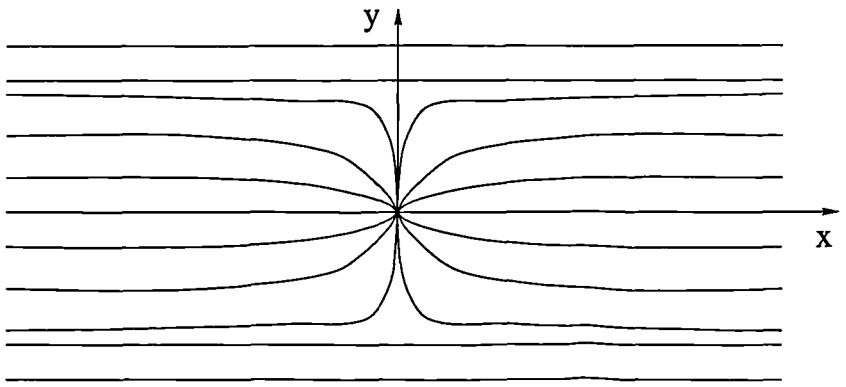

Figure 7.5: +1 line disclination along $x = y = 0$.

replacing all but the singularity at $x = y = 0$ by the director configuration $\mathbf{n} = (1,\ 0,\ 0)$ this solution can be used to model a single disclination line. The region of influence of the defect in the y direction is therefore of order $2\pi\left(\frac{K}{W\sqrt{1+\zeta^2}}\right)$.

From equation (7.14) it is seen that if $x,\ y \gg K/W$ then the solution is simply $\phi = 0$ (or $\phi = 0$) so that the boundary is dominating the director orientation. By comparing this to the region of influence of the defect previously found, the unkown constant ζ may be estimated to be $\sqrt{4\pi^2 - 1}$.

The next region to consider is away from the boundary where $z \gg W/K$. From (7.8) when $z \gg x,\ y$ this equation reduces to,

$$\frac{\partial^2\phi}{\partial x^2} + \frac{\partial^2\phi}{\partial y^2} = 0 \tag{7.17}$$

which has the solution,

$$\phi = \arctan\left(\frac{y}{x}\right) \tag{7.18}$$

The importance of the parameter W/K can be seen in Figure 7.6.

When $W/K \ll 1$ the region of influence of the disclination line is larger than that of the boundary alignment and visa versa when $W/K \gg 1$. In Region 1 in Figure 7.6 the disclination line dominates the director orientation and it is essentially $\phi = \arctan(y/x)$. In Region 2 the boundary dominates the director orientation and is essentially $\phi = 0$.

This model of a +1 disclination does not allow for an escaped core. Including escape leads to more complicated equations but, if possible, may be solved

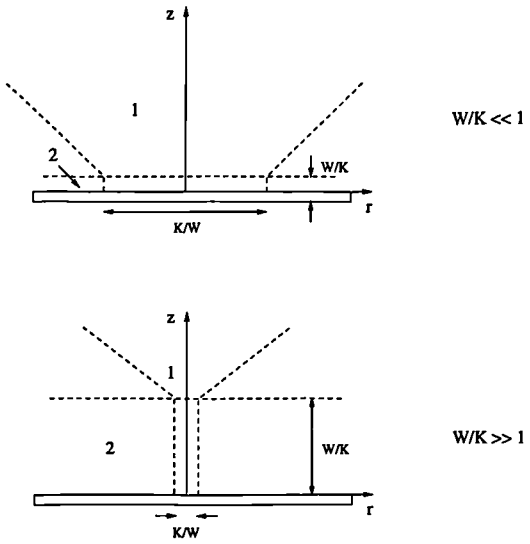

Figure 7.6: Disclination lines attached to a boundary for $W/K \ll 1$ and $W/K \gg 1$. In Region 1 the defect distortions dominate and in Region 2 the boundary alignment dominates.

analytically using more restrictive approximations. When considering the governing equations (7.8) for strength $\pm 1/2$ disclinations any solution of the form $\phi = (1/2)\arctan(f(x,y,z)$ will *not* satisfy the boundary conditions. It is interesting that if the surface energy is modelled by the function, $F_0 = W(\sin 2\phi)^2$ then the boundary condition is $\phi_z = (W/K)\sin(4\phi)$ and the solution is,

$$\phi = \phi_2 = \frac{1}{2}\phi_1 \tag{7.19}$$

and the solution is similar to a $\pm 1/2$ disclination line in a field whose strength decreases with increasing z.

7.3 Disclination line cores

Previously the core of a disclination line was simply taken as a cylinder $r < r_c$ which had a finite energy E_c. In this section a different continuum theory is used which allows for changes in biaxiality and scalar order parameter so that the details of the core may be investigated.

Previous authors have suggested that the scalar order parameters of the order parameter tensor (2.3) will change within the core of a disclination so that

the liquid crystal melts [19] and/or becomes biaxial [80]. A continuum theory which includes these effects within the core has been developed by Ericksen [33] and, using Landau-de Gennes theory, by various authors including Schophol and Sluckin [80]. The continuum theory used by Virga ([11], [87]) based on these theories will subsequently be followed. In Section 7.3.1 the continuum theory is discussed and the governing equations are found. In the rest of this chapter the core of a disclination line in studied using this continuum theory and in the next chapter wall defects are considered with the same theory.

7.3.1 Governing Equations

In biaxial liquid crystals the two eigenvalues S_1 and S_2 are not equivalent and the order parameter cannot be simplified from the form (2.3). Assuming a 2-dimensional director orientation so that the directors $\mathbf{n}_1$ and $\mathbf{n}_2$ can be written as,

$$\mathbf{n}_1 = (-\sin\phi,\ \cos\phi,\ 0) \tag{7.20}$$

$$\mathbf{n}_2 = (0,\ 0,\ 1) \tag{7.21}$$

and the order parameter may be transformed using,

$$S_1 = S - \alpha \tag{7.22}$$

$$S_2 = S + \alpha \tag{7.23}$$

so that when $\alpha = 0$ the eigenvalues are equivalent and the order parameter reduces to that of a uniaxial nematic with scalar order parameter S. The variable α is therefore a measure of the biaxiality of the liquid crystal. The order parameter becomes,

$$\mathbf{Q} = \begin{pmatrix} (S-\alpha)\sin^2\phi - \frac{2}{3}S & -(S-\alpha)\sin\phi\cos\phi & 0 \\ -(S-\alpha)\sin\phi\cos\phi & (S-\alpha)\cos^2\phi - \frac{2}{3}S & 0 \\ 0 & 0 & \frac{1}{3}S - \alpha \end{pmatrix} \tag{7.24}$$

the free energy density can then be calculated from,

$$F_D = \frac{K}{2}\left(|\nabla\mathbf{Q}|^2 + \sigma(\mathbf{Q})\right) \tag{7.25}$$

where $|\nabla \mathbf{Q}|^2 = tr\left((\mathbf{Q}_{,x})^2 + (\mathbf{Q}_{,y})^2 + (\mathbf{Q}_{,z})^2\right)$. The minimization of the free energy integral is then carried out with respect to the three dependent variables ϕ, S and α.

The potential $\sigma(\mathbf{Q})$

The potential will be assumed to be the sum of two functions of S and α modelling the effects on the free energy of changes in phase and biaxiality respectively,

$$\sigma(\mathbf{Q}) = \frac{h_1}{K}\sigma_1(S) + \frac{h_2}{K}\sigma_2(\alpha) = \frac{\kappa_1}{2}\sigma_1(S) + \frac{\kappa_2}{2}\sigma_2(\alpha) \tag{7.26}$$

where κ_1 and κ_2 are positive. The first potential has been studied by both de Gennes [23] and Doi [29] and can be written as,

$$\sigma_1(S) = aS^4 + bS^3 + cS^2 + d \tag{7.27}$$

where the coefficients a, b, c, and d are temperature dependent. The quantity d contributes a constant term to the free energy and therefore does not come into the minimization and can be neglected. The potential may therefore be written as,

$$\sigma_1(S) = S^2\left(\frac{S^2}{4} - (S_u + S_b)\frac{S}{3} + \frac{S_u S_b}{2}\right) \tag{7.28}$$

so that when there are two turning points they occur at $S = S_u$ and $S = S_b$. The effect on the potential function $\sigma_1(S)$ of varying S_u is equivalent to varying temperature T, and is shown in Figure 7.7. The characteristic temperatures of a liquid crystal T^*, T_c and T^+ can be defined as follows. In an undistorted liquid crystal sample then below T^* the liquid crystal is crystalline. Between T^* and T_c the liquid crystal state and the isotropic state are stable but the first is a global minimizer of the energy functional and the second is a local minimizer. Between T_c and T^+ the isotropic state is a global minimizer and the liquid crystal state is locally stable. Above T^+ the only stable state is the isotropic one. Subsequently the temperature is assumed to be in the range, $T^* < T < T^+$ so that the liquid crystalline state is always at least locally stable.

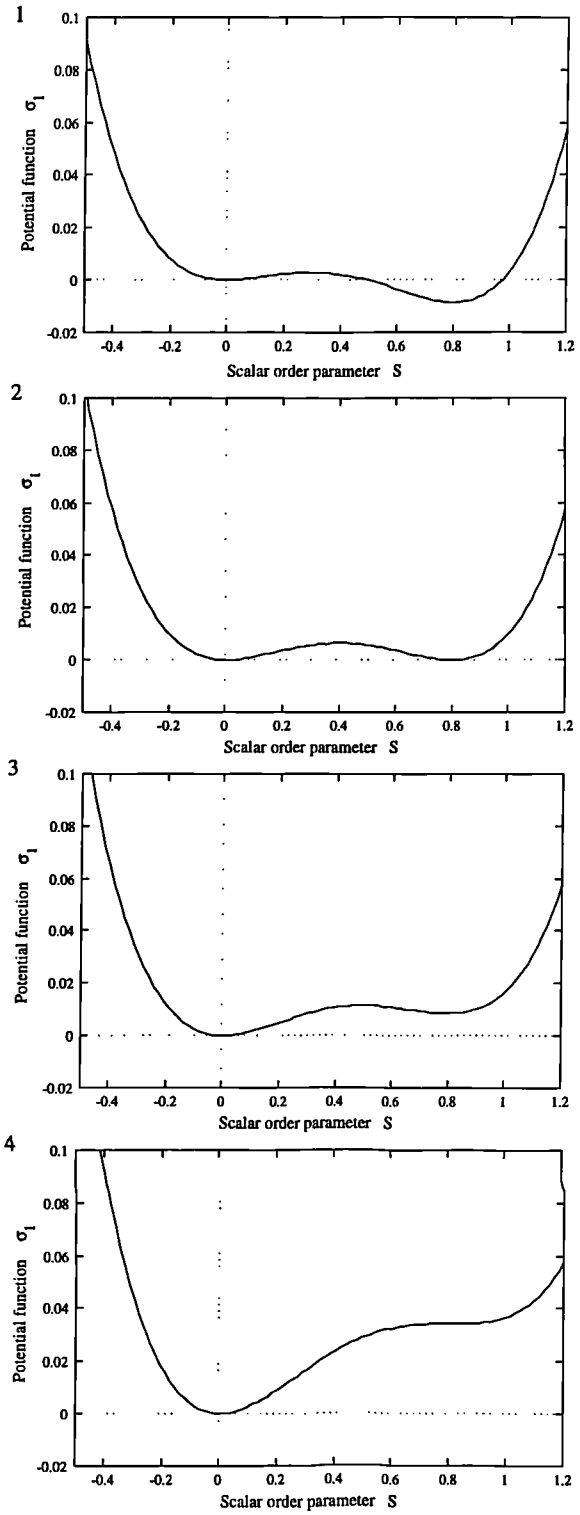

Figure 7.7: Scalar order parameter energy potential $\sigma_1(S)$ at temperatures 1. $T^* < T < T_c$, 2. $T = T_c$, 3. $T_c < T < T^+$, 4. $T = T^+$ for $S_b = 0.8$

The second potential σ_2 should represent the nature of the material to support biaxial states. If the nematic is assumed to be uniaxial in the temperature range $T^* < T < T^+$ then σ_2 will have a minimum at $\alpha = 0$. Following Virga [11], the simplest form of such a potential,

$$\sigma_2(\alpha) = \alpha^2 \tag{7.29}$$

is used. The ratio κ_1/κ_2 will indicate the relative importance of each potential function in the minimization of the energy. If κ_1/κ_2 is large it is energetically more favourable to minimize σ_1 rather than σ_2 and visa versa if κ_1/κ_2 is small. With the above potentials the free energy density becomes,

$$F_D = \frac{K}{2}\left(|\nabla \mathbf{Q}|^2 + \frac{\kappa_1}{2}S^2\left(\frac{S^2}{4} - (S_u + S_b)\frac{S}{3} + \frac{S_u S_b}{3}\right) + \frac{\kappa_2}{2}\alpha^2\right) \tag{7.30}$$

where $\mathbf{Q}$ is (7.24) so that,

$$\begin{aligned} F_D &= \frac{K}{2}\left((S-\alpha)^2(\nabla\phi)^2 + \frac{1}{3}(\nabla S)^2 + (\nabla\alpha)^2 \right. \\ &\quad \left. + \frac{\kappa_1}{2}S^2\left(\frac{S^2}{4} - (S_u + S_b)\frac{S}{3} + \frac{S_u S_b}{2}\right) + \frac{\kappa_2}{2}\alpha^2\right) \end{aligned} \tag{7.31}$$

and the governing equations are the Euler-Lagrange equations of the Lagrangian F_D with respect to the dependent variables ϕ, S and α,

$$0 = \frac{\partial}{\partial x_i}\left(\frac{\partial F_D}{\partial S_i}\right) - \frac{\partial F_D}{\partial S} \tag{7.32}$$

$$0 = \frac{\partial}{\partial x_i}\left(\frac{\partial F_D}{\partial \phi_i}\right) - \frac{\partial F_D}{\partial \phi} \tag{7.33}$$

$$0 = \frac{\partial}{\partial x_i}\left(\frac{\partial F_D}{\partial \alpha_i}\right) - \frac{\partial F_D}{\partial \alpha} \tag{7.34}$$

where the summation convention is assumed and $S_i = \partial S/\partial x_i$. Using (7.31) leads to the governing equations,

$$0 = \nabla^2 S - 3(S-\alpha)(\nabla\phi)^2 - \frac{3\kappa_1}{4}S(S-S_u)(S-S_b) \tag{7.35}$$

$$0 = \nabla^2\phi + \nabla(S-\alpha).\nabla\phi \tag{7.36}$$

$$0 = \nabla^2\alpha + (S-\alpha)(\nabla\phi)^2 - \frac{\kappa_2}{4}\alpha \tag{7.37}$$

In this chapter these equations (7.35, 7.36, 7.37) are used to consider the core of a disclination line. In the next chapter they will be used to model a wall defect within a twisted nematic layer.
At this point it is noted that from (7.36) the Euler-Lagrange equation for ϕ can be simplified if

$$\nabla(S-\alpha).\nabla\phi = 0 \tag{7.38}$$

Knowing the Oseen-Frank description of line disclinations (6.3) models the director angle ϕ well, the director angle is taken to be $\phi = \phi(\theta)$. Then if $S = S(r)$ and $\alpha = \alpha(r)$ (7.38) is automatically satisfied and the Euler-Lagrange equation for ϕ becomes $\phi_{\theta\theta} = 0$ and the Oseen-Frank disclination structure is recovered,

$$\phi = c_1\theta + c_2 \tag{7.39}$$

The free energy density is now,

$$\begin{aligned} F_D &= \frac{K}{2}\left((S-\alpha)^2(\frac{c_1}{r})^2 + \frac{1}{3}(rS_r)^2 + (r\alpha_r)^2 \right. \\ &\quad \left. + \frac{\kappa_1}{2}S^2\left(\frac{S^2}{4} - (S_u+S_b)\frac{S}{3} + \frac{S_uS_b}{3}\right) + \frac{\kappa_2}{2}\alpha^2\right) \end{aligned} \tag{7.40}$$

and the Euler-Lagrange equations for S and α are,

$$0 = S_{rr} + \frac{1}{r}S_r - 3(S-\alpha)\left(\frac{c_1}{r}\right)^2 - \frac{3\kappa_1}{4}S(S-S_u)(S-S_b) \tag{7.41}$$

$$0 = \alpha_{rr} + \frac{1}{r}\alpha_r + (S-\alpha)\left(\frac{c_1}{r}\right)^2 - \frac{\kappa_2}{4}\alpha \tag{7.42}$$

If there exists a disclination at $r = 0$ the energy of the system will be unbounded unless the liquid crystal region is bounded and the first term in the free energy (7.40) is bounded. Hence to obtain a finite free energy the region is restricted to $r \leq R$ and the condition $S - \alpha = 0$ at $r = 0$ is assumed. The governing equations can now be nondimensionalise using $r = Rr^*$. to give,

$$0 = S_{r^*r^*} + \frac{1}{r^*}S_{r^*} - 3(S-\alpha)\left(\frac{c_1}{r^*}\right)^2 - \frac{3\kappa_1R^2}{4}S(S-S_u)(S-S_b) \tag{7.43}$$

$$0 = \alpha_{r^*r^*} + \frac{1}{r^*}\alpha^*_r + (S-\alpha)\left(\frac{c_1}{r^*}\right)^2 - \frac{\kappa_2R^2}{4}\alpha \tag{7.44}$$

The equation parameters are therefore c_1, S_b, κ_1R^2, κ_2R^2 and S_u.

7.3.2 Boundary conditions

The condition that the energy is bounded has supplied a boundary condition at $r = 0$,

$$S(0) = \alpha(0) \tag{7.45}$$

Two forms of boundary conditions at $r = R$ will now be considered, Dirichlet and Neumann conditions. Dirichlet boundary conditions fix the order parameter on the boundary $r = R$ and can be used to model a disclination at $r = 0$ in a cylindrical surface $r = R$. If this surface exhibits an ordering that is equivalent to a scalar order parameter S_0 and is uniaxial then the boundary conditions are,

$$S(R) = S_0 \tag{7.46}$$

$$\alpha(R) = \alpha_0 \tag{7.47}$$

This value S_0 of the scalar order parameter at the boundary will usually be taken to be greater than the value of S in the bulk of the liquid crystal (approx. S_b) since the crystalline structure of the bounding surface is assumed to have more order than the liquid crystal.
Neumann conditions fix the gradient of the order parameter on the boundary $r = R$. This situation can be used to model a disclination in a large region where the boundary has little effect on the structure of the core of the disclination. By ensuring the boundary has little effect on the disclination the system is equivalent to a bounded region embedded in an infinite region. The boundary conditions are,

$$S_{r^*}(R) = 0 \tag{7.48}$$

$$\alpha_{r^*}(R) = 0 \tag{7.49}$$

For Dirichlet boundary conditions there are therefore three boundary conditions (7.45, 7.46, 7.47) and for Neumann boundary conditions there are three boundary conditions (7.45, 7.48, 7.49). For each case the three boundary

conditions are insufficient to find a unique solution to the two second order ordinary differential equations (7.43, 7.43). The essential features of the system may be found by considering the Neumann boundary conditions and therefore the Dirichlet conditions are not considered further in this chapter. In the next chapter Dirichlet conditions will be used to investigate a different system.
The extra boundary conditions needed for a unique solution can be found by investigating the governing equations. If the region close to $r = R$ is considered then $r^* \approx 1$ and since $3\kappa_1 R^2 \gg 1$ the equations reduce to,

$$0 = \frac{3\kappa_1 R^2}{4} S(S - S_u)(S - S_b) \tag{7.50}$$

$$0 = \frac{\kappa_2 R^2}{4} \alpha \tag{7.51}$$

So since $S = S_u$ is an unstable solution there are two extra boundary conditions,

$$S(R) = S_b \text{ or } 0 \tag{7.52}$$

$$\alpha(R) = 0 \tag{7.53}$$

Now looking close to the centre of the disclination line so that the region $r^* \ll 1$ is considered (ensuring that $1/r^* \gg 3\kappa_1 R^2$) then the equations reduce to,

$$0 = S_{r^*r^*} + \frac{1}{r^*} S_{r^*} - 3(S - \alpha)\left(\frac{c_1}{r^*}\right)^2 \tag{7.54}$$

$$0 = \alpha_{r^*r^*} + \frac{1}{r^*} \alpha_r^* + (S - \alpha)\left(\frac{c_1}{r^*}\right)^2 \tag{7.55}$$

which have solutions,

$$S = \lambda_1 (r^*)^n + S(0) \tag{7.56}$$

$$\alpha = \lambda_2 (r^*)^n + S(0) \tag{7.57}$$

where $n = \pm 2|c_1|$, $\lambda_2 = -\lambda_1/3$ and λ_1 is a constant. The derivatives are,

$$S_{r^*}(0) = 2|c_1|\lambda_1(r^*)^{(2|c_1|-1)} \tag{7.58}$$

$$\alpha_{r^*}(0) = -\frac{2}{3}|c_1|\lambda_1(r^*)^{(2|c_1|-1)} \tag{7.59}$$

The gradient at $r = 0$ therefore depends on the strength of the defect. If $c_1 = \pm 1/2$ then the boundary condition is,

$$S_{r^*}(0) = -3\alpha_{r^*}(0) \tag{7.60}$$

and if $c_1 = \pm 1,\ \pm 3/2,\ \pm 2, \ldots$ then,

$$S_{r^*}(0) = 0 \tag{7.61}$$

$$\alpha_{r^*}(0) = 0 \tag{7.62}$$

There are now sufficient boundary conditions to uniquely determine the solution to the problem. For a strength 1/2 disclination line, which will subsequently be considered, these boundary conditions are (7.45, 7.48, 7.49, 7.52, 7.53, 7.60),

$$\begin{aligned} S(0) &= \alpha(0) \\ S_{r^*}(0) &= -3\alpha_{r^*}(0) \\ S_{r^*}(R) &= 0 \\ \alpha_{r^*}(R) &= 0 \\ S(R) &= S_b \text{ or } 0 \\ \alpha(R) &= 0 \end{aligned} \tag{7.63}$$

Solving the governing equations analytically is attempted only in the limited regions above and for the linearised equations below. For the full equations the continuation package AUTO [28] is used to find a numerical solution and investigate how this solution is affected by certain significant parameter changes.

7.3.3 Linear solutions

To obtain a solution near $r^* = 0$ using a linearised set of equations it is not possible to simply linearise using $S \ll 1$, $\alpha \ll 1$ since this is not certain to be true in this region. The boundary condition at $r^* = 0$ is $S - \alpha = 0$ and therefore the only linearisation possible is in the variable $u = S - \alpha$ or equivalently using the approximation $S \approx \alpha$. The governing equations (7.43 ,7.44) then become,

$$0 = \alpha_{r^*r^*} + \frac{1}{r^*}\alpha_{r^*} - \frac{3\kappa_1 R^2}{4}\alpha(\alpha - S_u)(\alpha - S_b) \tag{7.64}$$

$$0 = \alpha_{r^*r^*} + \frac{1}{r^*}\alpha_{r^*} - \frac{\kappa_2 R^2}{4}\alpha \tag{7.65}$$

The choice of potential $\sigma_1(S)$ has therefore led to the necessary conditions, $\alpha \ll 1$ and $\kappa_2 = 3\kappa_1 S_u S_b$. If a quadratic potential function had been chosen for $\sigma_1(S)$ (see for example [11]) then the only necessary condition would be of the kind $\kappa_2 \propto \kappa_1$. However the linearised equations are now valid for near uniaxial situation and for potential coefficients related by $\kappa_2 = 3\kappa_1 S_u S_b$. To first order $\alpha = 0$ and $S(0) = 0$ and the governing equation is,

$$S_{r^*r^*} + \frac{1}{r^*}S_{r^*} - 3\left(\frac{c_1}{r^*}\right)^2 S - \frac{3\kappa_1 R^2}{4}S(S - S_u)(S - 1) = 0 \tag{7.66}$$

which can be further nondimensionalised using $S = S_b S^*$,

$$S^*_{r^*r^*} + \frac{1}{r^*}S^*_{r^*} - 3\left(\frac{c_1}{r^*}\right)^2 S^* - \frac{3\kappa_1 R^2 S_b^2}{4}S^*(S^* - S^*_u)(S^* - 1) = 0 \tag{7.67}$$

where $S^*_u = S_u/S_b$. If a disclination with a specific strength ($c_1 = \pm 1/2, \pm 1 \ldots$) is considered the equation parameters are $\kappa_1 R^2 S_b^2$ and S^*_u. When $S^* \ll 1$ (7.67) is linearised to obtain the equation,

$$S^*_{r^*r^*} + \frac{1}{r^*}S^*_{r^*} - 3\left(\frac{c_1}{r^*}\right)^2 S^* - \frac{3\kappa_1 R^2 S_b^2}{4}S^*_u S^* = 0 \tag{7.68}$$

which has the solution,

$$S^*(r^*) = \mathrm{I}_{\pm\eta}\left(\sqrt{\left(\frac{S^*_u S_b^2 \kappa_1 R^2}{4}\right)}r^*\right) \tag{7.69}$$

or

$$S(r) = S_b\, \mathrm{I}_{\pm\eta}\left(\sqrt{\left(\frac{S_u S_b \kappa_1}{4}\right)}r\right) \tag{7.70}$$

where $\eta = \sqrt{(3c_1^2)}$ and $\mathrm{I}_{\pm\eta}(z)$ is the modified Bessel function [1]. This solution is shown in Figures 7.8 and 7.9 for disclination lines of strength $+1/2$ and $+1$ with the same material parameters as those used in the next section.

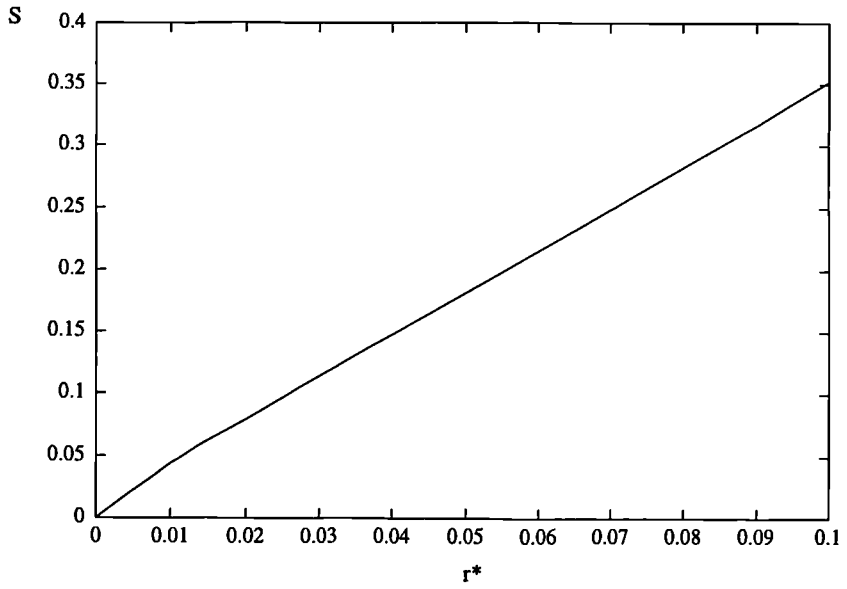

Figure 7.8: Modified Bessel function solution for a strength $+1/2$ disclination line ($c_1 = 0.5$) with $S_b = 0.7$, $S_u = 0.35$, $\kappa_1 R^2 = 1000$.

When $r^2 \ll 1/(\kappa_1 S_b^2)$ this becomes,

$$S(r) \approx \frac{S_b}{\Gamma(\eta+1)} \left(\frac{S_u S_b \kappa_1}{4}\right)^{\eta/2} r^{\eta} \tag{7.71}$$

which is equivalent to (7.54) with $\alpha = 0$.

7.3.4 Numerical solutions

The numerical package, AUTO [28], is used throughout this section to compute the solutions, stability and bifurcation structure of the system. This package is explained in more detail elsewhere [28] and only a summary of its use in the present situation is given here.

AUTO is a numerical package used to find solutions to sets of ordinary differential equations. In this thesis it is used to solve two or three (in Chapter 8) time independent nonlinear ordinary differential equations. Initially the system parameters from the governing equations and the boundary conditions are

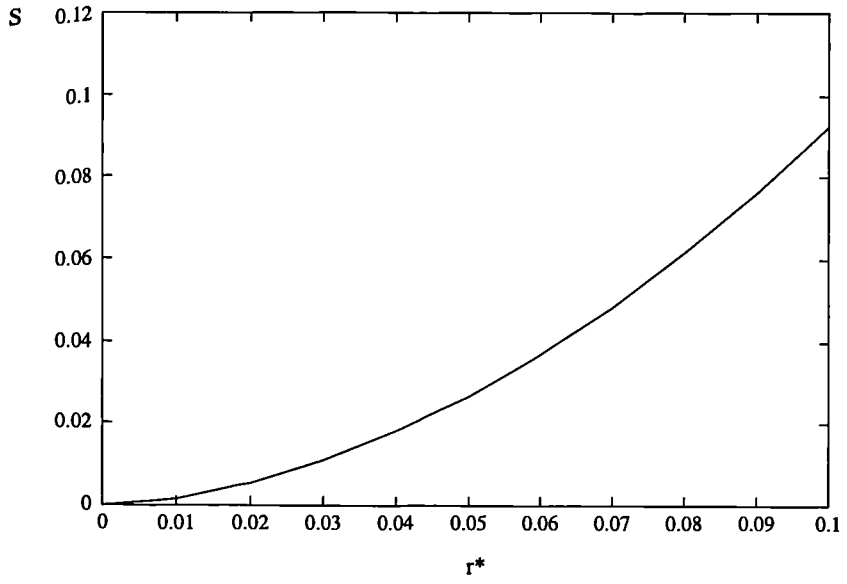

Figure 7.9: Modified Bessel function solution for a strength +1 disclination line ($c_1 = 1$) with $S_b = 0.7$, $S_u = 0.35$, $\kappa_1 R^2 = 1000$.

fixed and the solutions of the equations are found. Once a solution has been found AUTO allows the user to vary up to two of the system parameters (or *continue in* the parameters) and follow the initial solution to investigate how changes in these parameters affect the solution. Along this branch of solutions in parameter space the stability of the solution is calculated and at each point on this branch the program checks if the system undergoes a bifurcation. If a bifurcation of the solution branch occurs the user may then follow the bifurcated branches as before. In the next two chapters AUTO will be used to find the solutions of governing equations and to investigate how these solutions change with variations in the important system parameters.

The governing equations (7.43, 7.44) do not allow for director *escape* ([21], [69]) in the z direction and since in most real liquid crystal layers (except capillary tubes with very small radius) stable integer strength defects ($c_1 = \pm 1, \pm 2, \ldots$) escape to minimize the free energy then these disclination lines cannot realistically be considered. It is interesting to note however that the numerical solution to the equations (7.43, 7.44) with Neumann conditions for a strength ± 1 disclination ($c_1 = \pm 1$) (Figure 7.10) compared to that for a strength $\pm 1/2$ disclination ($c_1 = \pm 1/2$) (Figure 7.11) has very little biaxiality and a much

larger core (the region where $S < S_b$). This agrees with experimental observations [18] that have shown that disclination lines of strength ± 1 are thicker than those of strength $\pm 1/2$.

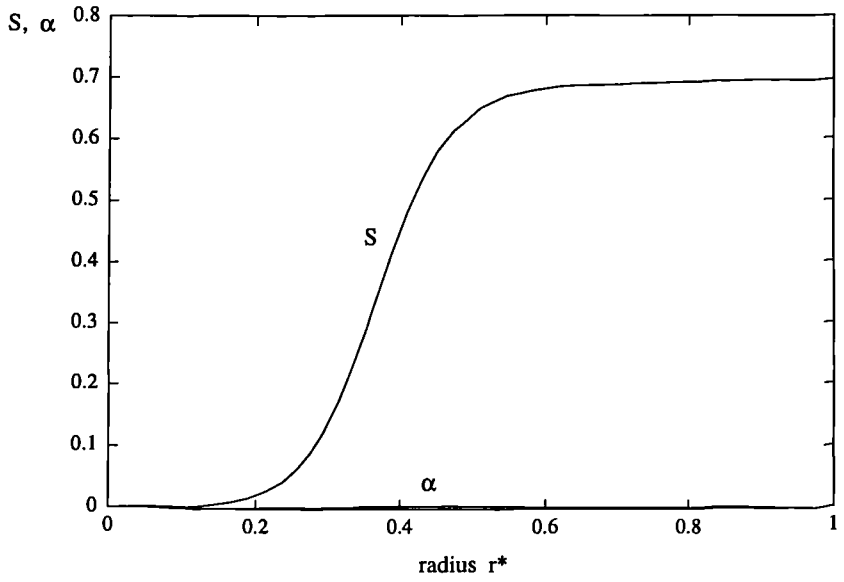

Figure 7.10: Solutions for S and α of a strength ± 1 disclination line for parameter values $c_1 = \pm 0.5$, $S_b = 0.7$, $\kappa_1 R^2 = 1000$, $\kappa_2 R^2 = 10000$, $S_u = 0.35$, $S_0 = 0.7$ and $\alpha_0 = 0$.

The system parameters for biaxial liquid crystals from (7.43, 7.44) and the boundary conditions are c_1, S_b, $\kappa_1 R^2$, $\kappa_2 R^2$, S_u and S_0 and α_0. Variation of the parameters S_b and S_0 yields no results of interest and therefore variation of the parameters $\kappa_1 R^2$, $\kappa_2 R^2$ and S_u whilst keeping the others fixed is considered. As mentioned above *escaped* disclination lines cannot be modelled with equations (7.43, 7.44) and since lines with strength $|c_1| > 1$ are rarely seen [18] only strength $\pm 1/2$ disclination lines are considered. Since a liquid crystalline state is to be modelled the non zero scalar order parameter for the potential minimum should be greater than 0.5 therefore $S_b = 0.7$ is chosen. Since only Neumann conditions are considered further the boundary conditions (7.63) give the values $S_0 = 0.7$ and $\alpha_0 = 0$. It is more convenient to rescale the remaining parameters so that they are $\kappa_1 R^2$, $\kappa = \kappa_2/\kappa_1$ and $S_u^* = S_u/S_b$.
Using AUTO the solution for Neumann boundary conditions shown in Figure 7.11 can be continued in each of the three parameters $\kappa_1 R^2$, κ and S_u^*. Chang-

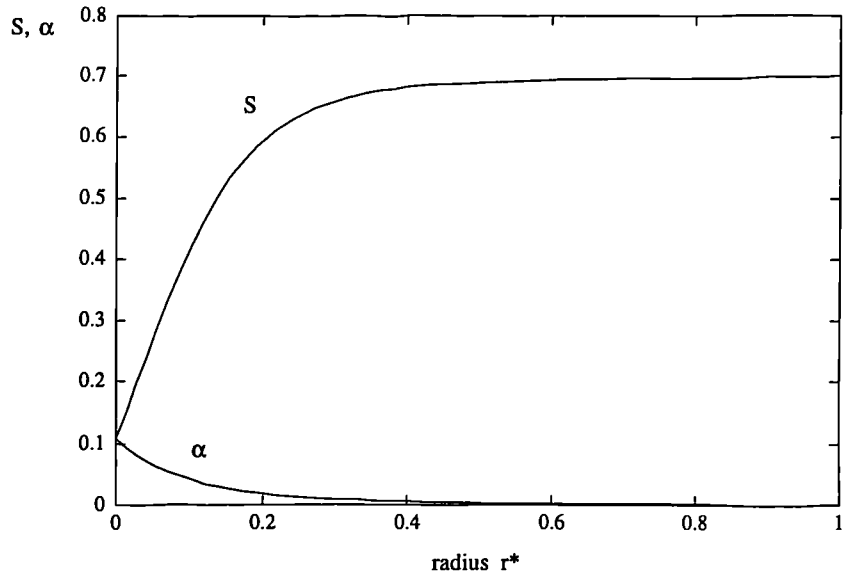

Figure 7.11: Solutions for S and α of a strength $\pm 1/2$ disclination line for parameter values $c_1 = \pm 0.5$, $S_b = 0.7$, $\kappa_1 R^2 = 1000$, $\kappa_2 R^2 = 10000$ and $S_u = 0.35$.

ing $\kappa_1 R^2$ is equivalent to a change in the radius of the region R. Therefore an increase/decrease of $\kappa_1 R^2$ is equivalent to a contraction/stretching of the r^* axis. As $\kappa_1 R^2 \to \infty$ the solution will tend towards the function,

$$S = \begin{cases} S(0) & \text{at } r^* = 0 \\ S_b & \text{elsewhere} \end{cases} \tag{7.72}$$

$$\alpha = \begin{cases} S(0) & \text{at } r^* = 0 \\ 0 & \text{elsewhere} \end{cases} \tag{7.73}$$

In calculating these solutions the value $\kappa_1 R^2 = 1000$ was used and the core width for this parameter value is $r_c \approx 0.1R = \sqrt{10/\kappa_1}$. The parameter κ_1 is the ratio of the coefficient of the potential, h_1 and the Frank constant K (7.26). The Frank constants are of the order of 10^{-11}N and so if the potential coefficient is known the core radius can be calculated from,

$$r_c = 10^{-5}\sqrt{\frac{1}{h_1}} \tag{7.74}$$

Alternatively if the core width is assumed to be of the order of 1000Å $= 10^{-7}$m [54] then the potential coefficient is $h_1 \approx 1$ Nm^{-2}.

Continuations in S_u^* are more interesting. If S_u^* is increased from 0 the solution curve reaches a limit point at $S_u^* = 0.56$ ($S_u = 0.56\ S_b$) (Figure 7.12). Figures 7.13, 7.14, 7.15, 7.16 and 7.17 details the S and α solutions along this branch. On the stable branch from a to b in Figure 7.12 the S and α vary only slightly. The main difference is that with increasing values of S_u^* the core width gets slightly larger, $S(0)$ and $S_{r^*}(0)$ decrease and $\alpha(0)$ decreases whilst $\alpha_{r^*}(0)$ increases.

After the limit point the branch consists of unstable solutions. At first these solutions have a core width which increases linearly with decreasing S_u^* until close to $S_u^* = 0.5$. At this point the *core* dominates the liquid crystal region and the system is attempting to approach the isotropic solution S, $\alpha \equiv 0$. It is at this point that the boundary between liquid crystal and isotropic fluid reaches the boundary $r = R$. The scalar order parameter on the boundary then reduces past zero to a negative value. The solution after this point is clearly unphysical since S must be positive and therefore is of no interest.

The potential function $\sigma_1(S)$ always has a local minimum at $S = 0$ in the parameter range $S_u = (0,\ S_b]$ and in this range there exists another solution branch consisting of the stable solution $S(r^*) \equiv 0$ corresponding to an isotropic fluid throughout the region. The energy of this solution is constant and equal to zero and it is this branch that the unstable solution branch connects to at $S_u^* = 0$.

If S_u^* is increased above the limit point value the system would *jump* down from the upper branch onto this lower energy branch. It has therefore been found that a liquid crystalline state can persist after the clearing point , T_c of an undistorted sample. How far into the isotropic region this liquid crystalline state can reach is determined by the value of S_u^* at the limit point. As the parameter S_u^* passes 0.5 the minimum at $S = S_b$ becomes only locally stable and the minimum at $S = 0$ becomes globally stable. Since the core of the disclination has a scalar order parameter close to zero, at some critical point (the limit point in Figure 7.12) the core will *drag* the rest of the liquid crystal into the lower potential well at $S = 0$ and the system jumps to an isotropic state. The bifurcation diagram (Figure 7.12) will not change when $\kappa_1 R^2$ is changed since, as mentioned previously, this parameter simply causes a stretching/contracting of the r^* axis. Therefore changes in the other equa-

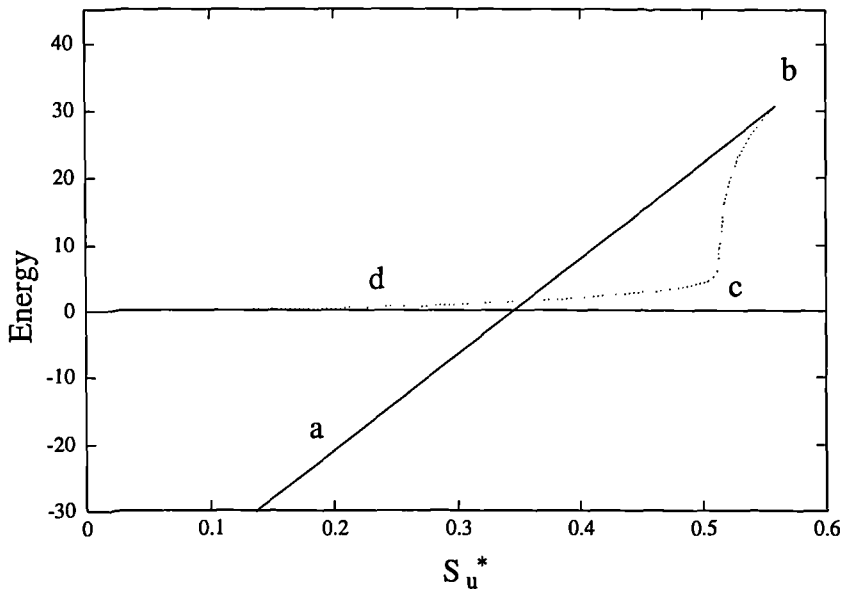

Figure 7.12: Bifurcation diagram showing the stable solution branch a-b, unstable solution branch b-c-d and the isotropic solution $E = 0$.

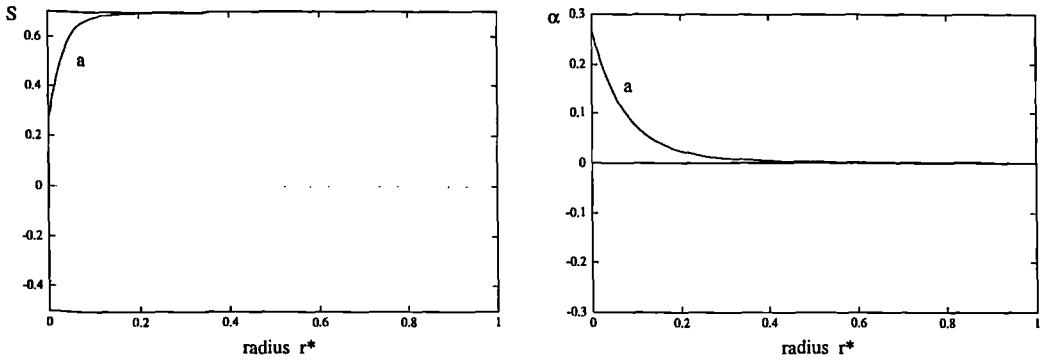

Figure 7.13: Scalar order parameter S and degree of biaxiality α solutions at position a in Figure 7.12.

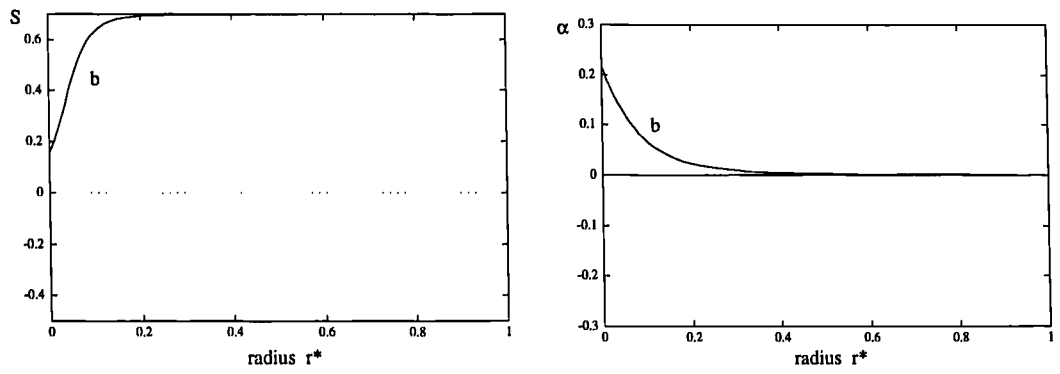

Figure 7.14: Scalar order parameter S and degree of biaxiality α solutions at position b in Figure 7.12.

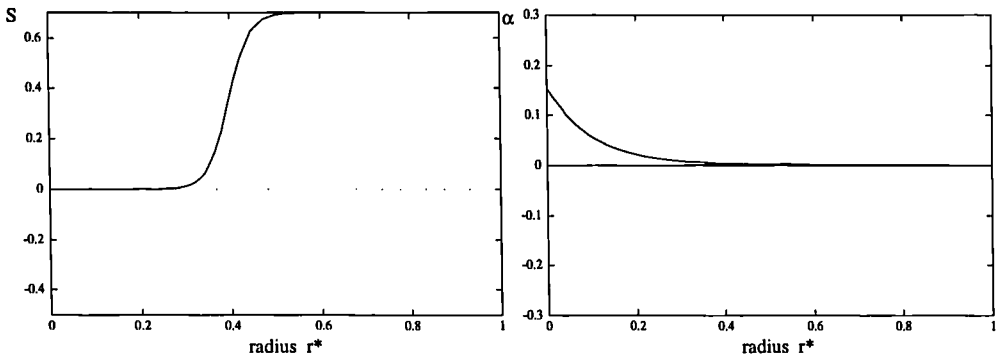

Figure 7.15: Scalar order parameter S and degree of biaxiality α solutions between b and c in Figure 7.12.

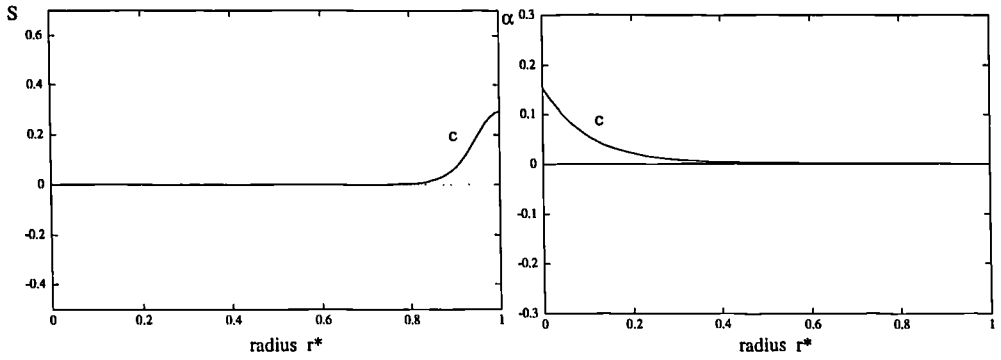

Figure 7.16: Scalar order parameter S and degree of biaxiality α solutions at position c in Figure 7.12.

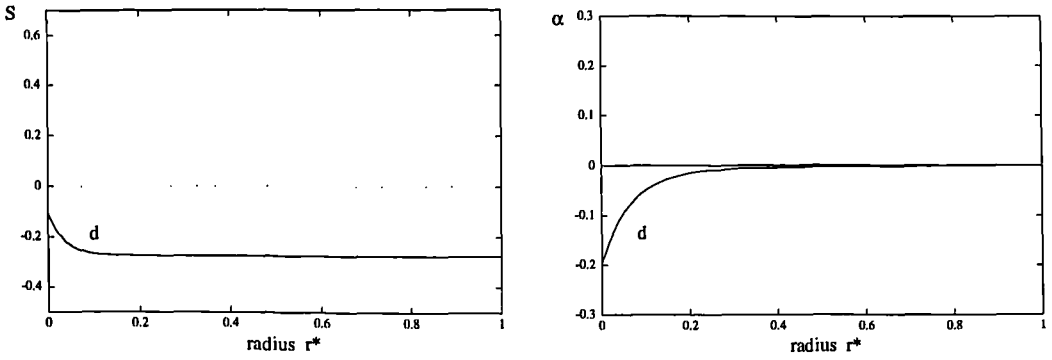

Figure 7.17: Scalar order parameter S and degree of biaxiality α solutions at position d in Figure 7.12.

tion parameter, κ which governs the comparative energetic favourability of the minimization of the potentials σ_1 and σ_2 will be considered.
When κ is large κ_2 is much larger than κ_1 and therefore minimization of the free energy forces the potential σ_2 to be very small. For the form of σ_2 used this means that α is small throughout the region. The liquid crystal is essentially uniaxial and therefore the asymptotic value of S_u^* is the uniaxial value.

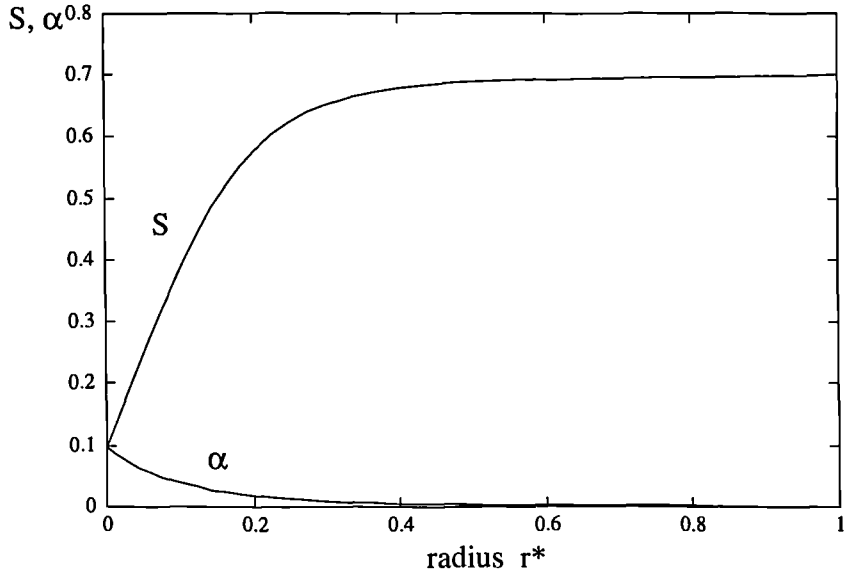

Figure 7.18: S and α solutions for $\kappa = 1$.

Figures 7.18 and 7.19 show the solution for values of the parameter $\kappa = 1$ and $\kappa = 0.001$ respectively. When κ is order 1 or larger the core *melts* to reduce the

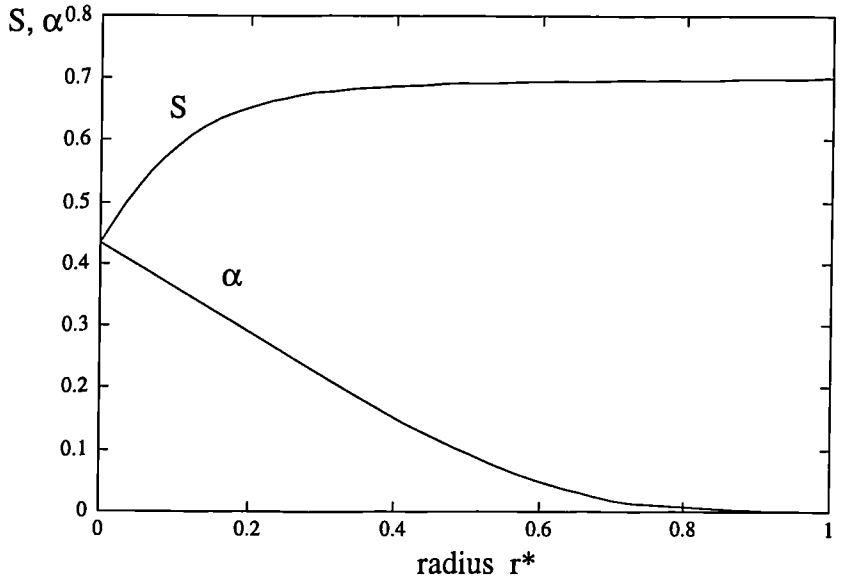

Figure 7.19: S and α solutions for $\kappa = 0.001$.

potential energy. When κ is small the biaxiality potential coefficient is small and the core prefers to have a higher biaxiality and consequently the scalar order parameter S is higher in this case.

Figure 7.20 shows the locus of the limit point in the κ, S_u^* parameter space. As $\kappa \to \infty$, S_u tends to the asymptotic value 0.5603 S_b and as $\kappa \to 0$, $S_u \to S_b$. When κ is very small κ_1 is much larger than κ_2 and minimization of σ_1 is necessary. This is achieved by either $S \approx 0$ or $S \approx S_b$ throughout the layer. If the system starts in a state which has $S \approx S_b$ throughout the layer, i.e. the stable branch with the limit point, then it will continue to have a solution such that $S \approx S_b$ until this state is not locally stable ($S_u = S_b$).

The change in the core and the value of S in the core when κ is altered causes a change in the position in the limit point of Figure 7.12. For low values of κ the core has a high value of S and its ability to *drag* the rest of the liquid crystal to the isotropic state is reduced. Therefore the fold in Figure 7.12 occurs at a higher value of S_u^* and the liquid crystalline state exists for higher values of S_u^* or equivalently, temperature.

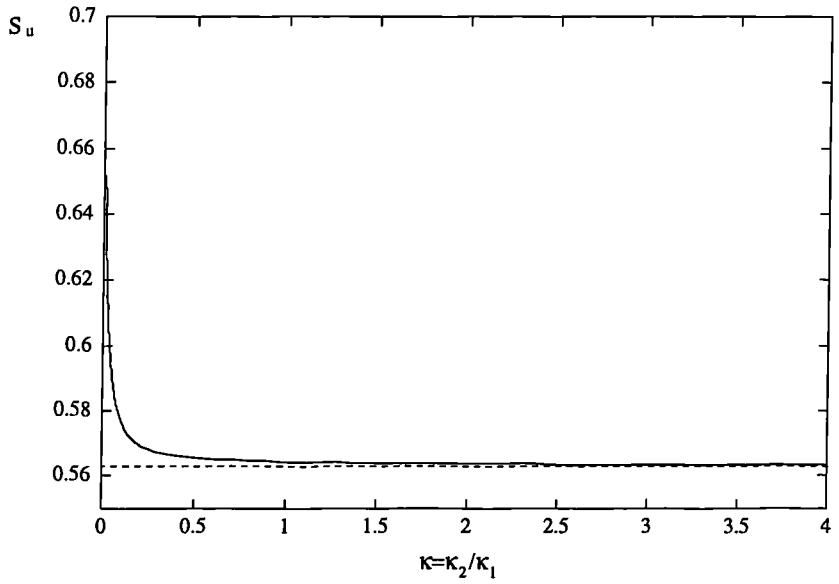

Figure 7.20: Locus of the limit point b (Figure 7.12) in the S_u^*, κ parameter space.

7.4 Summary

In this chapter disclination lines have been considered. In Section 7.1 disclination lines within liquid crystal layers that were attached to each bounding plate were considered. It was found that the anchoring at the boundary caused the disclination line to be repelled from the boundary thus causing the line to attach at right angles to the wall. This conclusion leads to an interesting problem related to the sinusoidal boundaries considered in previous chapters. The disclination line may move within the layer to minimise its free energy. There may be points on the bounding plates such that if the disclination line was attached at these points the line would have minimum energy.
Consider an out of phase sinusoidal boundary cell (Figure 7.21) under the constraint that the line attaches at right angles the disclination line would move to reduce the line length which is proportional to its energy (Figure 7.21 case 1). In an in-phase sinusoidal boundary cell the line would move to the minimum or maximum points on the boundary (Figure 7.21 case 2) or possibly to the line where the distance from the two boundaries is minimized (Figure 7.21 case 3). Since the presence of disclination lines in a liquid crystal display

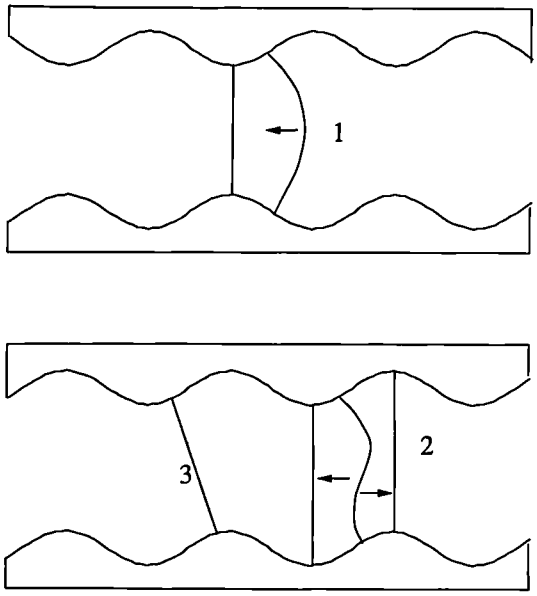

Figure 7.21: Movement of attached disclination lines between out of phase boundaries (1) and in-phase boundaries (2 and 3).

greatly affect the display characteristics the ability to prescribe the regions where these lines exist could be of great value.

In Section 7.2 the director field was calculated near the boundary where the disclination line attaches at right angles. It was found that the alignment on the boundary induced an orienting effect similar to an electric or magnetic field where the effective *field strength* decreased the further the distance from the boundary. The Oseen-Zöcher-Frank continuum theory was used to obtain the director field solution for this situation and it was assumed that there existed a fixed core $r < r_c$ with finite energy at the centre of the disclination line. This core was then investigated in detail using a continuum theory which included the scalar order parameters as dependent variables thus allowing for phase changes and biaxiality to be modelled. The full three dimensional problem of a disclination line attached to a boundary was not considered. Results were found for a disclination line in the bulk of the liquid crystal layer, away from the influence of the boundaries. Analytic solutions were found for the regions near to and far from the disclination line axis. The numerical continuation package AUTO was then used to obtain exact solutions and to investigate the stability and bifurcation structure of these solutions.

Once a solution was found using AUTO continuation in the two parameters S_u^*, the nondimensionalised scalar order parameter at the unstable maximum of the potential $\sigma_1(S)$ and a measure of the temperature, and κ, the ratio of the two potential coefficients κ_2 and κ_1 effectively measuring the relative susceptibility of melting to biaxiality. Increasing S_u^* and equivalently, temperature caused the potential $\sigma_1(S)$ to change so that the liquid crystalline state was only locally stable. The core of the disclination where the scalar order parameter S was near to zero was therefore in the global minimum of the potential and caused the system to jump (at around $S_u = 0.56\ S_b$ for high $\kappa = \kappa_2/\kappa_1$) to the isotropic state. When variations of κ were considered it was found that for low values of κ the core of the disclination had a higher value of S and therefore the minimum of the potential at $S = 0$ had to be *more* stable than the minimum at S_b or equivalently the parameter S_u^* had to be larger to produce the jump to an isotropic state. For lower values of κ the liquid crystalline state was therefore stable at higher temperatures.

In the next chapter the same continuum theory used in Section 7.3 will be used to consider wall defects in twisted nematic layers.

Chapter 8

Twist layers

A twist layer is formed when a nematic liquid crystal sample is sandwiched between two treated surfaces which induce strong homogeneous boundary conditions. If one of the surfaces is twisted the torque exerted by the surface will induce a twist in the director field (Figure 8.1). When a field is applied to the cell it is possible to induce a concentration of the twisting into a small region of the cell. This high distortion region is a Helfrich wall [45]. It is a form of defect where the director is defined at *all* points in the cell (unlike in a line disclination where the director is undefined along the line $r = 0$) but the orientation of the director is changed from one value to another across a very short distance. In this chapter a twist cell with *no* applied field is considered but the liquid crystal scalar order parameters are allowed to vary. In this way Helfrich walls are obtained without a field where the minimization of the energy is possible due to melting around the wall. In Section 8.2 it is assumed that there is no twist and analytic solutions to the governing equations are presented. In Section 8.3 the full equations are solved numerically using the continuation package AUTO used in the Section 7.3.

The continuum theory of Section 7.3 is used and for the system described in Figure 8.1 where all dependent variables depend only on the z coordinate then, when nondimensionalised by $K/4$, the free energy (7.31) becomes,

$$F_D = \frac{2}{3}S_z^2 + 2\alpha_z^2 + 2(S-\alpha)^2\phi_z^2 + \kappa_1\sigma_1(S) + \kappa_2\sigma_2(\alpha) \tag{8.1}$$

where ϕ is the azimuthal or twist angle, that is the angle in the xy-plane from the director to the x axis. The other two dependent variables are the uniaxial

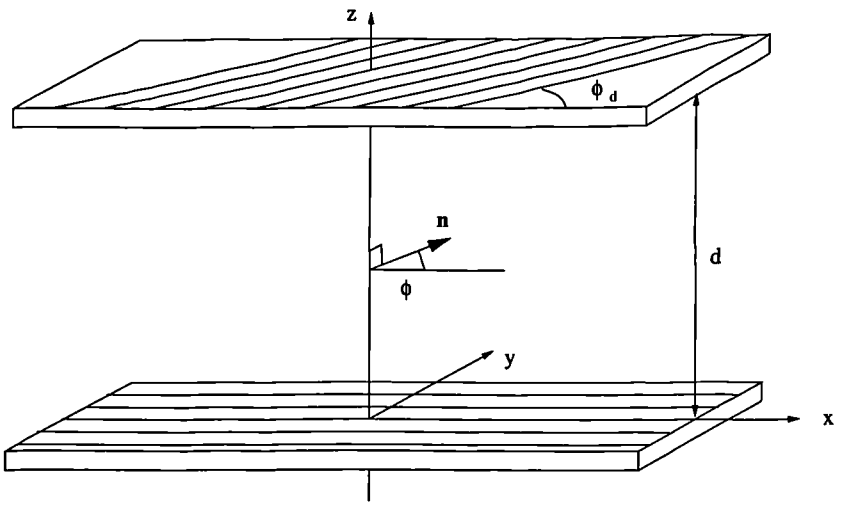

Figure 8.1: Schematic of a twisted nematic layer

scalar order parameter S and the degree of biaxiality α as discussed in Section 7.3.1. The Euler-Lagrange equations are then,

$$0 = S_{zz} - 3(S-\alpha)\phi_z^2 - \frac{3\kappa_1}{4}\frac{\mathrm{d}\sigma_1}{\mathrm{d}S} \tag{8.2}$$

$$0 = \alpha_{zz} + (S-\alpha)\phi_z^2 - \frac{\kappa_2}{4}\frac{\mathrm{d}\sigma_2}{\mathrm{d}\alpha} \tag{8.3}$$

$$0 = \left((S-\alpha)^2\phi_z\right)_z \tag{8.4}$$

The boundary conditions for ϕ are derived from the fact that there exists strong homogeneous anchoring on the surfaces $z = \pm d$ so that the director is fixed parallel to the boundary. Without loss of generality $\phi = 0$ on $z = 0$ is assumed and the general form of the ϕ boundary conditions is therefore,

$$\begin{aligned} \phi &= 0 \quad \text{on} \quad z = 0 \\ \phi &= \phi_d \quad \text{on} \quad z = d \end{aligned} \tag{8.5}$$

The Dirichlet boundary conditions described in Section 7.3.2 are used for S and α the general form of which are,

$$S = S_0 \quad \text{on} \quad z = 0$$

$$
\begin{aligned}
S &= S_d \quad \text{on} \quad z = d \\
\alpha &= \alpha_0 \quad \text{on} \quad z = 0 \\
\alpha &= \alpha_d \quad \text{on} \quad z = d
\end{aligned}
\tag{8.6}
$$

In Section 8.2 where the twist angle $\phi_d = 0$ a solution is found for the general boundary conditions. However in Section 8.3 it is assumed that the boundaries are identical so that $S_0 = S_d$ and $\alpha_0 = \alpha_d$. It is also assumed that the boundaries prescribe a scalar order parameter $S_0 = S_d$ greater than the liquid crystal bulk scalar order parameter S_b and are uniaxial so that the boundary conditions are,

$$
\begin{aligned}
S_0 &= S_d > S_b \qquad (8.7) \\
\alpha_0 &= \alpha_d = 0 \qquad (8.8)
\end{aligned}
$$

The values $S_d = 0.8$ and $S_b = 0.7$ will therefore be taken throughout this chapter. More general boundary conditions may be used in numerically solving the governing equations but the above simplification gives the essential features of the defect structure within the layer. It is possible to solve the governing equations analytically for two simplified cases. The first is when there is constant twist and the boundaries are not present and the second when there is no twist present in the layer. These two cases are considered in the next two chapters.

8.1 Constant Twist

By considering the *bulk* of the liquid crystal so that the boundaries do not influence the liquid crystal the governing equations (8.2, 8.3, 8.4) may be solved when the layer has constant twist so that $\phi_z = \lambda$. Then the equations reduce to,

$$
0 = S_{zz} - 3(S - \alpha)\lambda^2 - \frac{3\kappa_1}{4}\frac{\mathrm{d}\sigma_1}{\mathrm{d}S} \tag{8.9}
$$

$$0 = \alpha_{zz} + (S-\alpha)\lambda^2 - \frac{\kappa_2}{4}\frac{\mathrm{d}\sigma_2}{\mathrm{d}\alpha} \tag{8.10}$$

$$0 = \left((S-\alpha)^2\lambda\right)_z \tag{8.11}$$

The third equation then has the solution,

$$S = \alpha \pm \sqrt{\frac{p}{\lambda}} \tag{8.12}$$

where p is constant. Substituting this into equation (8.9) and (8.10) leaves the equations,

$$0 = S_{zz} \mp 3\lambda^2\sqrt{\frac{p}{\lambda}} - \frac{3\kappa_1}{4}\frac{\mathrm{d}\sigma_1}{\mathrm{d}S} \tag{8.13}$$

$$0 = S_{zz} \pm \lambda^2\sqrt{\frac{p}{\lambda}} - \left.\frac{\kappa_2}{4}\frac{\mathrm{d}\sigma_2}{\mathrm{d}\alpha}\right|_{\alpha=S\mp\sqrt{\frac{p}{\lambda}}} \tag{8.14}$$

If the scalar order parameter is *not* constant then for the two equations (8.13) and (8.14) to be consistent the potentials σ_1 and σ_2 and the constants κ_1 and κ_2 must satisfy the equation,

$$0 = \pm 4\lambda^2\sqrt{\frac{p}{\lambda}} + \frac{3\kappa_1}{4}\frac{\mathrm{d}\sigma_1}{\mathrm{d}S} - \left.\frac{\kappa_2}{4}\frac{\mathrm{d}\sigma_2}{\mathrm{d}\alpha}\right|_{\alpha=S\mp\sqrt{\frac{p}{\lambda}}} \tag{8.15}$$

In general this does not occur (for non-constant S) and therefore the only other solution occurs when $S_{zz} = 0$. For the potentials discussed in Section 7.3.1 (7.29, 7.28) the only solution is in fact when $S_z = 0$ and then S and α are constant. Substituting the potentials,

$$\sigma_1(S) = S^2\left(\frac{S^2}{4} - (S_u + S_b)\frac{S}{3} + \frac{S_u S_b}{2}\right) \tag{8.16}$$

$$\sigma_2(\alpha) = \alpha^2 \tag{8.17}$$

into (8.13, 8.14) gives,

$$p = \lambda\left(\frac{S\kappa_2}{2\lambda^2 + \kappa_2}\right)^2 \tag{8.18}$$

and S must satisfy the cubic equation,

$$0 = S(S-S_u)(S-S_b) + \frac{4\lambda^2\kappa_2}{\kappa_1(2\lambda^2+\kappa_2)}S \tag{8.19}$$

which, with $\lambda = \phi_d/d$ has the solutions,

$$S = 0 \tag{8.20}$$

$$\begin{aligned} S = {} & 0.5S_b + 0.5S_u + 0.5\Big((2\kappa_1 S_b^2\phi_d^2 + \kappa_1 S_b^2\kappa_2 d^2 - \\ & 4\kappa_1 S_u S_b \phi_d^2 - 2\kappa_1 S_u S_b \kappa_2 d^2 + 2\kappa_1 S_u^2 \phi_d^2 + \\ & \kappa_1 S_u^2 \kappa_2 d^2 - 16\kappa_2\phi_d^2)/\kappa_1(2\phi_d^2 + \kappa_2 d^2)\Big)^{1/2} \end{aligned} \tag{8.21}$$

$$\begin{aligned} S = {} & 0.5S_b + 0.5S_u - 0.5\Big((2\kappa_1 S_b^2\phi_d^2 + \kappa_1 S_b^2\kappa_2 d^2 - \\ & 4\kappa_1 S_u S_b \phi_d^2 - 2\kappa_1 S_u S_b \kappa_2 d^2 + 2\kappa_1 S_u^2 \phi_d^2 + \\ & \kappa_1 S_u^2 \kappa_2 d^2 - 16\kappa_2\phi_d^2)/\kappa_1(2\phi_d^2 + \kappa_2 d^2)\Big)^{1/2} \end{aligned} \tag{8.22}$$

Then α is calculated using (8.12) with (8.18) so that,

$$\alpha = \left(\frac{1}{1 + (\kappa_2 d^2)/(2\phi_d^2)}\right) S \tag{8.23}$$

The two solutions (8.21) and (8.22) are real when,

$$\left(\frac{d}{\phi_d}\right)^2 > \frac{16}{\kappa_1(S_b - S_u)^2} - \frac{2}{\kappa_2} \tag{8.24}$$

If this condition is not met then the only solution is $S = 0$. It will be seen in later sections that there are certain regions in the ϕ_d-d parameter space where the bulk of the liquid crystal has melted so that $S = 0$, regions where the order parameter is close to S_b and some regions where it is possible to obtain both forms of solutions. The above solution for S is shown in Figure 8.2.
After $d/\phi_d = 7.87$ there are three solutions one melted ($S = 0$), one liquid crystal ($S > 0.45$) which are both stable (due to the minima of the potential function $\sigma_1(S)$) and an unstable solution ($0 < S < 0.45$).

8.2 No Twist

To solve the governing equations with the boundary conditions analytically the assumption that there is *no* twist present will be used so that $\phi_d = 0$. The equation (8.4) therefore has the solution $\phi \equiv 0$ and using the potentials discussed in Section 7.3.1 the governing equations reduce to,

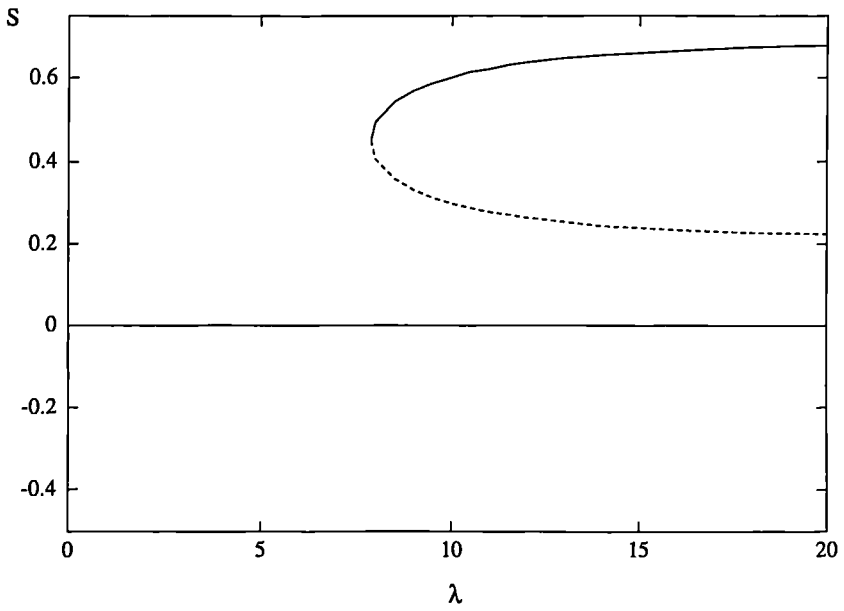

Figure 8.2: Solutions for constant S in a constant twist cell with parameter values $S_b = 0.7$, $S_u = 0.2$, $\kappa_1 = \kappa_2 = 1$.

$$0 = S_{zz} - \frac{3\kappa_1}{4} S^2 (S - S_u)(S - S_b) \tag{8.25}$$

$$0 = \alpha_{zz} - \frac{\kappa_2}{4}\alpha \tag{8.26}$$

with the boundary conditions,

$$\begin{aligned} S(0) &= S_0 \\ S(d) &= S_d \\ \alpha(0) &= \alpha_0 \\ \alpha(d) &= \alpha_d \end{aligned} \tag{8.27}$$

The solution to the second equation (8.26) subject to the boundary conditions (8.27) is,

$$\alpha = \alpha_d \frac{\sinh\left(\sqrt{\kappa_1} z/2\right)}{\sinh\left(\sqrt{\kappa_1} d/2\right)} - \alpha_0 \frac{\sinh\left(\sqrt{\kappa_1}(z-d)/2\right)}{\sinh\left(\sqrt{\kappa_1} d/2\right)} \tag{8.28}$$

The first equation can be solved by multiplying the equation by S_z and integrating to obtain,

$$0 = (S_z)^2 - \frac{3\kappa_1}{4}\sigma_1(S) + D_1 \tag{8.29}$$

where $\sigma_1(S)$ is the potential discussed in Section 7.3.1 and D_1 is a constant. It may be assumed, without loss of generality, that $S_0 \geq S_d$. There are then three possibilities,

1. $S(z)$ attains its maximum in the layer
2. $S(z)$ attains its minimum in the layer
3. $S(z)$ attains its minimum at $z = d$

Then (8.29) can be evaluated at the max/min point to obtain D,

1. $D_1 = \frac{3\kappa_1}{4}\sigma_1(S_{max})$
2. $D_1 = \frac{3\kappa_1}{4}\sigma_1(S_{min})$
3. $D_1 = \frac{3\kappa_1}{4}\sigma_1(S_d) - ((S_z)_d)^2$

where S_{max}, S_{min} are the maximum/minimum values of S and $(S_z)_d$ is the value of S_z at $z = d$. In all three cases the value of D_1 ensures that equation (8.29) does not imply an imaginary value for S_z.
Thus (8.29) has the solution,

$$z = \int_z^{S_0} \frac{\mathrm{d}S}{\left(\frac{3\kappa_1}{4}\sigma_1(S) + D_1\right)^{1/2}} + D_2 \tag{8.30}$$

which leads to the implicit solution given in Byrd and Friedman [17],

$$S(z) = \arccos\left(\mathrm{cn}((z - D_2)/g, k)\right) \tag{8.31}$$

where,

$$g = 1/\left(AB\right)^{1/2} \tag{8.32}$$

$$k^2 = \frac{(A+B)^2 - (2(S_0 - S_u))^2}{4AB} \tag{8.33}$$

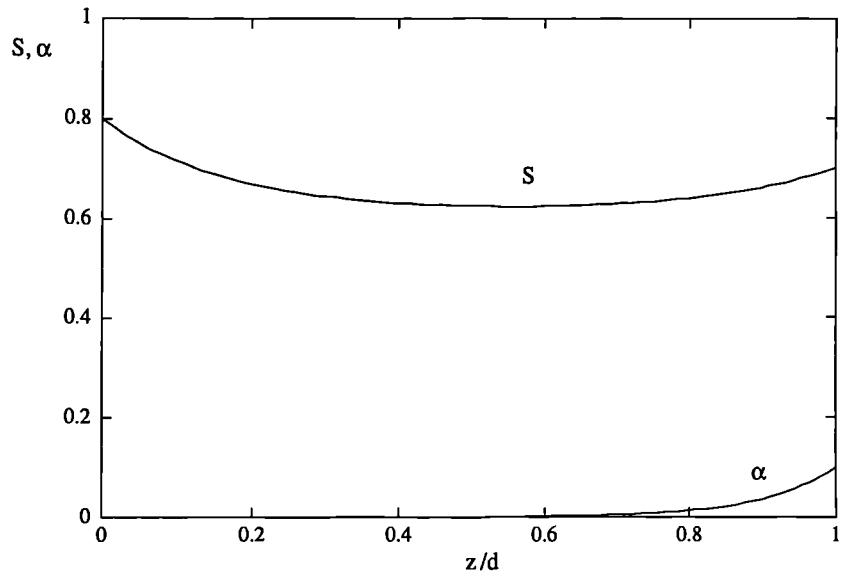

Figure 8.3: Solutions for S and α in a no twist cell with parameter values $S_0 = 0.8$, $S_d = 0.7$, $S_b = 0.6$, $S_u = 0.3$, $\alpha_0 = 0$, $\alpha_d = 0.1$, $\kappa_1 = \kappa_2 = 1$ and $d = 1$.

where $A^2 = (S_0 - \mathrm{Re}(c))^2 + (\mathrm{Im}(c))^2$, $B^2 = (2S_u - S_0 - \mathrm{Re}(c))^2 + (\mathrm{Im}(c))^2$ and c and $\bar{c}$ are the complex roots of the polynomial, $\frac{3\kappa_1}{4}\sigma_1(S) + D_1$.
The two constants of integration, D_1 and D_2 can then be found using the boundary conditions $S(0) = S_0$ and $S(d) = S_d$. The solutions for S and α for particular parameter values are shown in Figure 8.3.
The solution in Figure 8.3 is typical and altering the various equation parameters and boundary conditions gives no unexpected results. The analytic solution does give insight into the effects of twist. When the numerical solution is found in the Section 8.3 it can be compared to Figure 8.4 which is the no-twist analytical solution found in this chapter using the same equation parameters and boundary conditions.

8.3 Numerical Solutions

The full equations (8.2, 8.3 and 8.4) with the boundary conditions (8.5, 8.6) and the potentials (7.28, 7.29) may be solved using the numerical package AUTO [28] described in Section 7.3.4. Using this package it is also possible

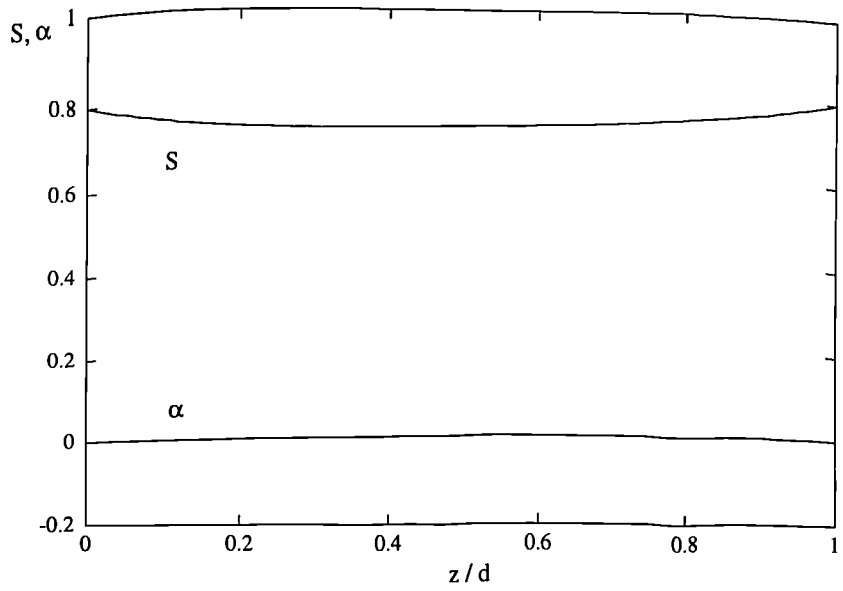

Figure 8.4: Solutions for S and α in a no twist cell with parameter values $S_0 = 0.8$, $S_d = 0.8$, $S_b = 0.7$, $S_u = 0.35$, $\alpha_0 = 0$, $\alpha_d = 0$, $\kappa_1 = \kappa_2 = 1$ and $d = 9$.

to investigate how the solution changes when parameters in the governing equations and boundary conditions are altered.

Figure 8.5 shows the S, α and ϕ solutions when $\kappa_1 = 1$, $\kappa_2 = 1$, $d = 9$, $S_0 = S_d = 0.8$, $S_b = 0.7$, $S_u = 0.35$, $\alpha_0 = \alpha_d = 0$ and $\phi_d = 1.6$. This solution may be compared to Figure 8.4 which is the analytic solution for no twist with the same parameter values. For the twist cell biaxiality, α, is present throughout the region and the scalar order parameter, S, is lower than the bulk scalar order parameter from the potential ($S_b = 0.7$) whereas in the no twist cell there is no biaxiality and the scalar order parameter never falls below $S_b = 0.7$.

The value of ϕ_z in Figure 8.5 shows that there is a larger amount of twist at the centre of the cell than at the boundaries and the scalar order parameter, S, reduces to compensate for the increased distortional energy. The other important point is that even though the biaxiality potential favours $\alpha = 0$ and the boundary conditions are $\alpha_0 = \alpha_d = 0$ there *is* biaxiality present in the cell. This is due to the second terms in (8.2) and (8.3). The relatively high twist at the centre leads to a high value of ϕ_z. The corresponding high energy is

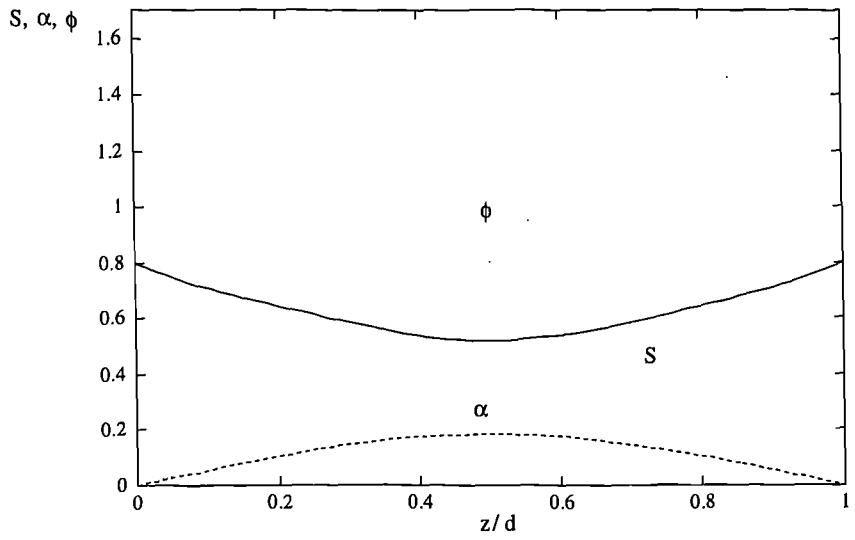

Figure 8.5: Twisted layer S, α and ϕ solutions for $\kappa_1 = 1$, $\kappa_2 = 1$, $d = 9$, $S_0 = S_d = 0.8$, $S_b = 0.7$, $S_u = 0.35$, $\alpha_0 = \alpha_d = 0$ and $\phi_d = 1.6$

reduced by a decrease in $S - \alpha$ or alternatively a decrease in S and an increase in α.

It is now possible using AUTO to investigate the changes to this solution as the parameters vary. The main geometrical parameter is the gap width, d. Figure 8.6 shows the free energy of the solution as AUTO follows the solution whilst varying the gap width d. There are two limit points, l_1 and l_2, in the solution branch at gap widths 8.4 and 29.7 between which the exists two stable solutions and one unstable solution. The units for the gap width cannot be found without knowing the order of the potential coefficients κ_1 and κ_2. From the approximate value found in Section 7.3.4 the units of gap width are 0.316 microns. Multiple solutions therefore exist between gap widths 2.65μm and 9.39μm. The stable solutions are shown in Figures 8.7, 8.8 and 8.9 in this region for a gap width $d = 20$ corresponding to 6.32μm.

In Figures 8.7, 8.8 and 8.9 Solution 1 has almost uniform twist with a relatively high scalar order parameter S denoting a liquid crystalline state and a small amount of biaxiality. Solution 2 however has a large twist gradient around the centre of the cell (near $z = d/2$), a corresponding region where the scalar order parameter S is low which indicates melting of the liquid crystal to an isotropic state and a concentration of biaxiality in the same region around $z = d/2$.

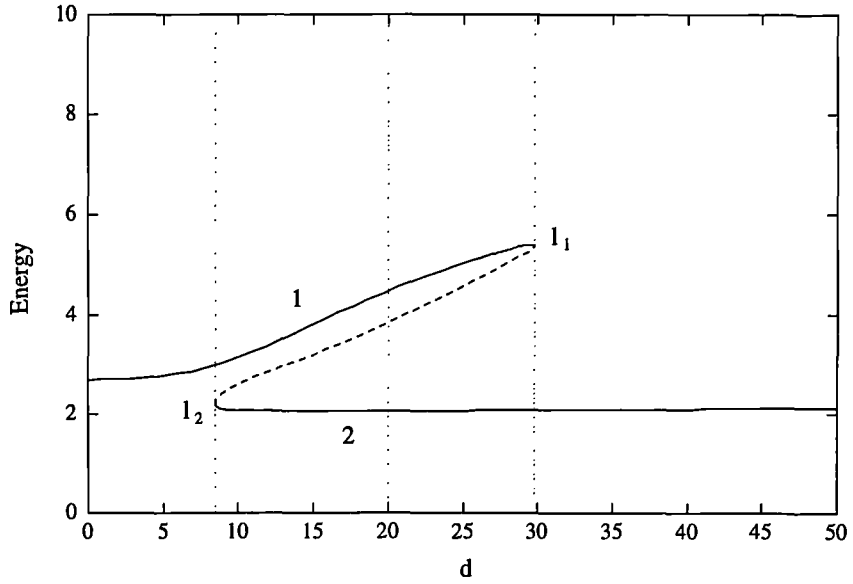

Figure 8.6: Fold in the solution curve as the gap width varies with the limit points l_1 and l_2 and the two stable solutions 1 and 2.

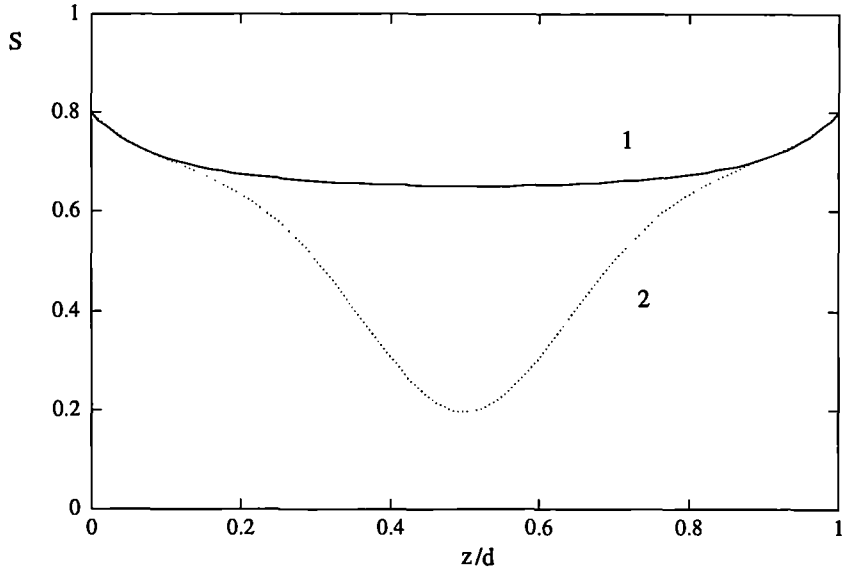

Figure 8.7: Multiple stable solutions of S in a twisted layer for d=20.

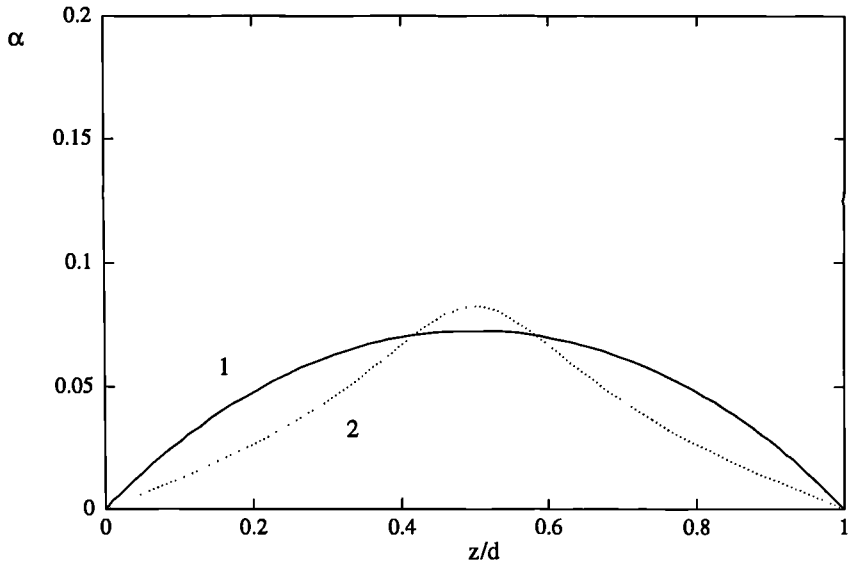

Figure 8.8: Multiple stable solutions of α in a twisted layer for d=20.

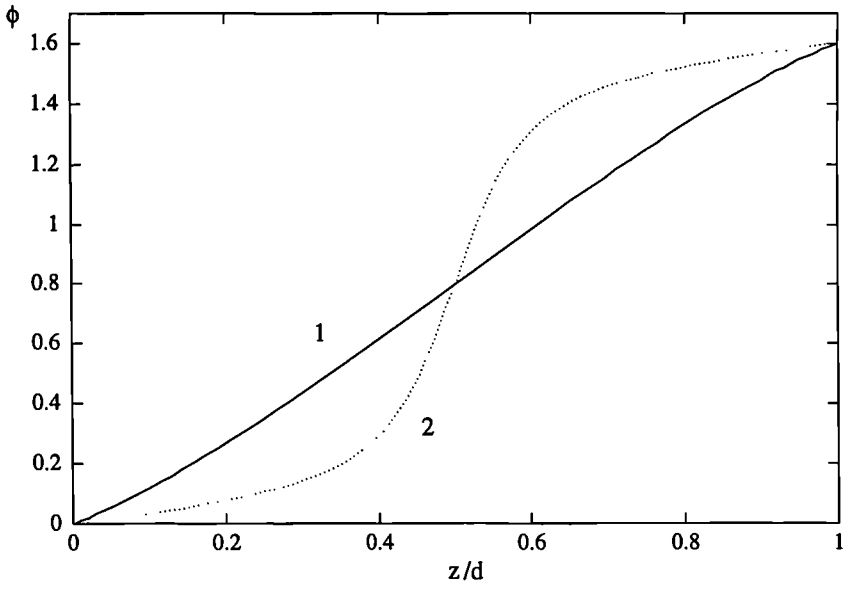

Figure 8.9: Multiple stable solutions of ϕ in a twisted layer for d=20.

This high energy distortion in solution 2 is compensated for by a decrease in the scalar order parameter S (Figure 8.7) and interestingly, although there is a concentration of the biaxiality around the centre of the cell, the maximum biaxiality α coefficient does not significantly increase.

The change to the region where multiple solutions exist when other parameters are altered can now be investigated. The most interesting changes occur when the coefficient of the biaxial potential κ_2 is varied. As κ_2 is varied the package AUTO finds the solutions to the equations and locates the two limit points l_1 and l_2 (in Figure 8.6). The region between these limit points is then where multiple solutions occur. Figure 8.10 shows this region up to a gap width of $d = 30$ where the numerical algorithm fails to converge to a solution. AUTO can find a solution along this branch for larger gap widths but it is difficult to *follow* the solution along this branch. By altering certain numerical parameters within AUTO and solving the equations for specific gap widths it is found that the locus of l_1 asymptotes to a straight line with gradient approximately equal to 1.

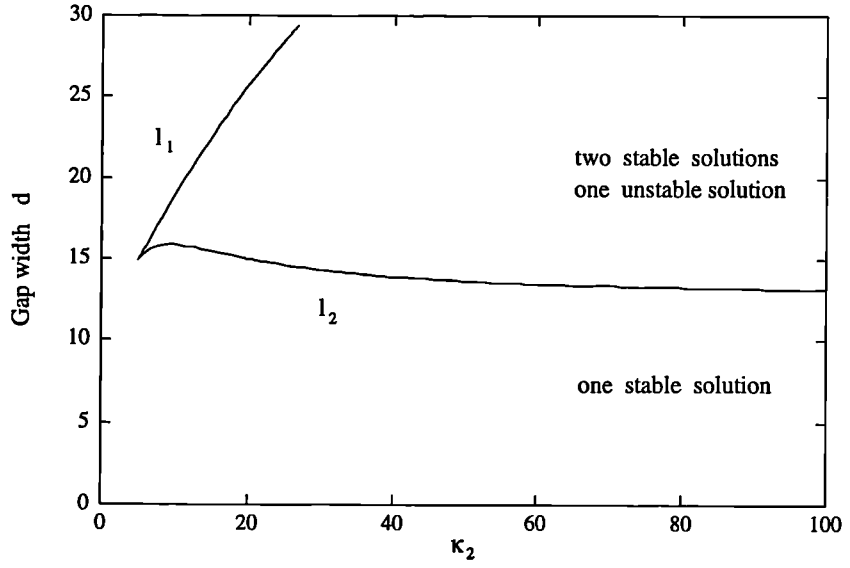

Figure 8.10: Locus of the limit points of Figure 8.6 forming a cusp in the κ_2, d parameter space

An increase in κ_2 makes biaxiality less favourable and when $\kappa_2 > 20$ biaxiality is energetically unfavourable and the liquid crystal is essentially uniaxial. Figure 8.10 shows that when there is biaxiality present in the layer ($\kappa_2 < 20$)

multiple solutions only occur within a small range of gap widths. In fact when $\kappa_2 < 4.99$ there is only one solution for any gap width. To investigate the multiplicity of solutions in this system κ_2 is fixed so that the liquid crystal is essentially uniaxial ($\kappa = 100$).
If it is assumed that $\alpha = 0$ then variations of S and ϕ need only be considered and the Euler-Lagrange equations are then,

$$0 = S_{zz} - 3S\phi_z^2 - \frac{3\kappa_1}{4}S(S - S_u)(S - S_b) \tag{8.34}$$

$$0 = \left(S^2\phi_z\right)_z \tag{8.35}$$

The number of parameters can be reduced by one if S is nondimensionalised using $S^* = S/S_b$. Then the equations become,

$$0 = S^*_{zz} - 3S^*\phi_z^2 - \frac{3\kappa_1^*}{4}S^*(S^* - S_u^*)(S^* - 1) \tag{8.36}$$

$$0 = \left((S^*)^2\phi_z\right)_z \tag{8.37}$$

with boundary conditions,

$$\phi(0) = 0 \tag{8.38}$$

$$\phi(d) = \phi_d > 0 \tag{8.39}$$

$$S^*(0) = S_0^* \tag{8.40}$$

$$S^*(d) = S_d^* \tag{8.41}$$

where $\kappa_1^* = \kappa_1 S_b^2$, $S_u^* = S_u/S_b$. The equation parameters are therefore κ_1^*, S_u^*, ϕ_d, d, S_0^* and S_d^*. Of these parameters only S_u^*, ϕ_d, d can be easily changed within a liquid crystal cell in a physical situation. As explained in Section 7.3.1 an increase in temperature is equivalent to an increase in S_u^*. In the present system which allows multiple stable solutions one solution of the equations exhibits a higher degree of melting than the other (Figures 8.7, 8.8, 8.9). The stability of these solutions is therefore expected to be affected by changes in S_u^* and will be investigated later in this chapter. The two parameters ϕ_d and d relate to the amount of twist in the layer and the distance over which the

director must twist and it will be shown below that changes in these parameters critically affect the stability and relative stability of the different possible solutions.

Variations of the gap width d and the amount of twist ϕ_d are initially considered. As before a solution is found for a specific set of parameters, $S_b = 0.7$, $\kappa_1 = 1$, $S_u^* = 0.5$, $\phi_d = 1.6$, $d = 9$, $S_0 = 0.8$. Figures 8.11 and 8.12 show the starting solutions for the above parameters.

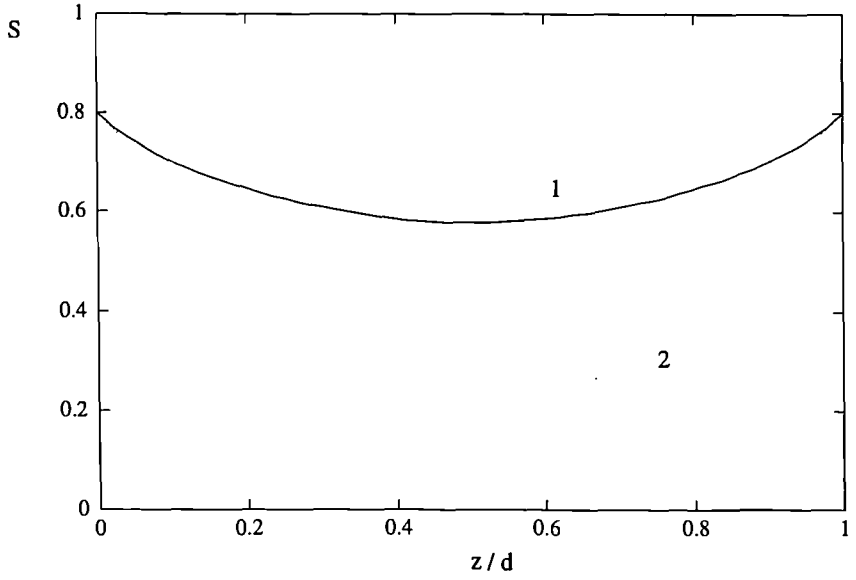

Figure 8.11: Uniaxial scalar order parameter stable solutions for a twist layer with parameters $S_b = 0.7$, $\kappa_1 = 1$, $S_u^* = 0.5$, $\phi_d = 1.6$, $d = 9$, $S_0 = 0.8$

If the solutions are followed as ϕ_d is continued through the range 0 to π the solution branches of the two solutions are linked by an unstable solution branch (Figure 8.13) and as in the biaxial case there are only three solutions in the range $\phi_d \in (1.36,\ 1.71)$ however there is no solution for angles past $\phi_d = 1.81$. After this point AUTO fails to converge on a solution and the L^2 norm which equals,

$$\|(S,\ \phi)\| = \int \sqrt{S^2 + (S_z)^2 + \phi^2 + (\phi_z)^2}\ \mathrm{d}z \tag{8.42}$$

tends to infinity (Figure 8.14). This failure to converge is due to the fact that the solution at this point in parameter space has extremely large values of ϕ_z

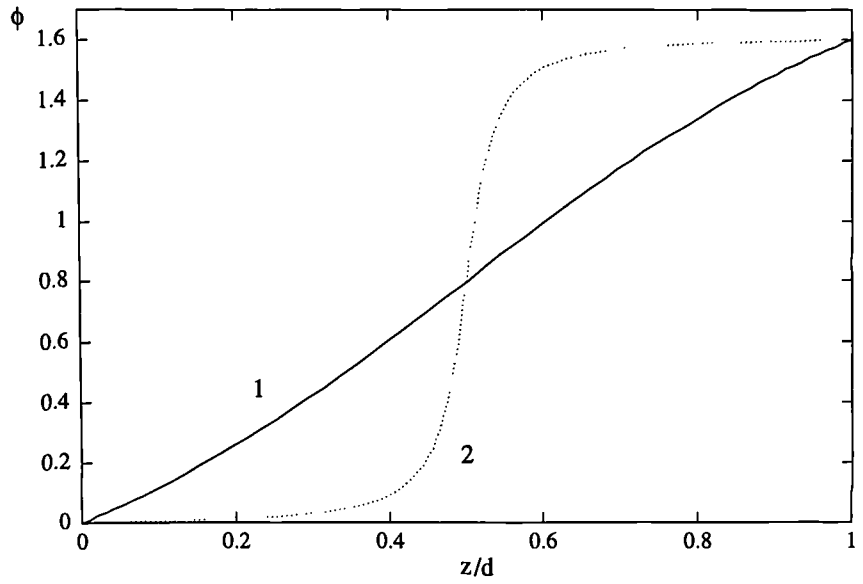

Figure 8.12: Uniaxial director angle stable solutions for a twist layer with parameters $S_b = 0.7$, $\kappa_1 = 1$, $S_u^* = 0.5$, $\phi_d = 1.6$, $d = 9$, $S_0 = 0.8$

near $z = d/2$. Figures 8.15 and 8.16 show the S and ϕ solutions for ϕ_d values before and after the fold.

There is a second possible configuration of the director for *any* point in parameter space due to the symmetry of the director. The directions $\mathbf{n}$ and $-\mathbf{n}$ are equivalent and therefore the director may twist in the opposite way from $\phi = 0$ on the lower boundary to $\phi = \phi_d + \pi$ on the upper boundary. There is therefore a second solution branch which is a reflection of the first in the line $\phi_d = \pi/2$ (Figure 8.17).

There are therefore two stable solutions when the twist parameter is in the regions $\phi_d \in (0,\ 1.36)$ or $\phi_d \in (1.78,\ \pi)$, there are three stable solutions and one unstable solution when $\phi_d \in (1.36,\ 1.43)$ or $\phi_d \in (1.71,\ 1.78)$ and there are four stable and two unstable solutions when $\phi_d \in (1.43,\ 1.71)$.

These regions, in which different numbers of solutions exist, can be investigated when another parameter is varied. Using AUTO the boundaries of the regions, which in this case are the limit point values of ϕ_d of the folds in Figure 8.16, may be followed as the gap width d is varied. Figure 8.18 shows the loci of the limit points values in the d, ϕ_d parameter space. For a cell with a gap width less than 6.49 there is only one possible solution. Between $d = 6.49$

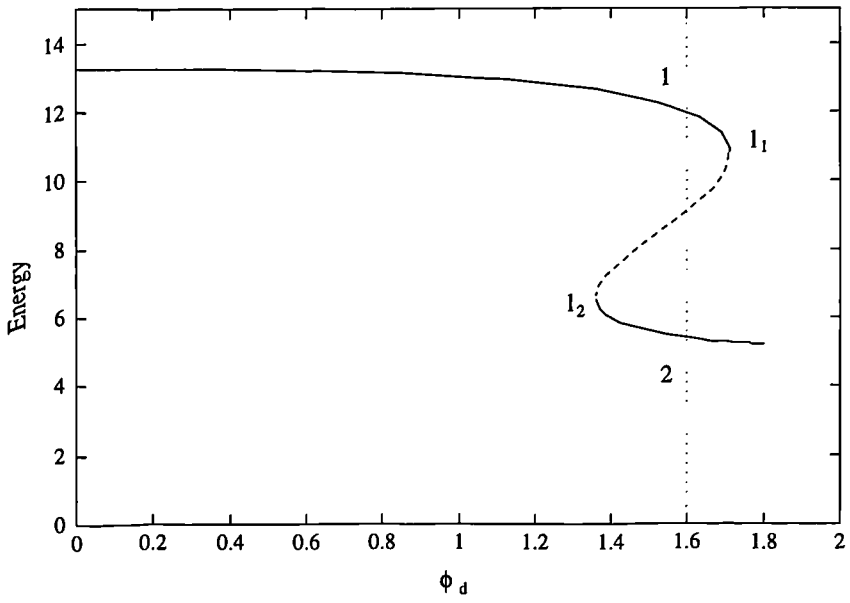

Figure 8.13: Fold in the Energy versus ϕ_d diagram for d=9.

and $d = 8.50$ the two cusps do not overlap so that there is a region around $\phi_d = \pi/2$ where there is one solution and within the cusp region there are two stable and one unstable solutions. After $d = 8.5$ the cusps overlap and there is a region around $\phi_d = \pi/2$ where there are four stable solutions and two unstable solutions possible at one point in parameter space.

As discussed before the parameter S_u has been set to be $S_b/2$ ($S_u^* = 0.5$) and hence the temperature is equal to the clearing point temperature T_c. At this point the two minima of the potential function are *both* global minimizers of the energy functional and hence the system can support multiple solutions. If the parameter S_u^* is changed so that the temperature is increased ($S_u^* \rightarrow 1$) or decreased ($S_u^* \rightarrow 0$) the system would be expected to prefer the high twist gradient, high melting solution or the uniform twist, low melting solution respectively. Figure 8.19 shows the development of one of the cusps from Figure 8.18 as S_u^* ($= S_u/S_b$) varies from 0 to 1.

Between the two cusps for $S_u^* = 0.5$ and $S_u^* = 0.55$ the asymptotic behaviour of the cusp changes. Less than a critical value of S_u^* the lower branch of the cusp asymptotes to a fixed twist parameter. More than the critical parameter and the branch asymptotes to a fixed gap width. This phenomena is associated with the fold in the solution curve for the disclination line situation (Figure

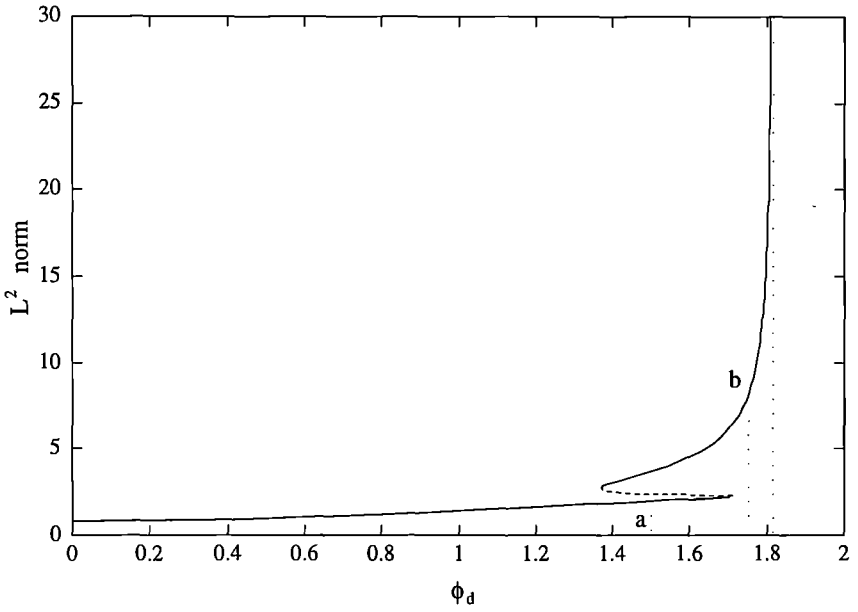

Figure 8.14: Fold and singularity in the L^2 norm versus ϕ_d diagram.

7.12). If S_u^* is high enough then for any value of the twist parameter there is a solution that involves melting and is the lowest energy solution. If S_u^* is lower than the critical value and if the twist parameter is low enough then the only solution is that with uniform twist and no melting.

8.4 Summary

In this chapter wall defects within twisted nematic layers have been considered. Analytical solutions are found for two cases. When the bulk of the liquid crystal layer is considered a solution is found for *constant* twist and when there is *no* twist present in the layer the governing equations uncouple and an analytic solution can be found. The full equations have been solved using the numerical continuation package AUTO. Multiple solutions were found for various regions in parameter space.

The symmetry of the system (reflection in the line $\phi_d = \pi/2$) leads to regions where 4 stable and two unstable solutions exist, regions where two stable and one unstable solution exist and regions where only one stable solution exists. Typically the stable solutions are of two kinds. The first solution involves a uniform twist between the two boundaries and a small decrease in the scalar

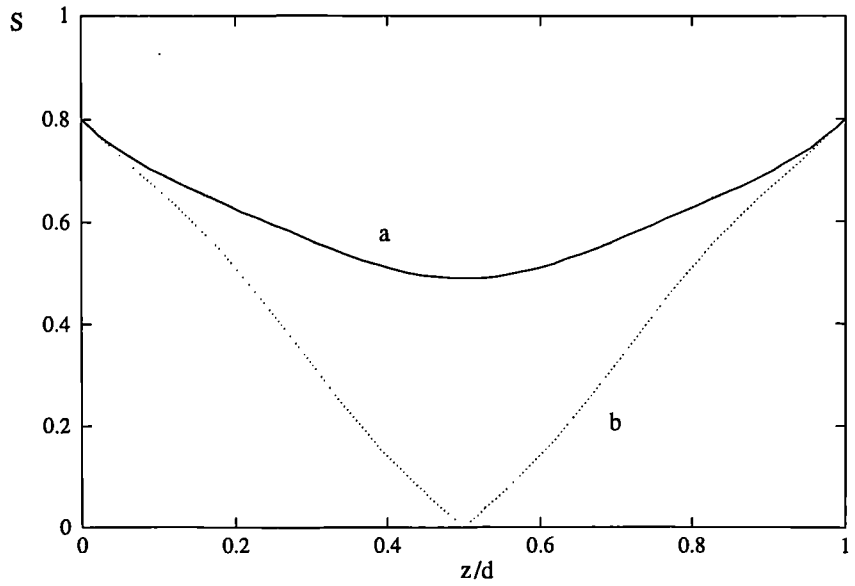

Figure 8.15: S solutions before the fold (a) and after (b) the fold near the L^2 norm singularity.

order parameter compared to the no-twist case. The second solution is a wall defect where the twisting necessary in the layer is concentrated around the centre at $z = d/2$ and the scalar order parameter decreases to values close to zero. The liquid crystal has therefore melted to an isotropic liquid in this region.

Figure 8.18 shows that for a greater amount of twist in the layer (ϕ_d larger) the wall defect solution will become the only stable solution and for less twist in the layer (ϕ_d smaller) the uniform twist solution will become the only stable solution and in the region in the middle both solutions are stable and the system exhibits hysteresis. Changes in the gap width, d, then determine the size of this region. As the gap width increases the director stress from the twist distortion decreases and the non-melting/uniform twist solution is stable over a larger range of twist angles ϕ_d.

Figure 8.19 shows that as the temperature increases (S_u increases) the asymptotic nature of the cusps in Figure 8.18 change. For values of S_u greater than a critical value the wall defect solution is stable (for d greater than some critical value) for any twist angle ϕ_d, even when there is no twist present. The critical dependence on S_u of the form of the cusp is equivalent to the critical

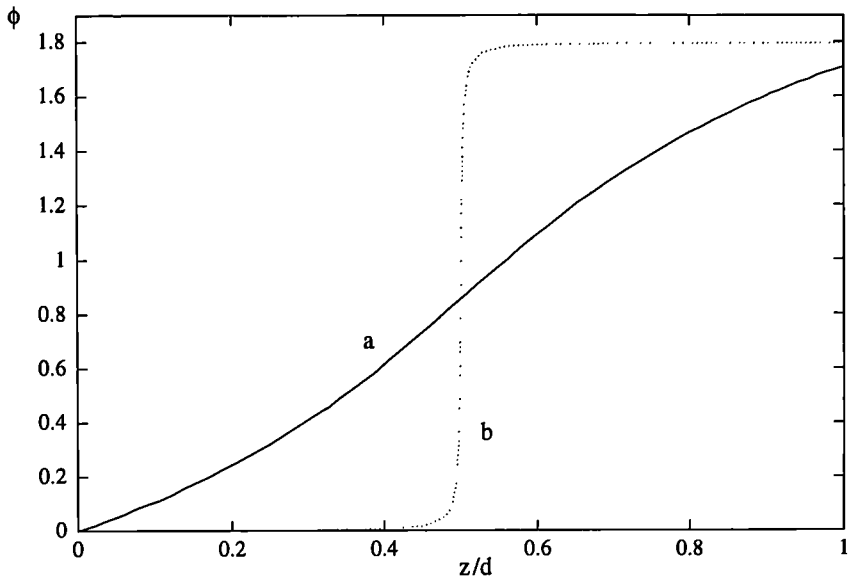

Figure 8.16: ϕ solutions before the fold (a) and after (b) the fold near the L^2 norm singularity

dependence on S_u of the disclination line structure in the previous chapter. In the next chapter the results of the thesis and possibilities for future research are discussed.

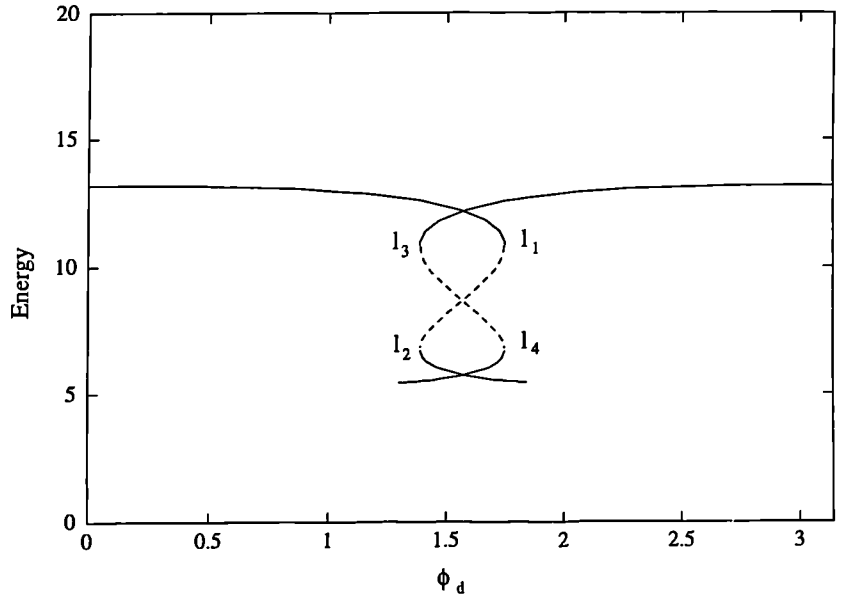

Figure 8.17: The effect of symmetry on the fold diagram is a reflection in the line $\phi_d = \pi/2$.

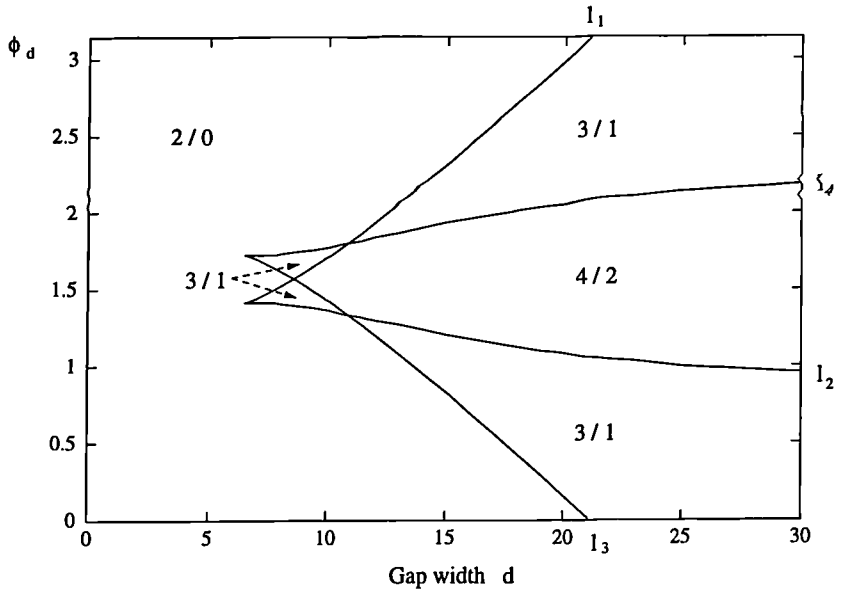

Figure 8.18: Locus of the *four* limit points (l_1, l_2, l_3 and l_4) in Figure 8.17 in the ϕ_d, d parameter space. In the regions i/j there exist i stable solutions and j unstable solutions.

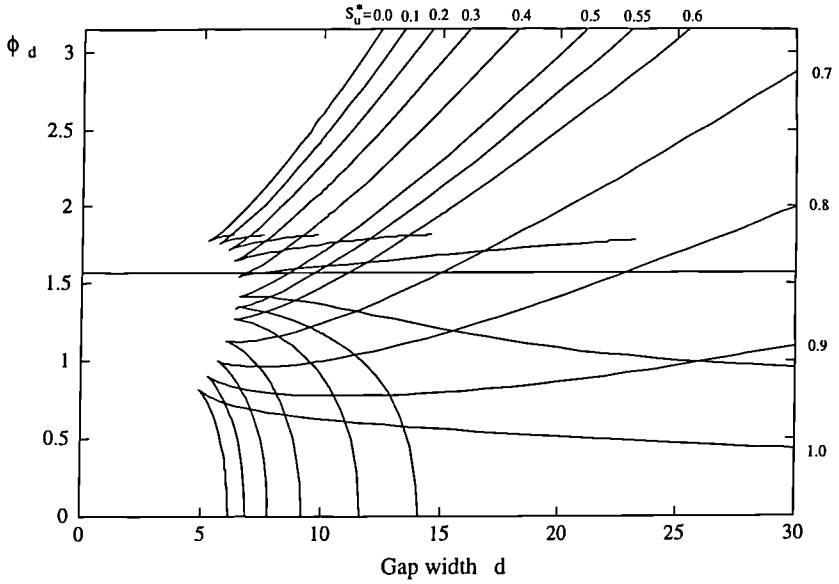

Figure 8.19: The change in one of the cusps (Figure 8.18) as S_u^* (or equivalently) temperature varies.

Chapter 9

Discussion

The aim of this study was to investigate the effects of various novel boundaries and boundary conditions on nematic liquid crystal behaviour. In the first half of the thesis the Freedericksz transition of a nematic sandwiched between non-planar and sinusoidal pre-tilt boundaries was studied using Oseen-Zöcher-Frank continuum theory. In the second half of the thesis the effects of certain boundary changes on disclination lines and twist wall defects using a continuum theory which allows for variable scalar order parameters were considered. In the next section the results of the previous chapters are discussed and in Section 9.2 some ideas for future work are presented.

9.1 Conclusions

In the first half of the thesis the effects of non-planar boundary conditions on the Freedericksz effect in a nematic liquid crystal layer were considered. For this problem a magnetic field is placed so as to compete with the surface alignment. The subsequent transition to alignment of the director with the field occurs at a critical field strength. Using the Oseen-Zöcher-Frank continuum theory the director configuration and the transition were considered in order to determine effects of the non-planar boundaries.

The governing equations and boundary conditions were discussed in Chapter 3 and two possible solutions to the simple case of the linear, zero field problem were found. In the first solution the boundaries dominate the director distortion and the director angle relaxes towards the centre of the cell although the

director angle is never identically zero. In the second solution the bulk of the liquid crystal cell is undistorted and boundary layers are formed at each of the glass plates. The second configuration therefore behaves as a planar liquid crystal cell during the Freedericksz effect and was not further considered. When a magnetic field was introduced to the governing equations the linearised equations predicted a singularity at a field parameter $\gamma_c = \pi^2/4+(Lk)^2$. When a perturbation expansion was used to investigate the (weakly) nonlinear nature of the equations the second term in the expansion predicted a second singularity at the field parameter $\gamma_c' = \pi^2 + 4(Lk)^2$. This singularity derived from the interaction between the boundary which has a wavenumber k and the distortions from linear solution which have wavenumber k which resulted in a distortion of wavenumber $2k$. Although the solutions from Section 4.2 predict singularities in the director angle the assumption that this angle angle is small implies that the solution is not valid near to the singularity. This means that the solution does *not* imply an unphysical spinning of the director as the critical field is approached but does imply that transition occurs from a low amplitude state to a high amplitude state.

In Chapter 5 greater consideration was given to the structure of this transition from low to high amplitude by analysing the amplitude of the dominant mode during the singularity. In this way it was possible to find the bifurcation diagrams and the stability of each solution branch. Since the classical Freedericksz transition is a pitchfork bifurcation, the introduction of slightly non-planar boundaries ($Ak \ll 1$) would be expected to result in a perturbed pitchfork bifurcation. Both singularities of the linear solution were found to be perturbed pitchfork bifurcations. It is therefore impossible to assign a critical field strength for the transition as there is no definitive point where the system changes from undistorted to distorted since there is always a certain amount of director distortion caused by the boundary. This perturbation also affects the growth and decay time constants for the transition (Appendix B). In terms of LCDs it takes a longer time for the director field to switch on and off than for a planar liquid crystal cell. The stability analysis showed that the middle branch of the second bifurcation was stable although the basin of attraction for this solution is extremely small. It is therefore possible that in a real situation this solution may be unattainable since in this high field state experimental errors

may be too large to keep the system on this branch and the system would switch to one of the outer branches of the first bifurcation. In fact the basin of attraction may be so small that molecular thermal vibration will be enough to switch the director. The reason this low director angle amplitude solution is stable (if it is attainable) at such a high field strength may be because of the *extra* distortion present. At this field strength the dominant mode is still the mode which has wavenumber $2k$. There is therefore more distortion at this point than if the mode with wavenumber k was dominant. This extra distortion in the bulk of the cell means that deformations are *spread* throughout the cell rather than just near the boundaries (as in the *switched* solution) and may therefore cause the solution to be stable. At this field strength the system is therefore bistable (tristable in fact if the two, virtually symmetric, switched states are included). It is conceivable that a liquid crystal display could be manufactured to take advantage of this behavior. The display would switching between the two stable states one with the director in the bulk aligned parallel to the layer normal and one with the director (on average) aligned perpendicular to the layer normal.

In the later half of the thesis defects in the liquid crystal layer were discussed. Using the same Oseen-Zöcher-Frank continuum theory it was possible to determine that a disclination line attached to a non-planar surface would attach at right angles. The director configuration around the point of contact was then found. The interaction between the high degree of splay and bend present in a disclination and the orienting effect of the boundary was found to be equivalent to a disclination line in a magnetic field. Where the effective magnetic field decreased further from the boundary. With this theory the disclination is assumed to possess a core $r < r_c$ with energy E_c to ensure the total energy is finite. In Section 7.3 a different continuum theory was then employed to model this core more realistically.

The scalar order parameter gradient at the centre of the disclination line $S_r(0)$ was found to be positive for disclinations with strength $\pm 1/2$ and zero for *all* other disclinations. It was noted that the core width for ± 1 lines (without escape) is much larger than for $\pm 1/2$ lines. This has been noticed experimentally by many authors. When the temperature is increased past the clearing temperature T_c the liquid crystal state is found to be stable. This state then

loses stability through a first order phase change and the only stable solution for higher temperatures is for an isotropic fluid. If there was no disclination present and the temperature is below the clearing temperature the liquid crystalline state would be the global minimizer of the system. If the temperature increases above the clearing point the liquid crystalline state is *still* stable and the system would continue to be stable until T^+ (Figure 7.7) when the liquid crystalline state loses stability to the isotropic state. The reason the system loses stability before T^+ is due to the presence of the core of the disclination. After T_c the melted core has a scalar order parameter S which is in the global minimizer of the potential $\sigma_1(S)$ (the isotropic state) and eventually the core will *drag* the order parameter throughout the region into the minimum potential well at $S = 0$. It is therefore the presence of the disclination that ensures the system becomes isotropic before T^+. It is also find that as the ratio of the coefficients of the biaxiality and *phase* potentials, κ, tends to zero the liquid crystalline state is stable for higher temperatures. When κ is small the biaxiality potential σ_2 contributes less energy than the scalar order parameter potential σ_1 and there is little melting near the core. Since it is this melting that causes the system to jump to the isotropic state, the smaller κ is the less likely the system will jump.

Chapter 8 applied the same continuum theory to twist layers and studied the effects of various boundary changes on twist wall defects. When the governing equations of the twist layer were solved using AUTO multiple solutions were found. All solutions involve a small amount of biaxiality but some solutions contain a uniform twist throughout the layer and very little melting in the bulk of the liquid crystal layer. Other solutions contain a concentration of the twist near the centre of the cell together with a significant amount of melting in the layer. Due to the symmetry of the problem ($\mathbf{n} = -\mathbf{n}$), in some regions of parameter space it is possible to find four stable and two unstable solutions coexisting. As with the disclination lines it is found that there is a critical value of S_u (or temperature) at which the behaviour of the cell changes drastically. At higher values of S_u the solution with a high degree of melting is dominant and below the low melting solution is dominant. The other general features of this system, which to some extent are expected, are that greater twist leads to a tendency for the liquid crystal to melt in order to minimize the

energy caused by the high twist deformations. Increasing the gap width has the opposite effect since the internal stress on the director is less if twisting is spread through a larger region.

9.2 Future work

In this thesis only a few of the possibilities for research into the effects of boundaries on liquid crystal cells have been considered. With regards to non-planar boundaries, only the static continuum theory of Ozeen-Zöcher and Frank has been considered and the dynamic theory of Ericksen and Leslie may be used to consider the effects of non-planar boundaries on phenomena such as Williams domains [30]. For the static system it is possible to solve the full nonlinear equations numerically using a package such as ENTWIFE. This would allow investigations of the exact solution and the bifurcation structure under any parameter changes in more detail.

The variable scalar order parameter theory of liquid crystals is still comparatively new and there are many possibilities for future research. The core structure of attached disclination lines, the interaction of two attached disclination lines, escaped disclination lines and disclination loops are just a few unresearched areas. The introduction of an electric/magnetic field to the twist layer to model Helfrich walls and the investigation of chiral nematics or nematics with a chiral dopant could be considered to model modern twisted nematic liquid crystal displays.

Only nematic liquid crystals have been considered in this thesis. The effect of boundaries on the inherently periodic structure of smectic and chiral nematic liquid crystals and disclinations within them is another area of future work.

The importance of boundaries on liquid crystal displays has been acknowledged for some time but there are clearly a great many untouched topics of research.

Appendix A

Oseen-Zöcher-Frank Continuum theory

In this appendix the continuum theory developed by Oseen, Zöcher and Frank is discussed. This theory, for a uniaxial nematic with director $\mathbf{n}$ and a fixed scalar order parameter S, uses various symmetries to reduce the number of terms in the free energy of the system. In Section A.1 the three terms contributing to the bulk free energy are found as functions of the director $\mathbf{n}$ and in Section A.2 the term contributing to the surface free energy is discussed.

A.1 Distortional free energy

Given a certain state of distortion described by the director $\mathbf{n}$. The variations of $\mathbf{n}$ are slow on the molecular scale so that $a\nabla\mathbf{n} \ll 1$ where a is a measure of molecular dimension. The free energy density due to distortion F_D will be zero if $\nabla\mathbf{n} = 0$ and therefore F_D may be expanded in powers of $\nabla\mathbf{n}$.
A local right-handed set of cartesian coordinates is chosen such that the director $\mathbf{n}$ is parallel to z at the origin and since $\mathbf{n}$ is a unit vector so,

$$n_x^2 + n_y^2 + n_z^2 = 1 \tag{A.1}$$

then locally $\mathbf{n} = (0,\ 0,\ 1)$ and,

$$0 = \nabla\left(n_x^2 + n_y^2 + n_z^2\right) = 2n_z\nabla n_z + 0 = 2\nabla n_z \tag{A.2}$$

Therefore all gradients of n_z are zero. The derivatives of $\mathbf{n}$ form the tensor,

$$\begin{pmatrix} \partial n_x/\partial x & \partial n_x/\partial y & \partial n_x/\partial z \\ \partial n_y/\partial x & \partial n_y/\partial y & \partial n_y/\partial z \\ 0 & 0 & 0 \end{pmatrix} \tag{A.3}$$

It is convenient to separate this tensor into its symmetric parts,

$$e_{ij} = \frac{1}{2}\left(n_{i,j} + n_{j,i}\right) \tag{A.4}$$

and antisymmetric parts,

$$(\text{curl } \mathbf{n})_z = \partial n_y/\partial x - \partial n_x/\partial y \tag{A.5}$$

$$(\text{curl } \mathbf{n})_y = \partial n_x/\partial z \tag{A.6}$$

$$(\text{curl } \mathbf{n})_x = -\partial n_y/\partial z \tag{A.7}$$

There are now three conditions that each term in F_D must satisfy,

1. F_D must be even in $\mathbf{n}$ since the two states $+\mathbf{n}$ and $-\mathbf{n}$ are indistinguishable.

2. There are no terms linear in $\nabla\mathbf{n}$ since the only terms that are invariant by rotations are,

   (a) div$\mathbf{n}$ which cannot be included since it is not invariant under the transformation $\mathbf{n} \rightarrow -\mathbf{n}$

   (b) $\mathbf{n} \cdot$ curl$\mathbf{n}$ which cannot be included since it is not invariant under the transformation $(x,\ y,\ z) \rightarrow -(x,\ y,\ z)$

3. The bulk free energy F_D is unchanged by the addition of pure divergence terms (div$\mathbf{u}$ for arbitrary $\mathbf{u}$) since their corresponding energy integral can be transformed, by the divergence theorem, to a surface term

With these conditions in mind it is possible to find all relevant terms in the free energy density by separating F_D into terms quadratic in e_{ij}, curl $\mathbf{n}$ and cross terms respectively,

$$F_D = F_{ee} + F_{cc} + F_{ec} \tag{A.8}$$

and looking at each term separately.
The most general form of F_{ee} is [56],

$$\begin{aligned} F_{ee} &= \lambda_1\, e_{zz}^2 + \lambda_2\, (e_{xx}+e_{yy})^2 + \lambda_3\, e_{ij}e_{ji} \\ &\quad + \lambda_4\, e_{zz}\,(e_{xx}+e_{yy}) + \lambda_5\, \left(e_{xz}^2 + e_{yz}^2\right) \end{aligned} \tag{A.9}$$

but $e_{zz} = 0$ and using the identity $e_{xx} + e_{yy} + e_{zz} = e_{xx} + e_{yy} = \text{div}\ \mathbf{n}$ this reduces to,

$$F_{ee} = \lambda_2\, (\text{div}\ \mathbf{n})^2 + \lambda_3\, e_{ij}e_{ji} + \lambda_5\, (\mathbf{n} \wedge \text{curl}\ \mathbf{n}) \tag{A.10}$$

Using the identities,

$$e_{ij}e_{ji} = (\text{div}\mathbf{n})^2 + (n_j\, n_{i,j})_i - (n_j\, n_{i,i})_j + \frac{1}{2}\,(\text{curl}\ \mathbf{n})^2 \tag{A.11}$$

$$(\text{curl}\ \mathbf{n})^2 = (\mathbf{n}\cdot\text{curl}\ \mathbf{n})^2 + (\mathbf{n}\wedge\text{curl}\ \mathbf{n})^2 \tag{A.12}$$

and since the third and fourth terms in (A.11) must be dropped by condition 3 then F_{ee} is the sum of the three terms,

$$(\text{div}\ \mathbf{n})^2,\ \ (\text{curl}\ \mathbf{n})^2 \ \ \text{and} \ \ (\mathbf{n}\wedge\text{curl}\ \mathbf{n})^2 \tag{A.13}$$

The term F_{cc} must have the general form,

$$F_{cc} = \mu_1\,(\text{curl}\ \mathbf{n})_z^2 + \mu_2\left((\text{curl}\ \mathbf{n})_x^2 + (\text{curl}\ \mathbf{n})_y^2\right) \tag{A.14}$$

$$= \mu_1\,(\text{curl}\ \mathbf{n})^2 + \mu_2\,(\mathbf{n}\wedge\text{curl}\ \mathbf{n})^2 \tag{A.15}$$

and the term F_{ec} has the form,

$$\begin{aligned} F_{ec} &= \nu_1\,(\text{curl}\ \mathbf{n})_z\,(e_{xx}+e_{yy}) \\ &\quad +\nu_2\left((\text{curl}\ \mathbf{n})_x\ e_{xz} + (\text{curl}\ \mathbf{n})_y\ e_{yz}\right) \\ &\quad +\nu_3\left((\text{curl}\ \mathbf{n})_y\ e_{zx} + (\text{curl}\ \mathbf{n})_x\ e_{zy}\right) \end{aligned} \tag{A.16}$$

The first term on the right-hand side is equal to $\nu_1\,(\mathbf{n}\cdot\text{curl}\ \mathbf{n})\,(\text{div}\mathbf{n})$ which is odd in $\mathbf{n}$ and can be discarded due to condition 1. The second term is equal

to zero since $e_{xz} = \frac{1}{2}(\text{curl } \mathbf{n})_y$ and $e_{yz} = -\frac{1}{2}(\text{curl } \mathbf{n})_x$. The last term is simply, $(\mathbf{n} \wedge \text{curl } \mathbf{n})^2$.

Hence grouping all three terms gives,

$$F_D = \frac{1}{2}K_1 (\text{div } \mathbf{n})^2 + \frac{1}{2}K_2 (\mathbf{n} \cdot \text{curl } \mathbf{n})^2 + \frac{1}{2}K_3 (\mathbf{n} \wedge \text{curl } \mathbf{n})^2 \qquad \text{(A.17)}$$

A.2 Boundaries

The boundaries of a liquid crystal cell can produce two kinds of theoretical boundary conditions, *strong* or *weak*. For strong boundary conditions the surface prescribes fixed values on the relevant dependent variables. In the weak case the boundary acts to contribute a surface energy term to the free energy of the system. The sum of the bulk free energy and the surface free energy is then minimized to obtain the governing equations and boundary conditions.

In the calculation of the bulk free energy density terms which could be expressed as the divergence of a vector were neglected. These terms are null Lagrangians and do not contribute to the bulk energy but to the surface energy . The surface energy will be composed of these terms from the distortional bulk free energy density and terms that model the interaction between the director and the aligning effect of the treated surface.

The term from the bulk free energy which can be written as a pure divergence term is,

$$F_{24} = \text{tr}(\nabla \mathbf{n})^2 - (\text{div } \mathbf{n})^2 = \nabla((\nabla \mathbf{n})\ \mathbf{n} - (\text{div } \mathbf{n})\ \mathbf{n}) \qquad \text{(A.18)}$$

so using the divergence theorem the free energy of this term is,

$$E = \int_{\mathcal{V}} F_{24}\, dv = \int_{\partial \mathcal{V}} \nabla((\nabla \mathbf{n})\ \mathbf{n} - (\text{div } \mathbf{n})\ \mathbf{n})\ ds \qquad \text{(A.19)}$$

The free energy due to the alignment can be simply modelled with a potential minimum function. The potential used in the thesis is that considered by Rapini and Popoular [76] and contributes a surface energy of the form,

$$E = \int_{\partial \mathcal{V}} \mathbf{n}^2\, ds \qquad \text{(A.20)}$$

When the boundaries induce strong anchoring the director is fixed on the boundary, all gradients of $\mathbf{n}$ are zero and F_{24} is zero. In this case the surface energy is constant and does not enter into the energy minimisation analysis.

Appendix B

Dynamics of the Freedericksz transition

In this chapter the dynamics of the Freedericksz transition is investigated and the switching times between the *on* and *off* states in the cell are found. By considering an approximation to the Ericksen-Leslie equations for the twisting Freedericksz transition the dynamic behaviour of the director orientation as the field is turned on or off is found [74]. The linearised equations are first considered to verify the critical field strength for the transition and then the nonlinear equations are used to find the time constant for the growth and decay during the transition.

The analysis for the other splay/bend Freedericksz transitions are more complex as the torsion on the director results in a translational motion. In the twist transition this does not occur and the fluid velocity may be assumed to be zero. If director inertia is neglected in the Leslie-Ericksen equations [62] the governing equation is,

$$K\nabla^2\psi + \chi_a H^2 \sin\psi\cos\psi + \lambda_1\frac{\partial\psi}{\partial t} = 0 \tag{B.1}$$

where $\lambda_1 = \mu_2 - \mu_3$ is the twist viscosity (the difference between the two Leslie coefficients μ_2 and μ_3) and ψ is the azimuthal director angle (see Chapter 4). If ψ is small then (B.1) can be approximated to,

$$K\nabla^2\psi + \chi_a H^2\left(\psi - \frac{2}{3}\psi^3\right) + \lambda_1\frac{\partial\psi}{\partial t} = 0 \tag{B.2}$$

The boundary conditions are $\psi = 0$ on $y = \pm L$ and knowing that there will be a sinusoidal x dependence in ψ leads us to Fourier decompose the twist angle,

$$\psi = \sum_n C_n(t) \cos(2n+1)\frac{\pi y}{2L} \sin kx \tag{B.3}$$

By neglecting higher harmonics and since symmetry arguments imply that ψ has a maximum at $y = 0$ this becomes,

$$\psi = \psi_{max}(t) \cos\frac{\pi y}{2L} \sin kx \tag{B.4}$$

By assuming ψ_{max}^3 is negligible so that,

$$-K\psi_{max}\left(\frac{\pi^2}{4L^2} + k^2\right) + \chi_a H^2 \psi_{max} + \lambda_1 \frac{\partial \psi}{\partial t} = 0 \tag{B.5}$$

the solution to the linearised equation is found to be,

$$\psi_{max} = C \exp\left[\left(K\left(\frac{\pi^2}{4L^2} + k^2\right) - \chi_a H^2\right) t/\lambda_1\right] \tag{B.6}$$

so if,

$$H^2 > \frac{K}{\chi_a L^2}\gamma_c \quad \text{then} \quad \psi_{max} \to \infty \text{ as } t \to \infty \tag{B.7}$$

$$H^2 < \frac{K}{\chi_a L^2}\gamma_c \quad \text{then} \quad \psi_{max} \to 0 \text{ as } t \to \infty \tag{B.8}$$

Hence the critical field strength is H_c as found in Chapter 4 (4.9).
For the nonlinear equations ψ_{max}^3 is not negligible and then the solution to (B.2) is,

$$\psi_{max}^2 = \frac{8\left(1 - (H_c/H)^2\right)}{3 - \exp\left[2\left(1 - (H_c/H)^2\right) t/\lambda\right]} \tag{B.9}$$

where $\lambda = \lambda_1/\chi_a H^2$. From the coefficient of t in the exponential function of the solution it is seen that ψ_{max} attains its maximum $\psi(\infty)$ with a growth time constant,

$$\tau(H) = \left(\left(H^2 - H_c^2\right)\chi_a/\lambda_1\right)^{-1} \tag{B.10}$$

Therefore when the field is switched on to strength H_{on} greater than the critical value the director angle grows at a rate,

$$\tau(H) = \left(\left(H_{on}^2 - H_c^2\right)\chi_a/\lambda_1\right)^{-1} \tag{B.11}$$

and when the field is switched off from a field strength above the critical strength to zero the decay time constant is therefore,

$$\tau(0) = \left(-H_c^2\chi_a/\lambda_1\right)^{-1} \tag{B.12}$$

Since the critical field strength H_c for sinusoidal boundaries is greater than that of planar boundaries the magnitudes of the growth and decay rates are *smaller* than for planar boundaries.

Bibliography

[1] M. Abramowitz and I. A. Stegun, editors. *Handbook of Mathematical Functions.* Dover, 1972.

[2] R. Barberi and G. Durand. Order parameter of a nematic liquid crystal on a rough surface. *Phys. Rev. A*, 41(4):2207, 1990.

[3] G. Barbero and G. Durand. Surface order transition in nematic liquid crystals induced by the flexoelectric polarization. *J. Appl. Phys.*, 68(11):5549, 1990.

[4] G. Barbero and G. Durand. Anchoring energy or surface melting in nematic liquid crystals? *Mol. Cryst. Liq. Cryst.*, 203:33, 1991.

[5] G. Barbero and G. Durand. Curvature induced quasi-melting from rough surfaces in nematic liquid crystals. *J. Phys. II*, 1:651, 1991.

[6] G. Barbero and G. Durand. Order parameter spatial variation and anchoring energy for nematic liquid crystals. *J. Appl. Phys.*, 69(10):6968, 1991.

[7] D. W. Berreman. Solid surface shape and the alignment of an adjacent nematic liquid crystal. *Phys. Rev. Lett.*, 28(26):1683, 1972.

[8] D. W. Berreman. Alignment of liquid crystals by grooved surfaces. *Mol. Cryst. Liq. Cryst.*, 23:215, 1973.

[9] P. Biscari, G. Capriz, and E. G. Virga. On surface biaxiality. *Liquid Crystals*, 16(3):479, 1994.

[10] P. Biscari and G. Guidone Peroli. A hierarchy of defects in biaxial nematics. *Quad. Dip. Mat. Pisa*, 811, 1994.

[11] P. Biscari and E. G. Virga. Biaxial nematics between two cylinders. *Quad. Dip. Mat. Pisa*, 841, 1995.

[12] L. M. Blinov. *Electro-Optical and Magneto-Optical Properties of Liquid Crystals.* Wiley, 1983.

[13] A. B. Borisov. Inverse problem for an elliptic sine-Gordon equation with an asymptotic behaviour of the cnoidal-wave type. *Inverse Problems*, 5:959, 1989.

[14] A. B. Borisov and V. V. Kiseliev. Topological defects in incommensurate magnetic and crystal structures and quasi-periodic solutions of the elliptic sine-Gordon equation. *Physica D*, 31:49, 1988.

[15] H. Brand and H. Pleiner. Hydrodynamics of biaxial discotics. *Phys. Rev. A*, 24(5):2777, 1981.

[16] G. H. Brown and W. G. Shaw. The mesomorphic state. *Chemical Reviews*, 57(6):1049, 1957.

[17] P. F. Byrd and M. D. Friedman. *Handbook of Elliptic Integrals for Engineers and Physicists.* Springer-Verlag, 1954.

[18] S. Chandrasekhar. *Liquid Crystals.* Cambridge University Press, 2nd edition, 1992.

[19] S. Chandrasekhar and G. S. Ranganath. The structure and energetics of defects in liquid crystals. *Advances in Physics*, 35(6):507, 1986.

[20] S. Chandrasekhar, B. K. Sadashiva, B. R. Ratna, and V. N. Raja. A biaxial nematic liquid-crystal. *Pramana*, 30:L491, 1988.

[21] P. E. Cladis and M. Kleman. Non-singular disclinations of strength $S = \pm 1$ in nematics. *J. de Physique*, 33:591, 1972.

[22] P. J. Collings. *Liquid Crystals: Nature's Delicate Phase of Matter.* Adam Hilger, 1990.

[23] P. G. de Gennes. Phenomenology of short-range-order effects in the isotropic phase of nematic liquid crystals. *Phys. Lett. A*, 30:454, 1969.

[24] P. G. de Gennes and J. Prost. *The Physics of Liquid Crystals.* Oxford University Press (Clarendon Press), 2nd edition, 1993.

[25] R. M. DeLeonardis, S. E. Trullinger, and R. F. Wallis. Theory of boundary effects on sine-Gordon solitons. *J. Appl. Phys.*, 51(2):1211, 1980.

[26] G. Derfel. Stationary states of the surface stabilized ferroelectric liquid crystal layers in electric field. *Liquid Crystals*, 8(3):331, 1990.

[27] G. Derfel. Effect of weak anchoring on the electric field induced deformations of nematic layers. *Liquid Crystals*, 17(3):429, 1994.

[28] E. J. Doedel. AUTO: A program for the automatic bifurcation analysis of autonomous systems. *Congressus Numeranti*, 30:265, 1981.

[29] M. Doi. Molecular dynamics and rheological properties of concentrated solutions of rod like polymers in isotropic and liquid crystalline phases. *J. Polymer Sci.*, 19:229, 1981.

[30] E. Dubois-Violette, G. Durand, E. Guyon, P. Manneville, and P. Pieranski. Instabilities in nematic liquid crystals. *Solid State Physics Supplement*, 14:147, 1978.

[31] J. L. Ericksen. Anisotropic fluids. *Arch. Rational Mech. Anal.*, 4:231, 1960.

[32] J. L. Ericksen. Conservation laws for liquid crystals. *Trans. Soc. Rheology*, 5:23, 1961.

[33] J. L. Ericksen. Liquid crystals with variable degree of orientation. *Arch. Rational Mech. Anal.*, 113:97, 1991.

[34] C. Fan. Disclination lines in liquid crystals. *Phys. Lett. A*, 34:335, 1971.

[35] F. C. Frank. On the theory of liquid crystals. *Discuss. Faraday Soc.*, 25:19, 1958.

[36] V. Freedericksz and V. Zolina. Forces causing the orientation of an anisotropic fluid. *Trans. Faraday Soc.*, 29:919, 1933.

[37] J. Frenkel and T. Kontorova. On the theory of plastic deformation and twining. *J. Phys. (USSR)*, 1:137, 1939.

[38] G. Friedel. Les états mésomorphes de la matiére. *Ann. Phys.*, 18:273, 1922.

[39] B. J. Frisken and P. Palffy-Muhoray. Electric-field-induced twist and bend Freedericksz transition in nematic liquid crystals. *Phys. Rev. A*, 39(3):1513, 1989.

[40] E. C. Gartland Jnr., P. Palffy-Muhoray, and R. S. Varga. Numerical minimization of the landau-de Gennes free energy: Defects in cylindrical capillaries. *Mol. Cryst. Liq. Cryst.*, 199:429, 1991.

[41] L. Gattermann and A. Ritschke. Azoxyphenol ethers. *Ber. deutsch. chem. Ges.*, 23:1738, 1890.

[42] E. Govers and G. Vertogen. Fluid dynamics of biaxial nematics. *Physica A*, 133:337, 1985.

[43] I. S. Gradshteyn and I. M. Ryzhik, editors. *Table of Integrals, Series and Products.* Academic Press, 1965.

[44] G. W. Gray. *Molecular Structure and the Properties of Liquid Crystals.* Academic Press, 1962.

[45] W. Helfrich. *Phys. Rev. Lett*, 21:1518, 1968.

[46] S. J. Hogan, T. Mullin, and P. Woodford. Rectilinear low-frequency shear of homogeneously aligned nematic liquid crystals. *Proc. R. Soc. Lond. A*, 441:559, 1993.

[47] O. Hudák. On vortex configurations in two-dimensional sine-Gordon systems with applications to phase transitions of the Kosterlitz-Thouless type and to Josephson junctions. *Physics letters*, 89 A(5):245, 1982.

[48] E. A. Jacobsen and J. Swift. Hydrodynamics of biaxial liquid-crystals. *Mol. Cryst. Liq. Cryst*, 78:311, 1981.

[49] Y. Kawata, K. Takatoh, M. Hasegawa, and M. Sakamoto. The alignment of nematic liquid crystals on photolithographic micro-groove patterns. *Liquid Crystals*, 16(6):1027, 1994.

[50] H. Kelker. History of liquid crystals. *Mol. Cryst. Liq. Cryst.*, 21:1, 1973.

[51] U. D. Kini. Isothermal hydrodynamics of orthorhombic nematics. *Mol. Cryst. Liq. Cryst.*, 108:71, 1984.

[52] U. D. Kini. Discontinuous orientational changes in nematics. effects of electric and magnetic fields. *Liquid Crystals*, 8(6):745, 1990.

[53] U. D. Kini. Magnetic and electric field induced bistability in nematics and cholesterics. *Liquid Crystals*, 10(5):597, 1991.

[54] M. Kleman. *Points, Lines and Walls: in Liquid Crystals, Magnetic Systems and Various Ordered Media.* Wiley, 1983.

[55] L. Lam and J. Prost. *Solitons in Liquid Crystals.* Springer-Verlag, 1991.

[56] L. D. Landau and E. M. Lifshitz. *Theory of elasticity.* Pergamon, London, 1959.

[57] E. S. Lee, P. Vetter, T. Miyashita, T. Uchida, and M. Kano. Control of liquid crystal alignment using stamped-morphology method. *Jpn. J. Appl. Phys.*, 32:L1436, 1993.

[58] O. Lehmann. Über physikalische isomerie. Dissertation, Strassburg, 1877.

[59] F. M. Leslie. Some constitutive equations for anisotropic fluids. *Quart. Journ. Mech. and Applied Math.*, 19(3):357, 1966.

[60] F. M. Leslie. Some constitutive equations for liquid crystals. *Arch. Rational Mech. Anal.*, 28:265, 1968.

[61] F. M. Leslie. Theory of flow phenomena in liquid crystals. *Advances in Liquid Crystals*, 4:1, 1979.

[62] F. M. Leslie. Continuum theory for nematic liquid crystals. *Continuum Mechanics and Thermodynamics*, 4:167, 1992.

[63] F. M. Leslie, J. S. Laverty, and T. Carlsson. Continuum theory for biaxial liquid crystals. *Q. J. Mech. Appl. Math*, 45(4):595, 1992.

[64] B. Lin and P. L. Taylor. Liquid crystal anchoring transitions induced by thermal motion. *Liquid Crystals*, 16(5):831, 1994.

[65] R. I. Lindsay. *Shear in Nematic Liquid Crystal Layers.* PhD thesis, University of Oxford, 1995.

[66] M. Lui. Hydrodynamic theory of biaxial nematics. *Phys. Rev. A*, 24:2720, 1981.

[67] F. Marchesoni. Exact solutions of the sine-Gordon equation with periodic boundary conditions. *Progress of Theoretical Physics*, 77(4):813, 1987.

[68] C. Mettenheimer. Ueber leptothrix ochracea. *Corr.-Blatt d. Vereins f. gem. Arbeit z. Förd. d. wissensch. Heilkunde*, 24:331, 1857.

[69] R. B. Meyer. On the existence of even indexed disclinations in nematic liquid crystals. *Phil. Mag.*, 27:405, 1973.

[70] V. P. Mineyev and G. E. Volovik. Planar and linear solitons in superfluid ^{3}He. *Phys. Rev. B*, 18(7):3197, 1978.

[71] K. Nakajama, Y. Onodera, T. Nakamura, and R. Sato. Numerical analysis of vortex motion on Josephson structures. *J. Appl. Phys.*, 45:4095–4099, 1974.

[72] A. H. Nayfeh. *Problems in perturbations.* Wiley, 1985.

[73] C. W. Oseen. The theory of liquid crystals. *Trans. Faraday Soc.*, 29:883, 1933.

[74] P. Pieranski, F. Brochard, and E. Guyon. Static and dynamic behaviour of a nematic liquid crystal in a magnetic field. *J. de Physique*, 34:35, 1973.

[75] K. Praefke, B. Kohne, B. Gundogan, D. Demus, and S. Diele. *Arbeitstagung Flüssigkristalle*, 18, 1989.

[76] A. Rapini and M. Popoular. Distorsion d'une lamelle nématique sous champ magnétique. conditions d'ancrage aux parois. *J. Phys. (Paris) Colloque*, C4:54, 1969.

[77] F. Reinitzer. Cholesterin. *Monatsh.*, 9:421, 1888.

[78] F. Rondelez and J. P. Hulin. Distortions of a planar cholesteric structure induced by a magnetic field. *Solid State Communications*, 10:357, 1972.

[79] A. Saupe. Elastic and flow properties of biaxial nematics. *J. Chem. Phys*, 75:5118, 1981.

[80] N. Schophol and T. J. Sluckin. Defect core structure in nematic liquid crystals. *Phys. Rev. Lett.*, 59(22):2582, 1987.

[81] A. G. Shagalov. Singular solutions of the elliptic sine-Gordon equation: models of defects. *Phys. Lett. A*, 165:412, 1992.

[82] J. M. Speight and R. S. Ward. Kink dynamics in a novel discrete sine-Gordon system. *Nonlinearity*, 7:475, 1994.

[83] A. Sugimura and T. Kawamura. Surface-induced nematic ordering using SiO_2 grating. *Japn. J. Appl. Phys.*, 23(2):137, 1984.

[84] V. A. Usol'tseva and I. G. Christiakoff. Chemical characteristics, structure and properties of liquid crystals. *Uspekhi Khim*, 32:1124, 1963.

[85] G. Valetin. *Die Untersuchung der Pflanzen-und der Tiergewebe im polarisierten Lichte.* Leipzig, 1861.

[86] R. Virchow. Ueber ein eigenthümliches verhalten albuminöser flüssig keiten bei zusatz von salzen. *Virchows Archiv*, 6:572, 1854.

[87] E. G. Virga. *Variational Theories for Liquid Crystals.* Chapman & Hall, 1991.

[88] L. J. Yu and A. Saupe. Observation of a biaxial nematic phase in potassium laurate-1-decanol-water mixture. *Phys. Rev. Lett*, 45:1000, 1980.

[89] H. Zöcher. The effect of a magnetic field on the nematic state. *Trans. Faraday Soc.*, 29:945, 1933.